UNIVERSITÄTSKLINIKUM HAMBURG-EPPENDORF

Zentrum für Molekulare Neurobiologie Hamburg
Institut für Molekulare und Zelluläre Kognition

Prof. Dr. Dietmar Kuhl

LTP in conventional and conditional Arc/Arg3.1 KO mice

Dissertation
zur Erlangung des Grades eines Doktors der Medizin
an der Medizinischen Fakultät der Universität Hamburg.

vorgelegt von:

Lilianna Stanislawa Kucharczyk
aus Kattowitz

Hamburg 2019

Angenommen von der
Medizinischen Fakultät der Universität Hamburg am: 25.06.2020

Veröffentlicht mit Genehmigung der
Medizinischen Fakultät der Universität Hamburg.

Prüfungsausschuss, der/die Vorsitzende: **Prof. Dr. Dietmar Kuhl**

Prüfungsausschuss, zweite/r Gutachter/in: **Prof. Dr. Robert Bähring**

INDEX

1 AIMS AND GOALS OF DISSERTATION

The correlation between Arc/Arg3.1, "a master regulator of synaptic plasticity" (Shepherd and Bear 2011) and activity regulated LTP (Cole et al. 1989, Tzingounis and Nicoll 2006) has become a major interest of many research groups. Because of its unique time course of expression and its multiple regulatory functions in plasticity and its essential role in memory formation, Arc/Arg3.1 protein has become the most studied activity-dependent IEG. This work aims to investigate in greater detail the role of Arc/Arg3.1 protein in TBS induced LTP in the CA1 region of the hippocampus; a form of LTP whose underlying cellular mechanisms are not yet understood. Through activity-dependent local synthesis of Arc/Arg3.1 protein, the amount of newly synthesized proteins may be critical for synaptic structural changes, and thereby regulate long-term synaptic response in prior activated dendritic synapses. Recent work using antisense oligodeoxynucleotides demonstrated that failure of memory consolidation results from partial reduction of Arc/Arg3.1 protein expression (Guzowski et al. 2000, Messaoudi et al. 2007). Thus, a second goal of this study is to reveal possible dose-response effects of Arc/Arg3.1 protein expression on TBS-LTP. To this aim, conventional Arc/Arg3.1 KO mice were compared to either heterozygous littermates harboring single Arc/Arg3.1 allele or WT littermates harboring two alleles. Furthermore, recent studies of neurogenesis in different Arc/Arg3.1 knockout models provide support for a developmental role of Arc/Arg3.1 protein in the formation of neuronal circuits in the brain (Kuipers et al. 2009, Mikuni et al. 2013). These studies raise awareness towards an involvement of Arc/Arg3.1 protein in brain development. A third aim of this study is to address this possibility by investigating synaptic plasticity in conditional Arc/Arg3.1 KO mice in which Arc/Arg3.1 was removed only postnatally.

To address these questions, LTP experiments were conducted *in vitro* from freshly obtained acute brain slices. Extracellular field recordings were conducted at CA1-CA3 synapses of hippocampal slices and monitored for several hours. The first set of LTP experiments examined the effects of stimulation intensities on the maintenance and duration of LTP in conventional WT mice. The second set of experiments compared LTP in heterozygous and homozygous Arc/Arg3.1 KO mice and their WT littermates. The third set of experiments, investigated LTP in the conditional Arc/Arg3.1 KO mice. Analyses of baseline synaptic transmission, connectivity strength, short-term modulation and LTP were performed for all experiments.

2 INTRODUCTION

The ability to learn and form memories is a fundamental characteristic of our brain and has been the focus of scientific research for many decades. Encoding, storing and retrieval of information rely on neural activity and synaptic plasticity within complex neural circuits. To receive information from the environments, our brain has to register external events via sensory organs and be able to convert these into a specific pattern of chemical or electrical stimuli. In this way, the perceived information is encoded in designated populations of neurons and can be stored in different regions of the brain, e.g. the hippocampus. The process by which sensory and short-term memory is converted into long-term memory is termed consolidation and allows the voluntary retrieval of memories. At each level of these processes, memory formation can be modified according to stimulation paradigms and filtered on the essentials. To handle the great amount of changes in the environment and avoid an overload of information, our brain sustains an equilibrium of memory formation and disruption which is mediated by synaptic plasticity. Synaptic plasticity is realized by rapidly adjusting the strength of synapses to alter neuronal output in response to similar input. It thereby ensures flexible changes in neuronal pathways throughout life.

Disturbances in neuronal activity or synaptic plasticity may lead to memory impairment. Normal memory loss occurs during aging (Davis et al. 2003, Rex et al. 2005) but is more pronounced in short- and long-term neurological disorders such as Alzheimer's disease (Shankar et al. 2008) or Epilepsy (Messas et al. 2008). Alzheimer's disease is characterized by the loss of short- and long-term memory and cognitive function which leads to severe impairment in social life. The current therapeutic options are limited and cannot adequately delay the disease's progression of the illness. Regarding semantic memorial impairment in the context of epilepsy, a range of effective therapies are available which for the most cases, control the episodic seizures. Epileptic seizures are known to result from abnormal cortical activity, but the triggering factors are yet unknown. At the present, neither of these diseases can be cured and leave many questions unanswered. The key challenge is to gain a better understanding of how altered neuronal activity shapes neural networks and thereby influences an individual's behavior. New methods and techniques enable the generation of unique animal models and their testing in behavioral or electrophysiological experiments, such as measurements of long-term potentiation (LTP), to gain new insights into the cellular and molecular mechanisms of memory formation.

2.1 Classification of memory

Brain lesion studies provided the first indication of distinct types of memory and suggested the hippocampus as a central structure required for memory formation (Scoville and Milner 1957). The most famous observation in these lesion studies was performed on the patient H.M. Because of his persistent epilepsy, the bilateral medial temporal-lobes including the major portion of the hippocampus were resected. This treatment reduced periodic seizures, but also induced a memory disorder. Patient H.M. developed a retrograde amnesia and severe deficits in long-term memory formation of novel experiences, whereas short-term and prior consolidated memories were unaffected. These observations provided a basis for an elaborated classification of memory depending on the content and the duration of memory and on the brain regions involved in its storage and retrieval. Short-term memory, i.e. working memory, is defined as the ability to store a small amount of information for a time period of minutes while long-term memory represents the final stage of memory formation which can store information over a longer period of days and weeks. Long-term memory can be further divided into explicit (declarative) and implicit (non-declarative) memory. Explicit memory, further subdivided into episodic and semantic memory, summarizes the factual knowledge and everyday events and is embedded in neocortical-hippocampal pathways which enable access to our consciousness (Eichenbaum 2000). Implicit memory ascribes motor and perceptual skills that are mediated by subcortical circuits in an unconscious manner. This type of memory is typically acquired by repetitive behaviors and practice, i.e. sensitization, classical conditioning or habituation.

2.2 The Hippocampus

The hippocampus is the most widely investigated region for learning and memory formation. Development of microelectrodes enabled extracellular recordings of the neuronal activity in the hippocampus *in vitro*. It was found that hippocampal neurons are very sensitive to artificially delivered stimulation and the degree to which they respond correlates with the cell discharge measured in field excitatory postsynaptic potential amplitude (fEPSP-A). The large field EPSP slopes recorded in the hippocampus resulted from favorable distribution of excitatory and inhibitory cell types, a synchronous activation of stimulated fibers and from cytoarchitectonic organization in the hippocampus.

2.2.1 Structure

As part of the limbic system, the hippocampus is located in the medial temporal lobe of the telencephalon and is anatomically subdivided in dentate gyrus (DG), Ammon's horn (CA1-4, only CA1 and CA3 are functional areas) and the subiculum. Collectively, these areas are known as the hippocampal formation and presented in a schematic transverse section as

showed in Figure 1. The different types of cells in these regions are organized in a three-layer architecture and can be differentiated by histological staining. In the hippocampus proper (CA1-4), cell bodies of pyramidal neurons are mostly embedded in the middle layer, stratum pyramidale, while their apical dendritic trees are mostly located in the distal part of the stratum radiatum. Superficially, the basal dendrites are positioned in a mostly cell-free layer that is called stratum oriens.

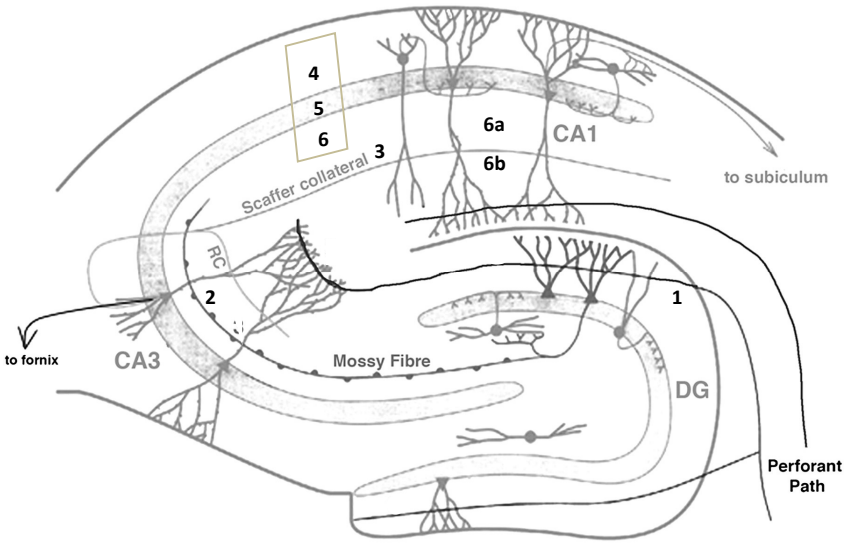

Figure 1: Schematic representation of the trisynaptic circuit in the hippocampus (Daumas et al. 2009). The principal input is carried by the fibers of the perforant pathway from the entorhinal cortex to the granule cells of the DG (1), whose axons (mossy fibers) project to pyramidal cells of CA3 (2). The fibers of CA3 synapses are projected in turn to CA1 area via the Schaffer collaterals (3) and leave the hippocampus by passing the subiculum. Stratum oriens (4), Stratum pyramidale (5) and stratum radiatum (6) incorporate the three laminar architecture of the CA1 area in the hippocampus. Additionally the proximal (6a) and the distal (6b) part of the stratum radiatum was marked to outline the heterogeneous distribution of dendrites.

The hippocampus is characterized as a trisynaptic circuit (David 1993). The main afferent input of the perforant pathway arises from the entorhinal cortex and projects to the dendrites of granule cells in the dentate gyrus. Subsequently, the axons of the granule cells termed mossy fibers reach for the apical dendrites of CA3 pyramidal cells whose fibers form the Schaffer collateral pathway. In turn, Schaffer collaterals project to the ipsilateral CA1 pyramidal cells, and to contralateral CA1 connections through commissural pathway. Hippocampal output mainly leaves by CA1 pyramidal cell axons which pass through the subiculum and project to the entorhinal cortex and to brain regions, e.g. the thalamus and the cortex.

2.2.2 Synapses in CA1 area

The principal cells in the CA1 area of the hippocampus are the pyramidal neurons. They transmit excitatory action potentials via glutamate neurotransmitters and represent the most abundant cell type in the CA1-4 area. Calculations of total number of synaptic input estimated that a single CA1 pyramidal cell has excitatory synapses in the order of 30 x 10^3 while the inhibitory input on this cell remains low at the approximately 1,7 x 10^3 (Megías et al. 2001). Furthermore, Megías and colleagues displayed a heterogeneous distribution of CA1 pyramidal cell dendrites and spines across lamina. Specifically the distal part of the stratum radiatum was reported to contain a high density of dendrites and to receive there the majority of excitatory CA3 input while inhibitory input was very low (Megías et al. 2001). In contrast, inhibitory GABAergic interneurons, the second type of cells in the CA1 area, are considerable less abundant and spread in all laminar layers. These GABAergic interneurons are heterogeneous in cell type, dendrites and function. Inhibitory synapses are rarely found in the distal part of the stratum radiatum and thus produce less $GABA_A$ tonic inhibition. For the above mentioned reasons the stratum radiatum represents a favorable area for LTP experiments and was chosen in this current study.

2.2.3 Principal receptors and synaptic function in the CA1 area

Glutamate is the most important excitatory neurotransmitter in the hippocampus and acts on several types of postsynaptic receptors. Besides other receptors, ionotropic receptors such as AMPA receptors (α-amino-3-hydroxy-5-methyl-4-isoxazolepropionic acid) and NMDA receptors (N-methyl-D-aspartate) are the principal mediators of synaptic plasticity. AMPA receptors are located at nearly all excitatory CA1/2 synapses and consist of different tetrameters of GluR1-4 subunits, preferably of GluR1 and GluR2 or GluR2 and GluR3 subunits (Wenthold et al. 1996). The distinct receptor complexes, especially the GluR2 units, are assumed to have a regulatory function on the receptor expression and thus determine the cell response to glutamate release (Sans et al. 2003). Once glutamate is released from the presynaptic site, it binds to the AMPA receptors and activates them. Following activation, the receptors are permeable for the monovalent ions Na^+ and K^+ for a few milliseconds.
NMDARs are mainly expressed at the postsynaptic density (PSD) of excitatory glutamate synapses and co-localized with AMPARs. In the CA1 pyramidal cells high levels of heteromultimeric assemblies consisting of NR1, NR2A and NR2B subunits were identified (Monyer et al. 1994). The functional properties of the diverse NMDAR subunit composition are assumed to play an important role in postnatal synaptogenesis and in synaptic plasticity (Constantine-Paton and Cline 1998). NMDA receptors contribute little to the initial negative resting membrane potential, but can be activated under two conditions: presynaptic firing and postsynaptic depolarization. Thereafter, the voltage-dependent Mg^{2+} block is released and enables large postsynaptic Ca^{2+} influx which increases cell potentiation. The discovery of these special features of NMDA receptors are assumed to be the cellular key role in

bidirectional synaptic plasticity, learning and memory formation and studied by a large group of scientists (Collingridge and Bliss 1987, Lisman 1989, Tsien et al. 1996, Nicoll and Malenka 1999).
Additionally, evidence demonstrated the existence of distinct ionotropic, heteropentameric $GABA_A$ receptors and diverse subtypes of metabotropic heterodimer $GABA_B$ receptors at the pre- and postsynaptic site of CA1 interneurons (Pozza et al. 1999, Mody and Pearce 2004). $GABA_B$ receptors can hyperpolarize the postsynaptic membrane by the influx of Cl^- and HCO_3^- ions and generate inhibitory postsynaptic potentials (IPSPs) which tighten the Mg^{2+} block of the NMDARs and curtail fEPSP slopes on excitatory synapses. Notably in a sequence of action potentials (AP), the presynaptic $GABA_B$ autoreceptors decrease IPSPs by temporary reduced presynaptic GABA release (Davies et al. 1991). This effect is used to impair tonic GABA inhibition and is favorable for the summation of fEPSP slopes in LTP experiments. Although important for encoding, their impact on CA3-CA1 plasticity is relatively low and they have not been dealt with in my thesis.

2.3 Long-term potentiation

"Long-term potentiation of synaptic transmission in the hippocampus is the primary experimental model for investigating the synaptic basis of learning and memory in vertebrates" (Bliss and Collingridge 1993). The idea that the mechanisms of memory formation are associated with cellular changes in synaptic strength emerged first by the work of Ramón y Cajal (Ramón y Cajal 1894). In 1948 the scientists Hebb and Konorski refined these ideas and proposed a synaptic model in which neurons strengthen their connections to enhance synaptic efficacy in response to neuronal activity: "*When an axon of cell A is near enough to excite a cell B and repeatedly or persistently takes part in firing it, some growth process or metabolic change takes place in one or both cells such that A's efficiency, as one of the cells firing B, is increased.*" (Konorski 1948, Hebb 1949). Some years later, the evidence of Hebbian plasticity was obtained *in vivo* and *in vitro* from animal experiments describing the first characters of long-lasting cell responses in the hippocampus (Bliss and Lømo 1973, Bliss and Gardner-Medwin 1973), and was coined the term "long-term potentiation" (Douglas and Goddard 1975). Particularly because of its persistence and its features, LTP attracted much interest and has been the candidate of research in a considerable number of studies.

2.3.1 Properties of LTP

Three basic properties were found to characterize LTP: cooperativity, associativity and input specificity. The features of cooperativity and associativity were demonstrated in the work of McNaughton and colleagues (McNaughton et al. 1978). The observation that weak stimulation which activates a small number of afferent fibers, cannot induce LTP in contrast

to strong stimulation suggests a threshold of co-activated fibers for LTP induction. However, when a weak stimulation is paired simultaneously with a strong tetanus to another but still convergent pathway, LTP can be produced due to the associative effect of stimulated fibers. Finally, LTP is input specific which describes the restrictive effect of delivered stimuli to the stimulated neuronal population without affecting adjacent pathways (Anderson et al. 1977). These characteristics of LTP can be explained through the activation of NMDA receptors, that are considered to be the molecular main mechanism of long-term potentiation in the hippocampus (Bliss and Collingridge 1993).

2.3.2 LTP induction

LTP is expressed as increased synaptic strength in response to electrical stimulation and can be characterized by its duration, magnitude and underlying molecular mechanisms. Early LTP (e-LTP) is characterized as a transient (1-3 hours) and protein synthesis independent form of LTP which can be converted into late LTP (l-LTP) when stimulation strength is sufficient (Huang and Kandel 1994). This following phase, the late LTP, develops slowly over a period of hours and requires *de novo* protein synthesis, activation of PKA and alterations in synaptic structure for its maintenance (Huang and Kandel 1994, Abraham and Williams 2003).

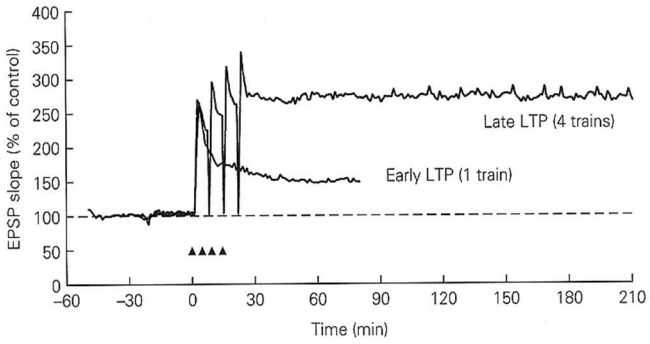

Figure 2: Early and late phase of LTP in the Schaffer collaterals (Kandel 2001). One train of HFS elicited early LTP for 2 hours while four trains of HFS evoked late LTP which lasts for more than 24 hours.

After the original description of LTP in the DG of the hippocampus (Bliss and Gardner-Medwin 1973), it was soon observed that specific patterns of repetitive stimulation protocols induce distinct components of LTP which are historically defined as early and late LTP. The most commonly used stimulation protocols in the CA1 region is high-frequency stimulation (HFS) also termed tetanic stimulation and is shown in Figure 2. This stimulation consists of a single train of 100 stimuli in one second (HFS at 100 Hz) and often generates only e-LTP. Multiple HFS trains applied at intervals in the range of seconds to minutes induce

large and long-lasting LTP (Frey et al. 1993, Huang and Kandel 1994, Nguyen and Kandel 1996, Kandel 2001, Park et al. 2014). In an attempt to mimic the most physiologically occurring firing patterns of hippocampal neurons (Larson et al. 1986) and to increase LTP induction reliability, a more complex stimulation protocol was designed and termed theta burst stimulation (TBS). There, LTP is typically induced by 10 bursts, each containing 4-5 stimuli at the rate of 200 Hz with inter-burst interval of 200msc (theta: 5Hz). Additional variations of TBS were also reported and investigated (Abraham and Huggett 1997, Nguyen and Kandel 1997, Kramer et al. 2004). Like HFS, the number of TBS trains regulate the duration of LTP maintenance. In contrast, other studies demonstrated conflicting results to these observations. The authors Bortolotto and Collingridge have shown that a single train of HFS was able to induce stable LTP for 5 hours in CA1 synapses (Bortolotto and Collingridge 2000). Furthermore, the latter also displayed that this stable form of LTP was resistant to potent PKA and PKC protein inhibitors indicating a possible different molecular pathway for l-LTP induction or simply, a protein synthesis independent form of LTP. Recent evidence of a protein synthesis independent form of lasting LTP, was demonstrated by Abbas and colleagues (Abbas et al. 2009) just as Villers and colleagues (Villers et al. 2012). However, it cannot be excluded that this form of LTP resulted from unspecific action of protein inhibitors which might have an inducible effect on LTP or equally possible, or from different protein kinases, like isoforms of PKA or PKC which were not blocked by the applied inhibitors (Brandon et al. 1997, Mellor and Parker 1998, Panja and Bramham 2013). Other reports focused investigations on temporal spacing in stimulation protocols and revealed the inter-tetanus interval as the decisive parameter determining induction of protein synthesis dependent or independent LTP, while the number of delivered stimuli was less crucial (Scharf et al. 2002, Woo at al. 2003). Park and colleagues elicited distinct long-lasting forms of LTP in response to single, compressed (3 HFS, 3-20 sec inter-burst interval) and spaced HFS trains (3 HFS, 5-10 min inter-burst interval) and examined these forms of LTP based on differences of mechanistic features (Park et al. 2014). Interestingly, 1 HFS- and compressed HFS-LTP were resistant to protein synthesis and PKA inhibitors while spaced HFS stimulation induced l-LTP was sensitive to these blockers. These findings proposed a co-existence of mechanistically distinguishable forms of LTP which could be recruited in response to different temporal stimulation protocols.

On a cellular level, LTP can also be induced by a signaling protein of the neurotrophin family, the brain-derived neurotrophic factor (BDNF) which is widely acknowledged as activity-dependent regulator of l-LTP at excitatory glutamatergic synapses in developing and adult synaptic plasticity (Lo 1995). In BDNF perfusion experiments in CA1 region and medial perforant pathway of hippocampal DG, BDNF-LTP was associated with slow and sustained increase of stable fEPSP slopes over a period of several hours (Kang and Schuman 1995, Messaoudi et al. 1998).

2.3.3 Cellular mechanisms during different phases of LTP

CA1 hippocampal synapses have been widely used as a major model to understand cellular signaling pathways in basal synaptic transmission and synaptic plasticity. These synapses are glutamatergic, highly plastic and can be structurally modulated. Conceptually, establishment of each phase, e-LTP and l-LTP, implicates the same initial cellular events while expression of e-LTP or l-LTP requires different mechanisms over a given time period.

LTP induction mechanisms

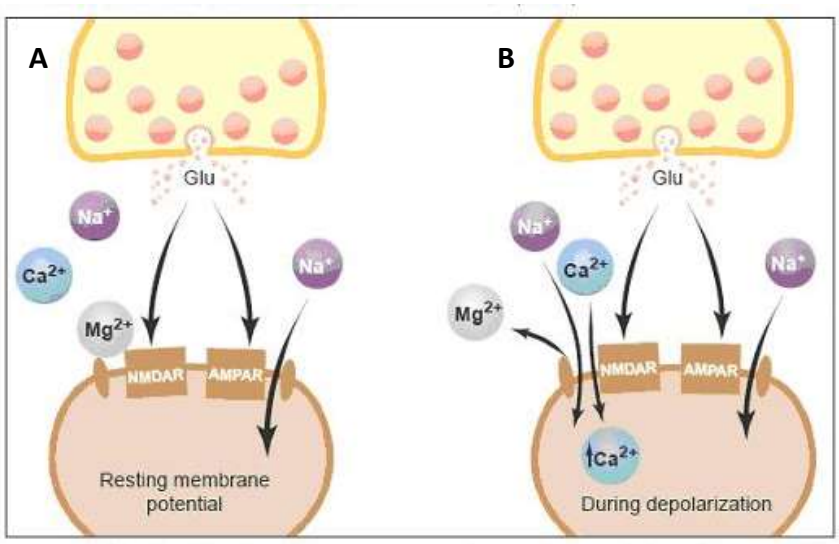

Figure 3: Model for cellular induction mechanisms of LTP (Malenka and Nicoll 1999). Glutamate release from the presynaptic bouton and its function on AMPA and NMDA receptors. **A** After release, glutamate binds to both AMPA and NMDA receptors. Only AMPA receptors permit Na^+ flow while NMDA receptors remain blocked by Mg^{2+} at resting membrane potential. **B** Sufficient depolarization of the postsynaptic membrane evoked by precedent stimulation relieves the Mg $^{2+}$ block and permits the additional Ca^{2+} flow through the NMDA receptors.

Electrical baseline stimulation at the presynaptic terminals leads to depolarization of the presynaptic membrane and to Ca^{2+} influx via voltage-gated Ca^{2+} channels. The increased intracellular Ca^{2+} concentration initiates vesicle fusion and release of neurotransmitters into the synaptic cleft. The neurotransmitters, in turn, initially act on AMPA receptors and cause postsynaptic depolarization by Na^+ and K^+ influx (Figure 3A). During the induction of LTP, depolarization and glutamate receptor binding are sufficient to relieve the Mg^{2+}-block from NMDA receptors, and lead to strong increase of intracellular Ca^{2+} in dendritic spines (Figure 3B, Larsen and Lynch 1988, Bliss and Collingridge 1993, Tsien et al. 1996, Malenka and Nicoll 1999). Additional to NMDA receptor mediated calcium influx, voltage-gated calcium channels and release of calcium from intracellular sources contribute to the postsynaptic

calcium elevation (Roberson et al. 1996). The transient rise of local Ca^{2+} concentration is considered as the major trigger for LTP induction and can directly promote protein synthesis which set in motion long-lasting changes at synapses to sustain LTP potentiation in each phase (Malenka and Nicoll 1999).

Early LTP expression

Following LTP induction, early LTP is initiated and is demonstrated to last over 1-3 hours until the late phase of LTP take over (Kandel and Huang 1994). During this initial phase, the calcium signal modulates a wide range of existing proteins, e.g. protein kinases, but only some of these were identified to play a key role during LTP. When activated, several protein kinases acquire a novel state of autonomous activation and remain activated over a transient period of time. In this context, protein kinases can act independently of the calcium or second messenger signal and maintain transient synaptic potentiation. For example, calcium/calmodulin protein kinase II (CaMKII) was assessed as an essential protein in e-LTP induction and expression. The protein kinase was found in constant high concentrations at stimulated dendritic synapses, in co-localization with glutamate receptors in the PSD (Otmakhov et al. 2004). CaMKII binds to NR2B subunit of NMDA receptors and possess the ability of autophosphorylation on Thr^{286}. Both processes support the prolonged activation of CaMKII and are independent of the presence of calmodulin and Ca^{2+} ions (Giese et al. 1998, Lisman et al. 2012). In turn, activated CaMKII phosphorylates directly Glu1 subunit of AMPA receptors and thus enhance their channel conductance during LTP (Barria et al. 1997). Moreover, activated CaMKII was also associated with AMPA receptor recruitment in silent synapses (Song and Huganir 2002). Similarly, the activation of protein kinase C (PKC) is induced by second messenger and maintained by autophosphorylation. Elimination of the neuron-specific isoform PKCγ in knockout mice demonstrated deficits in HFS-LTP while synaptic response to low-frequency stimulation was unaffected (Abeliovich et al. 1993). Although protein kinase A (PKA) was generally assessed as a protein kinase in l-LTP, some reports have described a role for PKA in e-LTP induction and AMPA receptor trafficking which represents a distinct mechanisms to contribute to synaptic plasticity. Blitzer and colleagues suggested that PKA might inhibit phosphatase activity and thus promote the function of CaMKII, PKC and other kinases (Blitzer et al. 1995). Studies of AMPA receptor trafficking revealed a regulatory role in which PKA and CaMKII might control the incorporation of AMPA receptors in the postsynaptic membrane (Esteban et al. 2003). Among the family of protein tyrosine kinase, BDNF and its receptor TrkB has gained the strongest interest among investigators. Since BDNF was found to be stored at glutamatergic synapses and released during strong stimulation patterns (Hartmann et al. 2001), several lines of evidence indicate a pre- and postsynaptic sites of BDNF storage and release (Hartmann et al. 2001, Leßmann and Brigadski 2009). However, the site which is responsible for LTP still needs to be elucidated. Genetical reduction of BDNF or TrkB function in transgenic mice was demonstrated to cause impairment in the early phase of LTP (Korte et al. 1995, Minichiello et al. 2002). Two independent groups investigated BDNF-LTP by

pharmacological blocking of BDNF and TrkB receptor activity, and have found that only TBS-LTP (induced by 1 or 3 trains of TBS) was impaired while HFS-LTP was normal (Kang et al. 1997, Chen et al. 1999). Furthermore, Kang and Schuman demonstrated immediate impairment of fEPSP slopes by inhibition of protein synthesis indicating a protein synthesis dependence of BDNF induced plasticity (Kang and Schuman 1996). These studies shed light on distinct signaling pathways in the early phase of LTP which were shown to depend on different LTP induction methods.

Besides, it is widely debated whether LTP also involves modification of presynaptic changes, in particular the probability of presynaptic transmitter release (Hjelmstad et al. 1997, Schulz et al. 1997). However, when presynaptic changes occurs, they are commonly triggered by the postsynaptic neuron though a retrograde signal. Several candidates for the retrograde signal were proposed, most notably a platelet-activating factor (Kato et al. 1994) and the diffusible nitric oxide (Arancio et al. 1996).

Late LTP expression

Considerably less is known about the cellular mechanisms in the late phase of LTP. Consistent with *in vivo* and *in vitro* studies, l-LTP is the most stable phase in all forms of long-term potentiation and can last several hours to months (Huang and Kandel 1994, Abraham 2002). The cellular hallmarks of l-LTP are *de novo* protein synthesis induced by up-regulated new gene expression and structural strengthening processes in locally stimulated dendritic spines (Nguyen et al. 1994, Martin et al. 2000, Scharf et al. 2002, Abraham and Williams 2003). Signaling cascade from cyclic adenosine monophosphate (cAMP)/PKA to mitogen-activated protein kinase (MAPK) and extracellular signal-regulated kinase (ERK) pathway and others were reported to phosphorylate and to activate the genomic cAMP response element-binding protein (CREB) and thereby increase new gene expression (English and Sweatt 1997, Waltereit and Weller 2003). However, further parallel signaling pathways which link electrical LTP induction to molecular signaling at the nucleus, were described revealing the complexity of individual cellular mechanisms (Pittenger et al. 2002). New gene expression was found to occur at a limited time window directly post LTP induction and to be based on post-translational modification of pre-existing proteins such as the transcription factor CREB (Nguyen et al. 1994). This class of genes was defined as immediate early genes (IEGs) and their increased expression was demonstrated to correlate with LTP induction (Abraham et al. 1991, Abraham et al. 1993). Identified IEGs like fos, jun or zif/268 were reported to contribute to the stabilization of LTP and thereby to regulate their own gene expression or induce other effector molecules which maintain l-LTP. New transcripts were thought to undergo protein synthesis in the soma of synaptic cell bodies or in locally stimulated synaptic dendrites which are equally equipped with ribosomes and translation machinery (Kang and Schuman 1996, Abraham and Williams 2003). Interestingly, Frey and Morris hypothesized that these new mRNAs or new proteins might be captured by a "synaptic tag" and thus be translocated rapidly from the synaptic soma to local potentiated synapses (Frey and Morris 1997). Although this group provided strong evidence and thus

lanced the question how these newly synthesized molecules can be targeted, the character of the "synaptic tag" remains still unknown. It has been well established that morphological growth of synaptic dendrites at which LTP has occurred results from new protein synthesis and are accompanied by long-lasting fEPSP potentiation (Yang et al. 2008). Initial spine changes were thought to be mediated by phosphorylation of existing AMPARs and actin polymerization while further spine plasticity was clearly associated with postsynaptic AMPAR incorporation, enlargement of PSD and generation of new dendritic spines (Yang et al. 2008, Hering and Sheng 2001, Lisman and Zhabotinsky 2001). A key element in all structural changes in dendritic spines is the dynamic reorganization of the actin cytoskeletal structure. The blockage of actin microfilaments polymerization in CA1 synapses was specifically demonstrated to destabilize LTP in the late phase while synaptic transmission and early LTP phase remained intact (Krucker et al. 2000, Fukazawa et al. 2003). Nevertheless, it is still difficult to identify causal roles of specific, synaptic activity-induced proteins in the l-LTP formation. Similarly to e-LTP, distinguishable forms of l-LTP were observed in response to BDNF, TBS and HFS LTP induction in hippocampal CA1 synapses. Typically, HFS-LTP involves transcription processes and new protein synthesis in the cell bodies as well as in locally stimulated dendrites (Nguyen et al. 1994, Frey et al. 1996). In contrast, BDNF- and TBS-LTP are independent of transcription and are restricted to local dendritic protein synthesis without participation of the cell bodies (Kang and Schuman 1996, Huang and Kandel 2005). In terms of synaptic capture, HFS-tetanus could generate a "synaptic tag" and attract new proteins to activated synapses while in TBS-LTP local protein synthesis is sufficient for l-LTP (Huang and Kandel 2005). Another difference in TBS and HFS induced l-LTP was revealed by the investigation of the time window of TrkB receptor activation. In HFS-LTP TrkB receptor activation occurred 30-60 min (not 70-100 min) after LTP induction whereas in TBS-LTP these receptors were activated 1-40 min post-TBS stimulation (Lu et al. 2011, Kang et al. 1997). Taken together these findings, long-term potentiation implies several cellular mechanisms in response to specific stimulation patterns that might have proper roles in the processing of memory formation.

2.4 Arc/Arg3.1 protein function

The IEG that attracted the most interest in molecular memory research is the multi-functional Arc/Arg3.1 gene (Guzowski et al. 2001, Shepherd and Bear 2011). The laboratory of Dietmar Kuhl and Paul Worley identified simultaneously but independently the same IEG mRNA by similar cloning techniques. They named it activity-regulated gene of 3.1 kb transcription length protein (Arg3.1 protein, Link et al. 1995) and activity -regulated cytoskeleton-associated protein (Arc, Lyford et al. 1995) respectively, hereinafter referred to as Arc/Arg3.1 gene/protein. The discovery and the unique correlation of Arc/Arg3.1 gene to neuronal activity provided crucial insights into the mechanisms of memory formation.

2.4.1 Genetic regulation of Arc/Arg3.1 expression

Activity-induced up-regulation of Arc/Arg3.1 expression was found to be localized to the nucleus, soma and dendrites of excitatory neuronal cells (Moga et al. 2004) and particularly enriched at activated synapses (Steward at al. 1998). Arc/Arg3.1 is tightly regulated on a transcriptional as well as on a translational level (Link et al. 1995, Lyford et al. 1995, Waltereit et al. 2001). Nevertheless, the signal transduction cascades which transfer neuronal activity to nucleus signaling has not been sufficiently revealed.

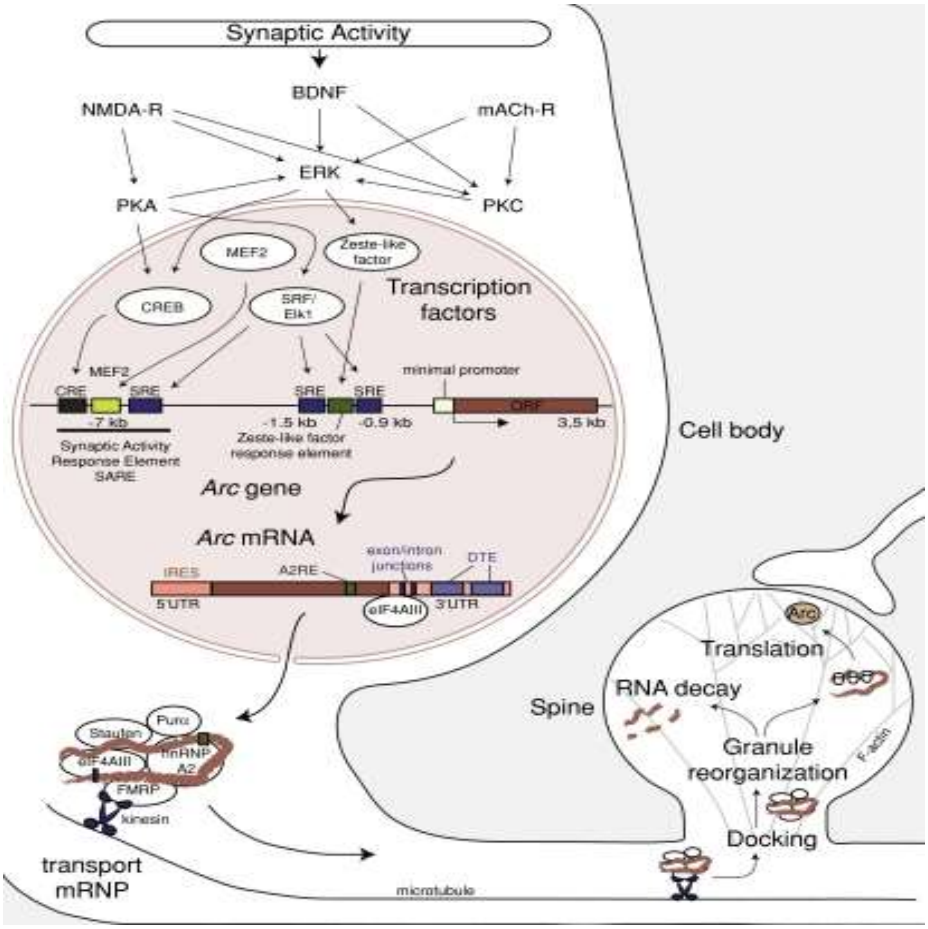

Figure 4: Arc/Arg3.1 gene regulation mechanisms (Bramham et al. 2010). Diverse signal cascades and transcription factors initiating Arc/Arg3.1 gene transcription in response to synaptic activity. Exemplary pathway via NMDA receptor-PKA, CREB binds to SRE located in the SARE promoter region of Arc/Arg3.1 gene and initiates Arc/Arg3.1 mRNA transcription. After its export of the nucleus, Arc/Arg3.1 mRNA interacts with transport proteins in order to reach recently activated synapses. In dendritic spines, Arc/Arg3.1 mRNA is subjected respectively to protein translation or non-sense mediated RNA decay.

Activity-dependent changes of Arc/Arg3.1 gene regulation are proposed preponderantly to be mediated by NMDA receptor activation, cAMP/PKA and MAPK/ERK signaling pathway which interacts with CREB (Steward and Worley 2001, Waltereit et al. 2001, Bramham et al.

2010). As demonstrated in Figure 4 the activated transcription factors, CREB and others, bind to specific sites in the Arc/Arg3.1 promoter region such as the serum response element (SRE) and thus enhance Arc/Arg3.1 transcription (Kawashima et al. 2009). The transcription-binding site termed as synaptic-activity responsive element (SARE) located at 7 kb upstream of Arc/Arg3.1 transcription initiation site was identified to be sufficient to induce rapid activity-induced Arc/Arg3.1 expression (Bramham et al. 2010). Interestingly, Arc/Arg3.1 transcription is also regulated by negative feedback mechanisms of activated AMPA receptors and appear to be temporally restricted during LTP (Rao et al. 2006). Consistently, work of Guzowski and colleagues have demonstrated that Arc/Arg3.1 mRNA accumulates rapidly in the nucleus post stimulation before it is transported by kinesin motor complex to the cytoplasm in the subsequent 30 minutes (Figure 4, Guzowski et al. 1999, Kanai et al. 2004). After one hour, Arc/Arg3.1 mRNA is actively transported from the cytoplasm to stimulated dendrites where it undergoes local protein synthesis (Kuhl and Skehel 1998). Recent publication from Huang and coworkers demonstrated that the distribution of somatic Arc/Arg3.1 mRNA to activated synapses requires synaptic-specific modification (Huang et al. 2007). Furthermore, these data suggested that locally targeting of Arc/Arg3.1 mRNA to specific synapses results from the combination of F-actin and ERK activation, as F-actin polymerization alone is not sufficient to capture these mRNA (Huang et al. 2007). In addition, identified Rho kinase protein was shown to play an important role in Arc/Arg3.1 mRNA targeting and F-actin polymerization (Huang et al. 2007).

As transcription, translation of Arc/Arg3.1 mRNA seems to be tightly regulated. The translation factor eukaryotic initiation factor 2α (eIF2α) and eIF4E, both part of a protein assembly of the initiation complex, were reported to be involved in Arc/Arg3.1 protein translation. Evidence showed that eIF4E activity, regulated via G_s-coupled receptor/PKA and NMDA receptor mediated MAPK/ERK/MAP kinase integrating kinase-1 (MNK1) pathway, correlates with the time course of Arc/Arg3.1 protein synthesis (Messaoudi et al. 2007, Bloomer et al. 2008, Panja et al. 2009). This represents a possible linkage between translation initiation and LTP consolidation. Genetic modification of eIF2α induced severe impairment of l-LTP and learning abilities in *in vitro* and *in vivo* experiments pointing to a critical role of intact translation machinery in LTP consolidation (Costa-Mattioli et al. 2009). Directly after transcription the amount of Arc/Arg3.1 protein synthesis appears to be regulated by translation-dependent non-sense mediated RNA decay (NMD) which is generally considered as a quality control supervision of abundant mRNA clearance (Peebles and Finkbeiner 2007, Bramham et al. 2010). Due to the integration of specific gene sequence within its stop codon, Arc/Arg3.1 mRNA is a natural target of NMD and can be down-regulated and limited in its protein expression (Bramham et al. 2010). The rapid elimination of Arc/Arg3.1 mRNA could be reconciled with the finding that the LTP consolidation requires a sustained time-dependent window of Arc/Arg3.1 protein synthesis.

Notably rapid turnover of proteins in dendrites seem to be subject to active cytoplasmic protein degradation and required for LTP (Karpova et al. 2006). Arc/Arg3.1 protein expression was shown to be a targeted towards proteasome by a binding site for ubiquitin-

protein ligase E3A (UBE3A) and by a specific gene sequence termed PEST (riche in proline (P), glutamate (E), serine (S) and threonine (T)) sequence (Rao et al. 2006, Geer at el. 2010). Both mechanisms control the amount of newly synthesized Arc/Arg3.1 protein and as such provide a way by which Arc/Arg3.1 protein can be returned to basal levels after stimulation.

2.4.2 Arc/Arg3.1 protein in synaptic plasticity

Most importantly, Arc/Arg3.1 gene plays an essential role in learning and memory formation just as in different forms of synaptic plasticity and homeostatic plasticity. Multiple evidence obtained from *in vitro* and *in vivo* experiments have shown that sufficient Arc/Arg3.1 protein is essentially required in the consolidation processes of hippocampal long-term potentiation. Its abnormal expression may contribute to cognitive illnesses (Guzowski et al. 2000, Plath et al. 2006, Messaoudi et al. 2007, Palop et al. 2007).

Intrahippocampal infusion of antisense (AS) oligodeoxynucleotides (ODN) in *in vivo* experiments have been used to inhibit specific synthesis of new proteins and thereby elucidate their role in signaling pathways as well as in behavioral patterns. Using these techniques, inhibition of Arc/Arg3.1 protein expression in awake animals resulted in severe impairment of monitored long-lasting fEPSP potentiation post HFS-LTP induction and also prevented long-term memory formation in these during the behavioral tasks (Guzowski et al. 2000). Here, neither the induction of recorded LTP nor the short-term memory in spatial training tasks was affected by Arc/Arg3.1 inhibition. Referring to these results Arc/Arg3.1 protein plays a major role in maintenance of long-term potentiation and seem to be less important for LTP induction and e-LTP mechanisms. However, a contribution of early Arc/Arg3.1 protein synthesis to the early phase of LTP cannot be excluded (Messaoudi et al. 2007).

The group of Dietmar Kuhl investigated the impacts of Arc/Arg3.1 gene deletion in a conventional knockout mouse model, termed Arc/Arg3.1 KO mice (Plath et al. 2006). The animals were tested in several behavioral tests, e.g. spatial learning strategies, fear conditioning, conditioned taste aversion and object recognition that include hippocampal dependent and hippocampal independent forms of memory as well as implicit and explicit memory. Consistently, memory consolidation failed in all behavioral tests whereas short-term memory formation seemed to be normal. For example in the novel object recognition task, mice were exposed to two familiar objects during training and to an additional novel object during a memory test. Exploration preference of the novel object was used as a proxy of the memory. Conventional WT and KO mice showed both increased exploring time for the novel object after 10 min, while after 24 hours only WT mice explored the novel objects. This test presented that KO mice possess intact short-term memory after 10 min but cannot consolidate newly learned contents into a long-lasting memory. The observed failure in long-term memory was shown to correlate with similar results in the study of extracellular fEPSP recordings (Guzowski et al. 2000, Plath et al. 2006). In hippocampal DG *in vivo* and in CA1 region *in vitro*, conventional Arc/Arg3.1 KO mice generated immediately an increased in

fEPSP slope post HFS stimulation (Plath et al. 2006). The potentiated synapses from these KO mice largely exceeded the magnitude of fEPSP slope of WT mice and declined to baseline levels within 90 min of recording time. Aside from alterations in e-LTP and l-LTP, Arc/Arg3.1 protein deletion did not affect basal synaptic transmission or synaptic structure (Plath et al. 2006).

In terms of bidirectional plasticity, Arc/Arg3.1 protein was also assessed to regulate long-term synaptic depression (LTD). In hippocampal CA1 region, LTD was demonstrated to be mediated by NMDA receptors and group 1 metabotropic glutamate receptors (mGluRs), and both associated with increased levels of Arc/Arg3.1 protein expression in dendritic synapses (Plath et al. 2006, Waung et al. 2008). Deletion of Arc/Arg3.1 protein in conventional KO mice showed smaller and faster decaying fEPSP slopes in response to low frequency stimulation compared to control mice and leaded to impaired NMDA-LTD (Plath et al. 2006). Likewise mGLuR mediated LTD was shown to be blocked by specific Arc/Arg3.1 protein AS ODNs (Waung et al. 2008).

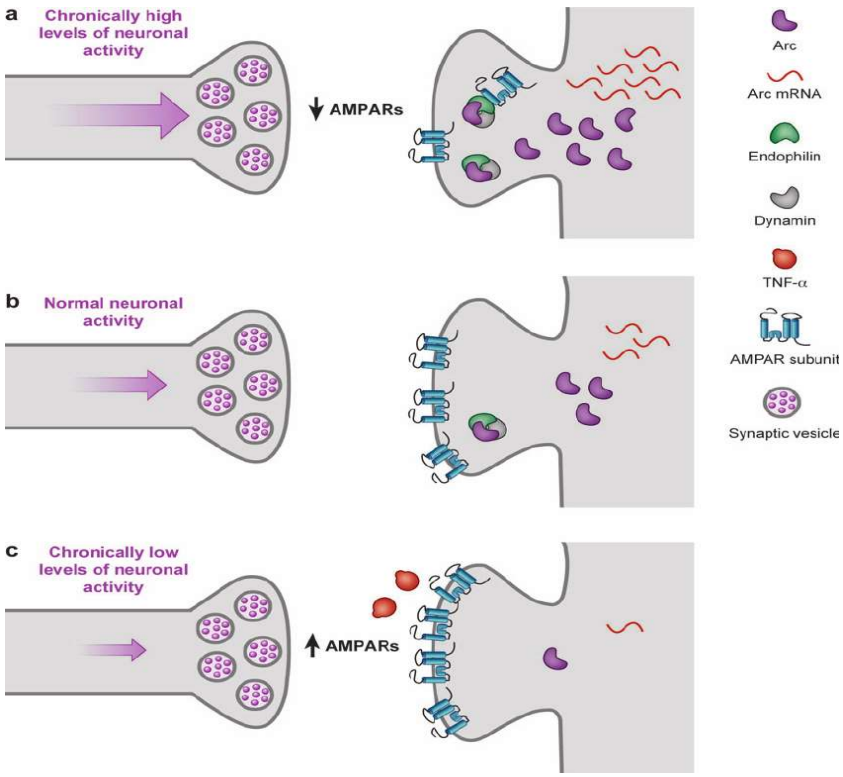

Figure 5: Arc/Arg3.1 protein function in bidirectional synaptic plasticity (Shepherd and Huganir 2007). Distinct distribution of surface AMPA receptors and Arc/Arg3.1-endophilin-dynamin interaction in response to high and low neuronal activity. The upper part of the picture (a) shows the reduced amount of postsynaptic AMPA receptors and increased Arc/Arg3.1 mRNA and Arc/Arg3.1 protein after constant strong stimulation. The complex of Arc/Arg3.1-endophilin-dynamin leads to internalization of AMPA receptors from the postsynaptic membrane. The lower part of the picture (c) depicts the lack of Arc/Arg3.1-endophilin-dynamin complex in association with an increased amount of AMPA receptors after chronically low stimulation. Fittingly Arc/Arg3.1 mRNA and protein is reduced here.

In the model of bidirectional synaptic plasticity LTP and LTD were shown to reinforce themselves by increasing or decreasing of their synaptic strength. To prevent extreme synaptic unbalance and avoid synaptic network saturation, Hebbian synaptic plasticity is thought to be compensated by homeostatic scaling (Shepherd et al. 2006). Following long-term increase or decrease in synaptic strength, neurons might regulate their synaptic weight by respectively down- or up-regulation of the output-firing rate and thus maintain the same average of neuronal output activity and strength. On a cellular level, the average firing rate was suggested to be regulated via the amount of AMPA receptors expressed on the postsynaptic surface which in turn is tightly regulated by components of the endocytic machinery and Arc/Arg3.1 protein expression (Chowdhury et al. 2006, Shepherd et al. 2006). As shown in Figure 5, high levels of activity induced Arc/Arg3.1 protein block homeostatic up-regulation of surface AMPA receptors and reduce the amount of these postsynaptic receptors. AMPA receptor endocytosis is thought to be mediated by an interaction of postsynaptic enhanced Arc/Arg3.1 protein with proteins of endocytic machinery such as dynamin and endophilin (Shepherd and Huganir 2007). The loss of Arg.3.1 protein in Arc/Arg3.1 deficient mice or low neuronal activity had an opposite effect and diminished endocytosis which raises the number of AMPA receptors on the postsynaptic membrane (Shepherd et al. 2006). However, it is not known yet how Arc/Arg3.1 protein controls the detailed changes in cell weight in response to LTP and LTD.

Based on abnormal Arc/Arg3.1 protein expression, previous work also proposed a contribution of Arc/Arg3.1 protein in cognitive and neuropsychiatric diseases. For example, in a mouse model of Alzheimer's disease, the Alzheimer's related human amyloid precursor protein (hAPP) derived amyloid β peptide was correlated with decreased Arg3.1 protein expression and leaded to hyperexcitability and seizure tendencies (Palop et al. 2007). Other KO mice with generated neuronal diseases such as the fragile X syndrome, the most common inherited cause of mental retardation and autisms (Park et al. 2008), or the Angelman Syndrome, a neurodevelopmental disorder (Geer et al. 2010) were presented to involve dysfunction of Arc/Arg3.1 dependent cellular mechanisms of respectively Arc/Arg3.1 mRNA translation and Arc/Arg3.1 protein degradation mechanisms. Nevertheless, the diseases are not directly referred to Arc/Arg3.1 gene mutations in knockout mice but involve altered Arc/Arg3.1 protein pathways, which entails pathological Arc/Arg3.1 expression.

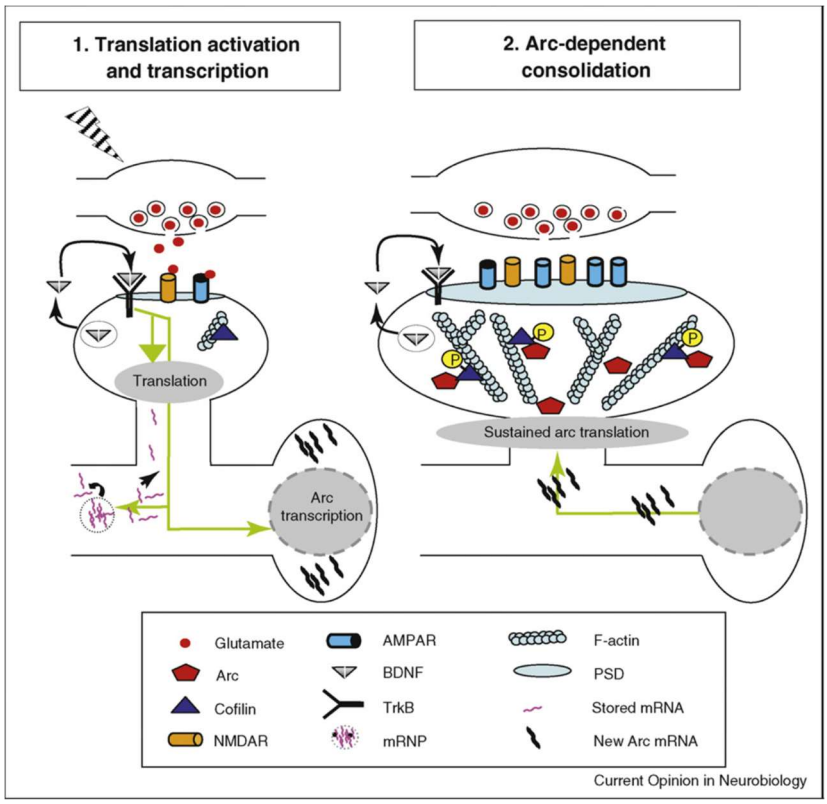

Figure 6: Arc/Arg3.1 dependent LTP consolidation (Bramham 2008, Figure adapted from Bramham and Wells 2007). Arc/Arg3.1 protein dependent structural changes in dendritic spines in response to synaptic activity. After activity induced activation of Arc/Arg3.1 translation and transcription, Arc/Arg3.1 mRNA is transported to stimulated dendrites and locally accumulated. The persistent transport of Arc/Arg3.1 mRNA is required for cofilin phosphorylation and formation of new F-actin microfilaments and leads to Arc/Arg3.1 dependent consolidation.

In terms of structural plasticity, activity induced Arc/Arg3.1 protein was originally discovered in co-localization with F actin microfilaments at potentiated dendritic spines and have lanced the interest of a function in synaptic remodeling processes (Lyford et al. 1995). Evidence from immunostaining and microscope imaging pointed to an Arc/Arg3.1 protein dependent increase in spine density which regulates dynamic spine morphology and thus stabilizes synaptic network in l-LTP (Peebles et al. 2010). In this work Arc/Arg3.1 protein was reported to increase specifically the thin portion of dendritic spines which were described as plastic and learning spines while other types of more stable spines decreased in their size. In agreement with these findings, neurons overexpressing Arc/Arg3.1 protein showed significant increase in spine density whereas the absence of Arc/Arg3.1 protein expression in KO mice leaded to decreased spine density (Peebles et al. 2010). Figure 6 represents structural changes in dendritic spines which require not only polymerization of new F-actin microfilament and phosphorylated cofilin but also involvement of Arc/Arg3.1 protein. In the study of Messaoudi and colleagues, LTP was reversed by Arc/Arg3.1 antisense infusion 2 hours post LTP induction and was reported to be accompanied by rapid down-regulation of

up-regulated Arc/Arg3.1 protein, dephosphorylation of hyperphosphorylated cofilin and disruption of F-actin microfilaments (Messaoudi et al. 2007). The reversibility of LTP was shown to be blocked by jasplakinolide, a F-actin stabilizing drug and thus provide strong suggestion of a linkage between Arc/Arg3.1 protein pathway and F-actin expansion. The Arc/Arg3.1 protein pathway might be reduced to constant cofilin phosphorylation during l-LTP which is maintained by late Arc/Arg3.1 protein synthesis (Messaoudi et al. 2007). Although the signaling cascades are not known by which Arc/Arg3.1 protein regulates cofilin phosphorylation, recently an actin-binding protein WAVE3 has emerged as Arc/Arg3.1 binding partner (Bramham et al. 2008). Furthermore, local reorganization of F-actin microfilament was shown to be necessary in Arc/Arg3.1 mRNA targeting and to induce selective Arc/Arg3.1 mRNA transport to activated synapses (Huang et al. 2007).
Recent work of Okuno and colleagues have proposed a role for Arc/Arg3.1 protein in the model of inverse synaptic tagging of inactive synapses (Okuno et al. 2012). They hypothesized that Arc/Arg3.1 mRNA is targeted to inactive or previously stimulated synapses in a process that is termed inverse synaptic tagging. Captured Arc/Arg3.1 is suggested to increase AMPA receptor endocytosis and thereby weaken further synaptic activity. Little is known about its mediating mechanisms, but however, since loss of CaMKIIβ was demonstrated to suppress Arc/Arg3.1 protein accumulation in silenced synapses (Okuno et al. 2012), this protein might be a critical candidate in inverse synaptic tagging and determinate the accumulation of Arc/Arg3.1 mRNA in synaptic dendrites. Taken together these results Arc/Arg3.1 protein regulates synaptic plasticity by specific weakening mechanisms and controls the level of neuronal activity. This model might reconcile contradictory results and connect the role of Arc/Arg3.1 protein in long-term potentiation, AMPA receptor trafficking and homeostatic plasticity.

2.4.3 Arc/Arg3.1 protein and neurogenesis

Neurogenesis occurs in the subgranular zone of the hippocampal dentate gyrus and is known to be an ongoing process throughout adult life in almost all mammals (Zhao et al. 2006). These days still little is known about the incorporation mechanisms of newborn neurons into the hippocampal circuits. However, Arc/Arg3.1 protein expression is supposed to play a role in the neuronal formation and remains an important subject to research.
An unique property among IEG is that Arc/Arg3.1 is expressed since the first day after birth and widely associated with long-term survival and neuronal differentiation of newly generated cells (Bramham et al. 2010). Kuipers and colleagues investigated neurogenesis in newborn hippocampal granule cells birthmarked by bromodeoxyuridine injection within the first 4 weeks during maturation and used IEG to map their functional maturation (Kuipers et al. 2009). Surprisingly, Arc/Arg3.1 expression did not increase in response to evoked LTP in these neurons assuming that newborn neurons are refractory to evoked Arc/Arg3.1 expression. Nevertheless, Arc/Arg3.1 expressing cells showed a higher probability of survival and incorporation in pre-existing hippocampal circuits while Arc/Arg3.1 negative new cells

gradually decreased (Kuipers et al. 2009). The connecting pathways from Arc/Arg3.1 expression to neuronal circuit maturation remain to be explored. The finding that Arc/Arg3.1 is transferred directly to the nucleus where it interacts with large protein complexes in order to promote proliferation, differentiation and apoptosis of cells indicate a contribution to neurogenesis.

3 MATERIALS AND METHODS

3.1 Animals

Conventional Arc/Arg3.1 KO mice were generated as described by Plath and colleagues (Plath et al. 2006). Shortly, a neomycin resistance cassette, flanked by two loxP sites, was inserted at position +2690 into the second intron. The Arc/Arg3.1 ORF was flanked by inserting a third loxP site at position -1720. The targeting vector was linearized at a unique NotI site and electroporated into R1 ES cells. Positive clones were identified by Southern blot analysis and one targeted ES cell clone was transiently transfected with Cre recombinase. The resulting recombination types were identified by Southern blot. A type I recombination clone was injected into C57Bl/6J blastocysts to generate chimeras with a deleted Arc/Arg3.1 allele. Type II recombination clones were selected and injected into C57Bl/6J blastocysts to generate mice carrying the floxed allele. Male chimeras were backcrossed into C57Bl/6J. Arc/Arg3.1 KO ($Arc/Arg3.1^{-/-}$), WT ($Arc/Arg3.1^{+/+}$) and heterozygous ($Arc/Arg3.1^{+/-}$) mice were obtained from breeding heterozygous animals ($Arc/Arg3.1^{+/-}$).
Conditional Arc/Arg3.1 mice: floxed Arc/Arg3.1 mice ($Arc/Arg3.1^{f/f}$) were bred to the cre transgenic mouse line Tg(CamKIIα-cre)1Gsc (Casanova et al. 2001). Offspring with the genotype $Arc/Arg3.1^{f/f,\ Cre+}$ exhibited full ablation of the Arc/Arg3.1 gene two weeks after birth and are termed conditional KO mice ($Arc/Arg3.1^{f/f,\ Cre+}$, cKO mice) in this thesis. WT-control mice were either $Arc/3.1Arg^{+/+}$, $Arc/Arg3.1^{f/f}$ or $Arc/Arg3.1^{+/+,\ Cre+}$, as indicated.
Male and female mice aged 9-26 weeks were used in all experiments.

3.2 Slice preparation

Mice were anesthetized with 100µl 2 Bromo 2 chloro 1, 1, 1, tritrifluoroethane and decapitated. Brains were quickly removed and placed in ice-cold gassed (95% O_2, 5% CO_2 and pH: 7.4) ACSF for 1-2 min. Subsequently slices were prepared: transverse hippocampal slices (350 µm) were prepared with a vibratom (HM 650V, MICROM) and two third of the dorsal-mid hippocampus was collected in a breaker containing warmed (37°C) and gassed ACSF and allowed to recover for 90 minutes followed by additional 15 min at room temperature. ACSF for slice preparation and recordings was the same and contained: NaCl 119 mM, KCl 2.5 mM, $NaHCO_3$ 26 mM, NaH_2PO_4 1.25 mM, $MgSO_4$ 1.3 mM, glucose 10 mM and $CaCl_2$ 2.5 mM.

3.3 Electrophysiological field recordings

Extracellular field recordings were made with Synchrobrain (Lohres research, Germany), a system of 4 parallel recording chambers (CH 1-4, Figure 7A), which allows the simultaneous recording of 4 brain slices. Recording chambers were continuously perfused with recirculated warmed (37°C) and gassed ACSF at a rate of 3 ml/min per chamber. Slices were transferred to the recording chambers and allowed to equilibrate for additional 30 minutes prior to recordings. Two extracellular electrodes (SE-100 concentric bipolar stainless steel) were placed independently into the stratum radiatum of CA1, as shown in Figure 7B, within approximately 300 µm from the stratum pyramidale. In each LTP experiment one stimulation electrode was chosen to deliver the LTP-inducing stimulus to the stimulation pathway (SE: stimulation pathway, from stimulation electrode) and the other electrode was used to monitor a control pathway (CE: control pathway, from control electrode). Recordings were made without GABA blockers. Signals were amplified 1000x and filtered at 1 KHz.

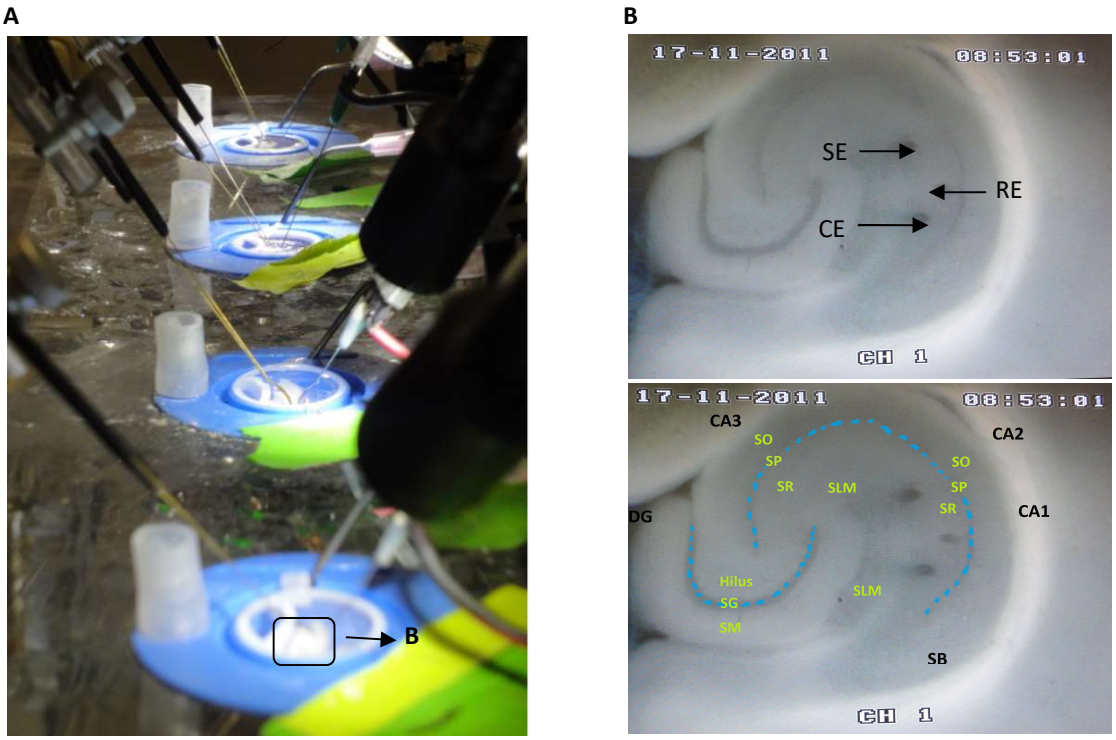

Figure 7: Recording chambers and arrangement of electrodes. (A) Photograph of 4 recording chambers and electrodes of Synchrobrain. **(B)** Upper example photograph from hippocampal slice preparation indicate the electrode setting (black fleshes in the upper picture) of SE, CE and RE (RE: recording electrode) in the CA1-stratum radiatum (CH 1: chamber 1). The photograph below shows the corresponding anatomical structures (CA1-4: cornu ammonis area 1-4, SB: subiculum, DG: dentate gyrus, SO: stratum oriens, SM: stratum moleculare, SG: stratum granulosum, SP: stratum pyramidale, SR: stratum radiatum, SLM: stratum locunosum-moleculare, dashed blue lines: cell bodies of neurons). All three pictures were made by myself.

3.4 Field excitatory postsynaptic potential: fEPSP

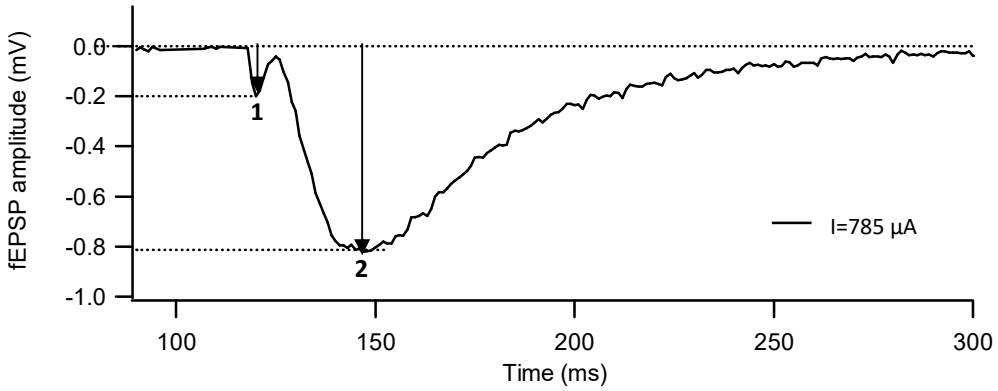

Figure 8: Exemplary fEPSP. A representative fEPSP trace evoked in response to a short bipolar stimulation (I = 784 µA) in stratum radiatum. Dashed lines indicate the size of FV (1) and fEPSP amplitude (2).

A short stimulus delivered in stratum radiatum evokes a fEPSP slope which is the extracellular potential generated when a population of neurons responds synchronously to the stimulus. After stimulation, an initial smaller and faster potential is obtained which represents the action potential evoked in the projecting CA3 axons, and is termed the fiber volley (FV). The fiber volley amplitude (FV-A) is proportional to the number of stimulated presynaptic fibers, and permits to estimate the recruitment and degree of excitability in the afferent input. The subsequent component, the field excitatory postsynaptic potential (fEPSP), reflects the local extracellular potential arising from the current flowing through the transmitter receptors opened in response to the action potential evoked in the CA3 axons. It is therefore a function of the number of evoked synapses, the amount of released transmitters and the current flowing through each receptor channel. The magnitude of fEPSP amplitude (fEPSP-A) also depends on the number of functional postsynaptic receptors versus silent receptors and the seize of single synapses. Thus, increasing or reinforcing of one of these parameters would lead to greater size of fEPSP amplitudes. An exemplary of fEPSP trace is demonstrated in Figure 8. Here, a short bipolar stimulus (200 µs) of 785 µA generated FV-A in the size of 0.20 mV, and a fEPSP-A of 0.82 mV.

3.5 Conditions and design of LTP experiments

At the beginning of each LTP experiment characteristic parameters of basal synaptic transmission were investigated, such as input/output curves (IO curves) and paired pulse facilitation tests (PPF). IO curves and PPF tests were performed to define the stimulation intensity (I_{half}) and to ensure input specificity. I_{half} is defined as the current needed to generate 50% of the maximal field excitatory postsynaptic potential amplitude ($fEPSP_{max}$-A):

fEPSP$_{half}$-A. The currents generating the smallest and the largest fEPSP slopes were first determined and a series of six to ten pulses within this range were randomly generated and applied to each stimulation electrode. For each recorded pathway (CE and SE), the fEPSP amplitudes were measured on line and fitted with sigmoidal function that was used to determine fEPSP$_{max}$-A and fEPSP$_{half}$-A. The current I_{half} yielding fEPSP$_{half}$-A was used subsequently as the stimulation intensity for all stimuli applied in the following LTP experiment. The maximal possible range of stimulation intensities in all experiments was 0-1600 µA.

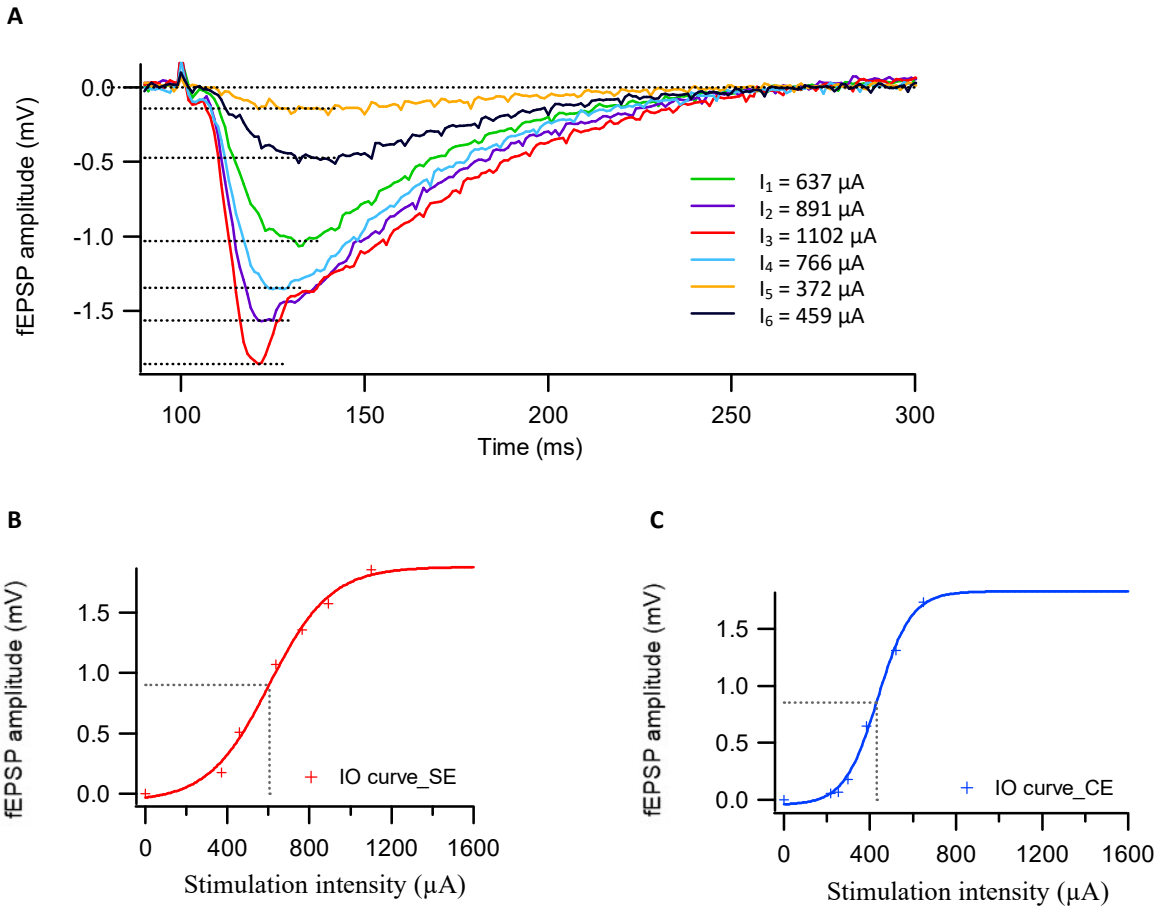

Figure 9: IO Curves of SE and CE. (A) Six individual fEPSP slopes extracted from the SE IO curve were plotted and showed increasing amplitudes with stronger stimulation intensities. The strongest current (here I_3) generated a population-spike. The dashed lines indicate the fEPSP peak amplitudes. **(B, C)** Six pulses of SE and CE were measured at different stimulation intensities (crosses) and fitted with a sigmoidal function of the stimuli rage for SE: 300-1200 µA and CE: 200-700 µA. The dashed line indicates respectively the size of corresponding I_{half} and fEPSP$_{half}$-A.

In Figure 9A, six traces were selected from the IO curve applied to SE and showed an increase in the fEPSP-A in response to higher stimulation intensities. The smallest injected current (here I_5 = 372 µA) elicited a small but detectable fEPSP-A which proportionally increased at intensities of I_6 = 459 µA, I_1 = 637 µA, I_4 = 766 µA and I_2 = 891 µA. Above a given

strength, here I_3 = 1102 µA, a population-spike was evoked that interrupted the fEPSP. The entire IO curves for SE and CE is demonstrated in Figure 9B and 9C. Each IO curve contained six pulses in the interval of minimal and maximal fEPSP-A (SE: 300-1200 µA and CE: 200-700 µA). The stimulation current I_{half} of SE was in the size of 604.54 µA and generated 0.903 mV of $fEPSP_{half}$-A while the control pathway stimulated $fEPSP_{half}$-A of 0.855 mV by I_{half} of 431.85 µA.

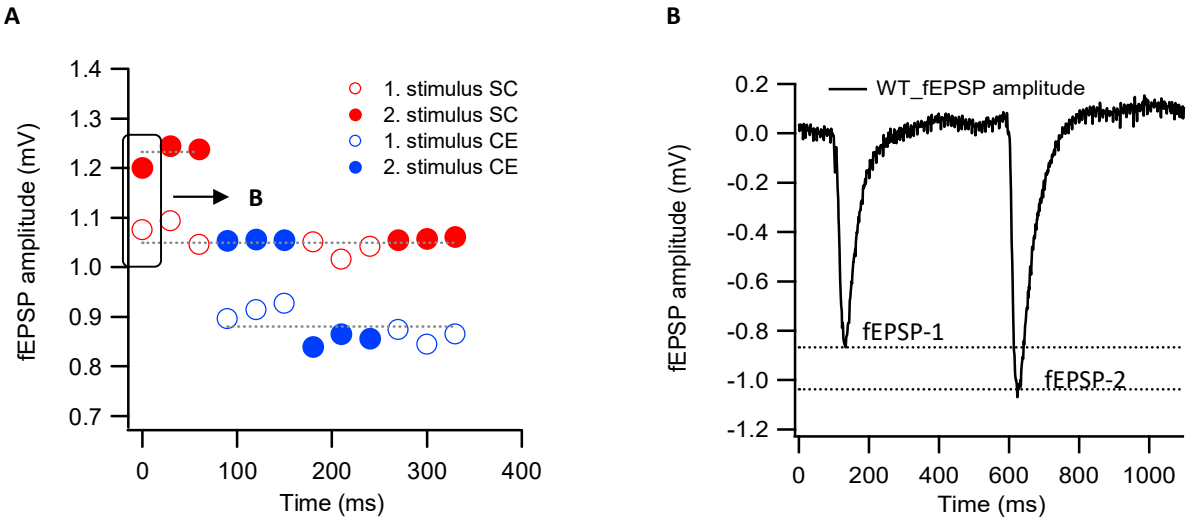

Figure 10: Paired pulse facilitation test. (A) Stimulation pattern of PPF test. Sequences of 3 paired pulses were delivered separately to each stimulating electrode followed by another sequence in which a stimulus to SE was altered with a stimulus to CE. In all paired stimuli, intervals were 50 ms. Each dashed line represents the averaged fEPSP amplitudes. **(B)** Increased fEPSP-2 in response to a pair of stimuli extracted from a pair of stimuli of the PPF test in Figure 10A. Dashed lines indicate the size of fEPSP-1 and fEPSP-2 amplitude.

I used the PPF test to assess a possible overlap between the two synaptic populations measured as stimulation and control pathways. The test was performed by delivering three subsequent pairs of stimuli at an interval of 50 ms to each pathway, separately. At this stimulus interval, synapses in CA1 normally exhibit facilitation of the second fEPSP amplitude (fEPSP-2) compared to the first fEPSP amplitude (fEPSP-1). The cellular mechanism underlying this facilitation is likely to be an increase of Ca^{2+} concentration during the second stimulus resulting in larger release of transmitter (Katz and Miledi 1968). Subsequently, three pairs of stimuli were delivered first to SE and 50 ms later to CE. If the two synaptic populations are independent of each other, than delivering a pair of stimuli to two distinct synaptic pathways should evoke fEPSP amplitudes that are identical to the prior fEPSP-1 amplitude in each pathway. However, if current injection to one electrode stimulates some or all the synapses at the other electrode, than the fEPSP amplitude measured in this sequence will be larger than the fEPSP-1 amplitude of this pathway. The entire sequence of PPF stimuli is plotted in Figure 10A together with the analysis of PPF ratio from an exemplary experiment. First, pairs of stimuli were delivered to SE and CE, separately, showing

facilitation of fEPSP-2 amplitude in both pathways. PPF ratio was calculated by normalizing the amplitude of the fEPSP-2 to the fEPSP-1 (SE: 1.15, CE: 1.16, values >1 indicate facilitation). Subsequently, pairs of stimuli were applied alternately to SE and CE. Values of calculated PPF ratio ≤1 indicate independence of both pathways (SE: 0.99, CE: 0.94). Additionally Figure 10B was added to show facilitation of fEPSP-2 in response to a pair of stimuli.

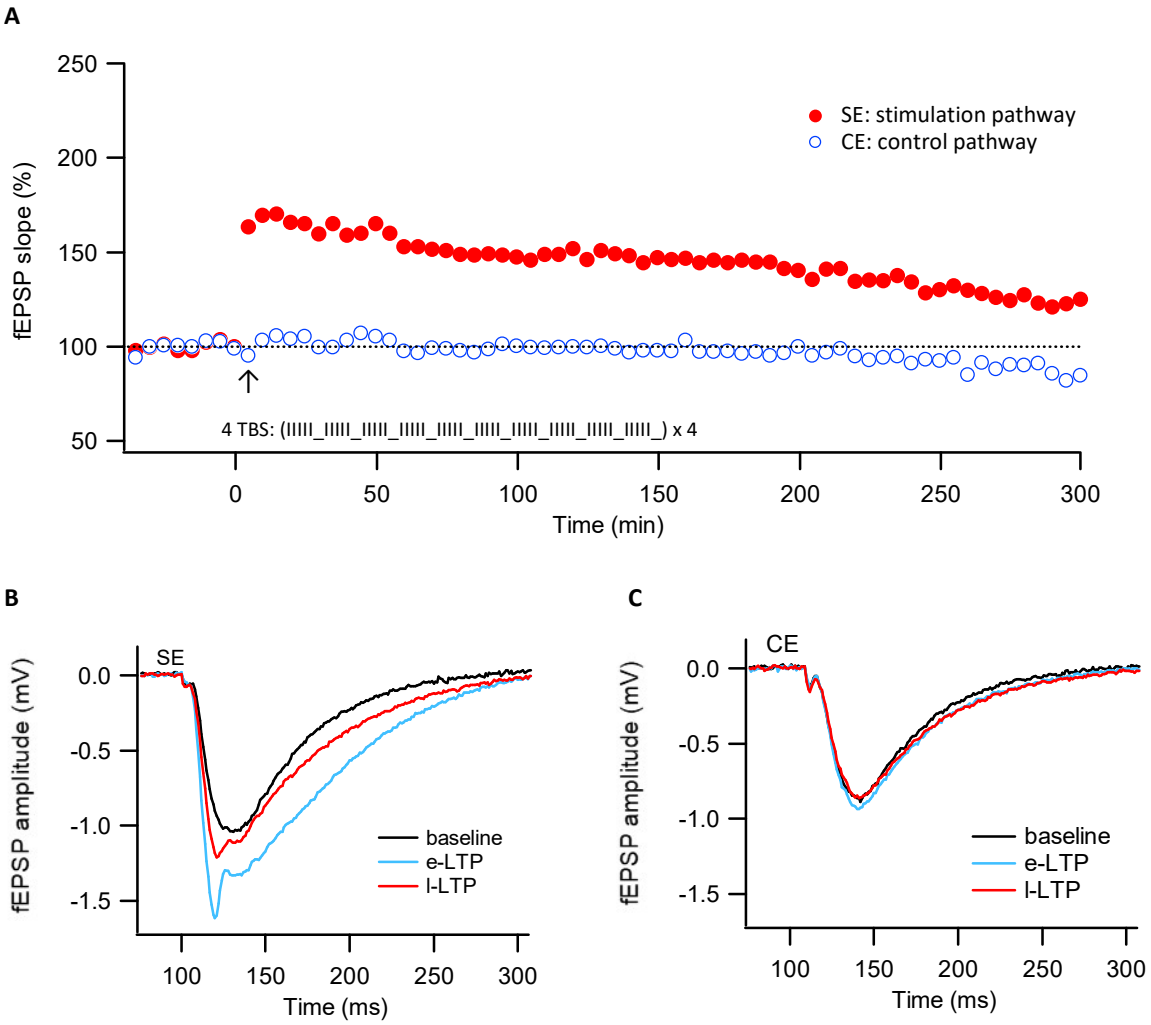

Figure 11: Recordings of one LTP experiment. (A) Representative LTP time course of one experiment induced by 4TBS stimulation protocol. FEPSP slopes were normalized to 100% of baseline stimulation and plotted against time in minutes. At the time point 0 min, only cell responses of SE (red filled circles) received TBS stimulation and showed enhanced fEPSP slopes which remained elevated over 5 hours. The stimulation pattern of one TBS train is illustrated schematically in the lower part of the figure. It consisted of 10 burst (inter-burst of 200 ms) of five stimuli each (intra-burst of 200 Hz). CE (blue unfilled circles) received only baseline stimulation and remained unstimulated by TBS trains. **(B, C)** Sweep analysis: fEPSP traces were extracted at the time points of baseline, e-LTP and l-LTP for SE and CE. Post TBS stimulation only SE exhibited increased fEPSP amplitudes at e-LTP and l-LTP time points. Annotation: here calculated I_{half} showed little larger fEPSP amplitudes of SE and CE than during IO curves measurement which might be due to an amelioration of slices in artificial physiological conditions in chambers.

The time course of an individual LTP experiment is plotted in Figure 11A. A schematic representation of the TBS stimulation protocol is represented below by a series of black lines. Prior to LTP induction, stimulation and control pathway received 80 stimuli each in the seize of calculated I_{half} (impulse of the second electrode had a delay of 1000 ms), at a rate of 0.033 Hz (30 sec intervals, total of 40 min) to measure the baseline fEPSP size. Subsequently, LTP was induced in the stimulation pathway by 4 trains of TBS. One TBS train consisted of 10 bursts of 5 stimuli each, applied at an intra-burst rate of 200 Hz and repeated at an inter-burst interval of 200 ms. Four TBS trains were applied with 30 sec intervals. In response to 4 TBS, stimulated fEPSP slopes increased immediately and reached a magnitude of 170 ± 0.43% of baseline stimulation. This value was calculated from the average of the first 10 min of fEPSP recording post TBS application and determined as early LTP (e-LTP). Following the LTP time course, fEPSP slopes slightly attenuated in size but remained elevated over 5 hours of recording. The last 30 min of recording were averaged to represent late LTP (l-LTP) and, which in this example was 124 ± 0.90% of baseline stimulation. The control pathway received only low frequency stimulation, as during baseline (0.033 Hz), throughout the experiment and showed unchanging fEPSP slopes.
To discriminate changes in fEPSP slope caused by experimental parameters (e.g. perfusate level or deterioration of slice health) from LTP induced changes by the high frequency stimulation, the FV-A and fEPSP-A were additionally analyzed in both control and stimulation pathways (Figure 11B and 11C). The graph of SE showed maximal enhanced fEPSP-A (population spike) post LTP induction at e-LTP time point and lasting increased fEPSP-A at l-LTP time point compared to baseline stimulation. FEPSP-A at corresponding time points in the control pathway showed constant fEPSP-A at all time points. Moreover, both pathways showed unaltered FV-A over the LTP recording time. Only experiments without major perfusion disturbances, or rundown of control pathway or of the FV, were included in the final analysis.
Further analysis of one single LTP experiment included FV, l-LTP probability and fEPSP slopes in TBS trains and were described in the result section.

3.6 Data analysis and statistics

All LTP experiments from conventional and conditional mice were digitized online and the fEPSP amplitudes and slopes were analyzed with the Synchrobrain software. Analyzed data was further processed in Microsoft Office Excel (Version 2007) and Igor Pro 6.06 (Wavemetrics). Only LTP experiments without perfusion disturbances, rundown of CE or FV and PPF ratio <1 were included in summary graphs. During each LTP experiment, the fEPSP slope was measured as initial 10-30% of fEPSP slope fall respectively in control and stimulation pathway. An increase of initial post-TBS fEPSP slope above 120% compared to baseline and over 30 min was defined as e-LTP, while continuously elevated fEPSP slopes above 110% were classified as successful l-LTP. Summary graphs of LTP time course divided

in successful and unsuccessful l-LTP experiments are demonstrated for each genotype. To compare the size of e-LTP and l-LTP, initial 10 min and final 30 min of increased fEPSP slopes were averaged for each experiment. The total magnitude of e-LTP and l-LTP as well as the induction rate of successful l-LTP are presented in bar diagrams. All results are shown as mean ± SEM (standard error of measurement) with number of animals (N) and slices (n) stated. Data of burst analysis and basal synaptic transmission were analyzed and are presented in graphs or bar diagrams. Annotated, results from basal synaptic transmission resumed data from SE and CE, whereas LTP analysis were performed separately.

Statistical comparisons of obtained data were conducted in SPSS and GraphPad Prism (Version 5). Mann-Whitney test (or student T-test) was used to compare fEPSP slopes in averaged LTP time courses and considered only in selected time points during LTP recording time. Time points corresponding to e-LTP (first 10 min post TBS stimulation: 2 time points) and l-LTP (last 30 min of recording time: 6 time points) were compared to baseline stimulation prior LTP induction (at least 5 min pre-TBS stimulation: 1 time point) and control pathway at equal time points as the stimulation pathway. Similarly, the exact time points of fEPSP slope decay in LTP time courses were identified and compared to baseline and control pathway. The Mann-Whitney test was used to reveal significance of two group comparisons in bar diagrams, while three group comparisons were analyzed by One Way ANOVA (post hoc bonferoni). The level of significance is indicated in each graph or bar diagram as braces and asterisks (* $p < 0.05$, ** $p < 0.01$ and *** $p < 0.001$).

In this study, the genotype of tested animals was only revealed after completion of LTP experiments and analysis, to avoid experimental bias.

4 RESULTS

4.1 LTP in conventional Arc/Arg3.1 mice

The following set of experiments demonstrates the TBS-LTP in hippocampal CA1 area. Conventional wild-type (WT, Arc/Arg3.1$^{+/+}$) and knockout (KO, Arc/Arg3.1$^{-/-}$) slices were investigated on distinct LTP components and synaptic basal transmission to detect Arc/Arg3.1 protein dependent alterations.

4.1.1 Stimulus dependent l-LTP in WT mice

To examine separately e-LTP and l-LTP in CA1 area of the hippocampus two different TBS protocols were applied to slices obtained from conventional Arc/Arg3.1 KO and WT littermates. 1 TBS protocol was reported to induce a transient potentiation decaying to baseline within 1-3 hours while 4 consecutive trains of TBS generated stable l-LTP which persisted for longer than 3 hours (Larson et al. 1986, Staubli and Lynch 1987, Nguyen and Kandel 1997, Raymond 2007).

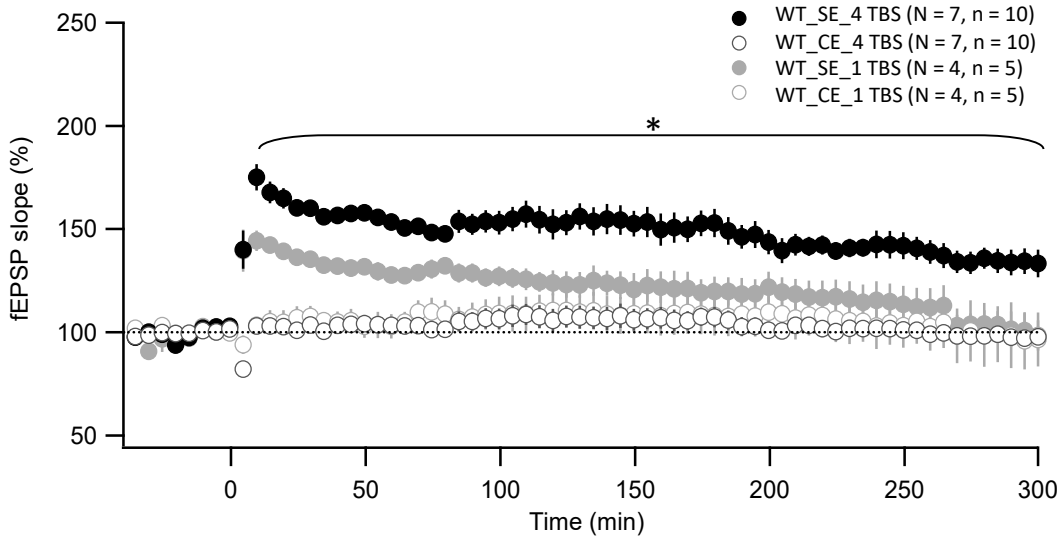

Figure 12: LTP time course of 1 and 4 TBS in WT mice. Pathways stimulated with 1 TBS showed smaller e-LTP, that decayed to baseline levels within 3-5 hours. In contrast, pathways stimulated with 4 TBS exhibited enhanced e-LTP which remained elevated for over 5 hours. Comparison of both stimulated pathways revealed significant difference over the entire recording time. Bars represent means ± SEM, and asterisks ($p < 0.05$).

Figure 12 shows averaged LTP time course in response to 1 and 4 TBS in WT mice (1 TBS-WT mice, N = 4, n = 5, 4 TBS-WT mice, N = 7, n = 10). After recording stable baseline fEPSP slopes in stimulation and control pathway for 40 min, either 1 or 4 TBS was applied to the stimulation pathway while control slices continued to receive baseline stimulation. In

response to 1 TBS, the averaged fEPSP slopes increased to 147 ± 5.48% within 5 min and were highly significant compared to the baseline fEPSP slopes ($n = 5$, $p < 0.001$). Subsequently, fEPSP slopes remained significantly elevated for 64.5 min compared to control pathway ($n = 5$, $p < 0.01$) and 139.5 min compared to baseline ($n = 5$, $p < 0.01$-0.05). Following the LTP time course, fEPSP slopes decayed to baseline without showing l-LTP ($n = 5$, l-LTP: 102 ± 5.68%, l-LTP to baseline: $p > 0.05$, l-LTP to CE: $p > 0.05$). In contrast to 1 TBS stimulated slices, 4 TBS application induced generally larger fEPSP slopes over the entire LTP time course. Significant increase of e-LTP and l-LTP was measured respectively in the seize of 174 ± 6.7%, compared to baseline ($n = 10$, $p < 0.001$) and 134 ± 5.65%, compared to baseline ($n = 10$, $p < 0.001$) and to control pathway ($n = 10$, $p < 0.001$). Comparison of the 1 and 4 TBS induced LTP time course detected significant differences over all recorded time points post stimulation (1 TBS-WT mice, $n = 5$, 4 TBS-WT mice, $n = 10$, $p < 0.05$). These results are in agreement with previous reports and showed that LTP maintenance is dependent on stimulus strength. 4 TBS stimulation protocols seem to be strong and sufficient to induce reliable l-LTP while 1 TBS stimulation protocols only generate a transient e-LTP.

4.1.2 Impairment of l-LTP in KO mice

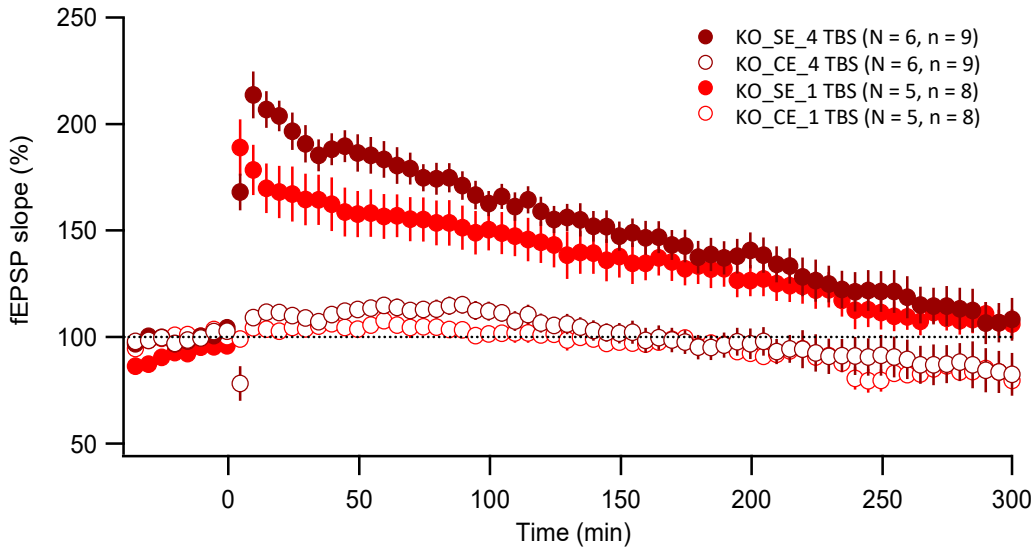

Figure 13: LTP time course of 1 and 4 TBS in KO mice. 4 TBS induced fEPSP slopes were initially increased but could not consolidate into l-LTP. 1 TBS stimulated slices showed less e-LTP compared to 4 TBS stimulated slices and similar decaying fEPSP slopes. Comparisons of both LTP time courses detected no significant differences. Bars represent means ± SEM.

The same 1 and 4 TBS stimulation protocols were applied to slices obtained from Arc/Arg3.1 KO mice (1 TBS-KO mice, N = 5, n = 8, 4 TBS-KO mice, N = 6, n = 9). Figure 13 represents the averaged time course of LTP induced by 1 and 4 TBS, respectively. The fEPSP slopes of e-LTP increased similarly in response to both stimulation protocols, (1 TBS-KO mice, n = 8, e-LTP: 197 ± 12.12%, 4 TBS-KO mice, n = 9, e-LTP: 214 ± 8.64%, $p > 0.05$) and were significantly higher than baseline (1 TBS-KO mice, n = 8, $p < 0.001$, 4 TBS-KO mice, n = 9, $p < 0.001$). After e-LTP induction with either 1 TBS and 4 TBS, fEPSP slopes remained significantly enhanced until 239.5 and 214.5 min compared to the baseline (1 TBS-KO mice, n = 8, $p < 0.01$-0.001, 4 TBS-KO mice, n = 9, $p < 0.01$-0.001) and until 300 and 219.5 min compared to the control pathway (1 TBS-KO mice, n = 8, $p < 0.001$, 4 TBS-KO mice, n = 9, $p < 0.001$-0.05). However, 1 and 4 TBS induced fEPSP slopes decayed back to baseline levels without generating l-LTP (1 TBS-KO mice ,n = 8, l-LTP: 108 ± 5.66%, l-LTP to baseline: $p > 0.05$, l-LTP to CE: $p > 0.05$, 4 TBS-KO mice, n = 9, l-LTP: 111 ± 9.63%, l-LTP to baseline: $p > 0.05$, l-LTP to CE: $p > 0.05$). Notably no significant differences between both LTP time courses were detected (1 TBS-KO mice, n = 8, 4 TBS-KO mice, n = 9, $p > 0.05$).

In addition, during the last hour of recording fEPSP slopes of the control pathway in 1 and 4 TBS stimulated slices decreased below baseline values to the level of 83 ± 1.20% and 84 ± 0.66%. Consequently, the relative magnitude of l-LTP to control pathway became significant in 1 TBS stimulated slices.

4.1.3 Comparison of LTP

To examine the effects of Arc/Arg3.1 protein on LTP induction and maintenance, averages of 4 TBS experiments were compared. Figure 14A demonstrates 4 TBS induced LTP time courses while Figure 14B summarizes the relation between the magnitude of e-LTP and l-LTP in response to stimulation intensity.

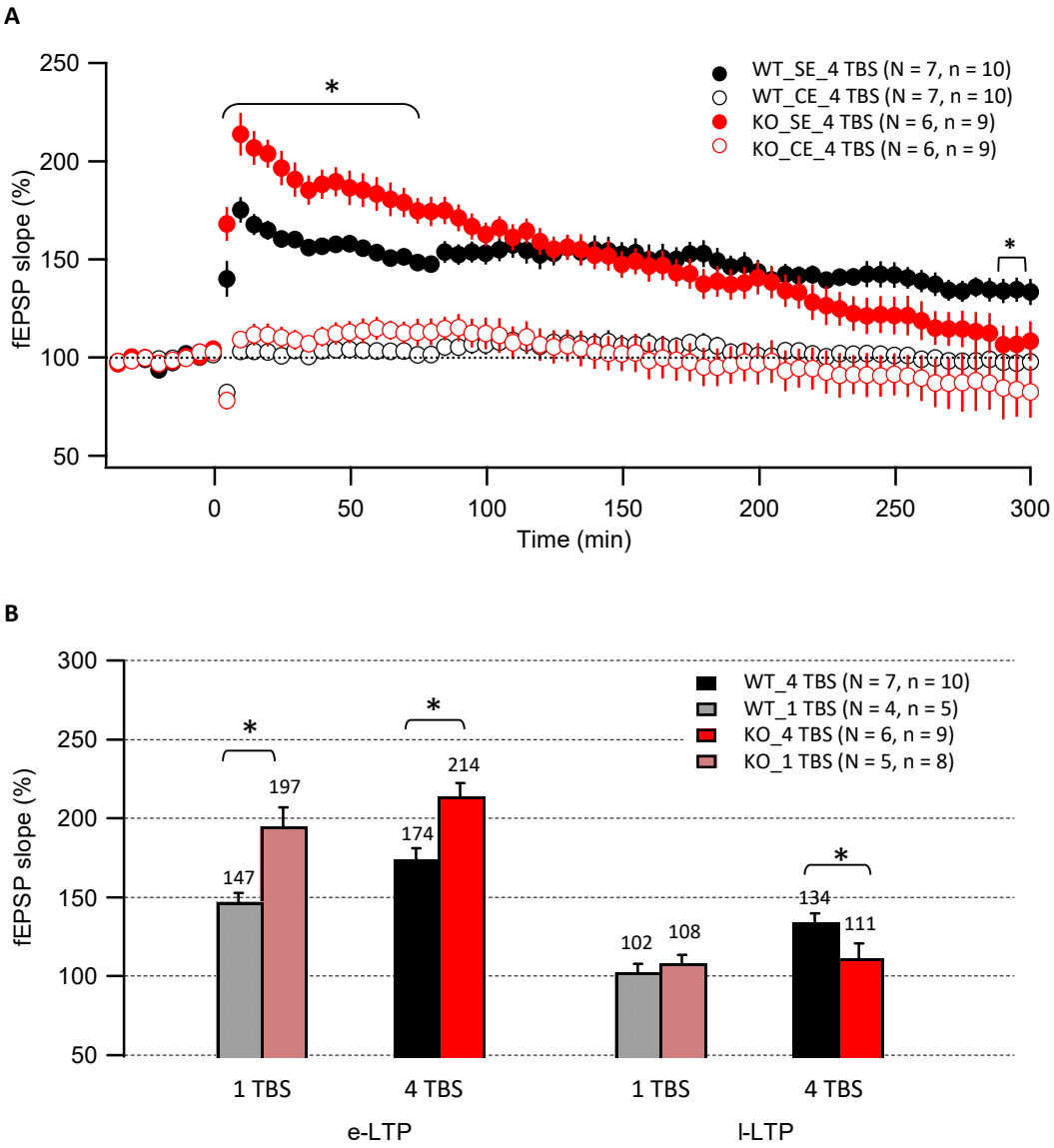

Figure 14: Comparison of LTP in WT and KO mice. (A) The averaged LTP time course of 4 TBS stimulated KO slices showed increased initial fEPSP slopes which clearly decayed over the recording time without consolidation into l-LTP, compared to WT slices. Asterisks ($p < 0.05$) showed significant differences between genotypes. **(B)** Overview of the magnitude of e-LTP and l-LTP in WT and KO slices. KO slices generated significant larger e-LTP in response to 1 and 4 TBS but no l-LTP. Only WT slices showed significant l-LTP in response to 4 TBS. Numbers over each bar indicate the values of e-LTP and l-LTP respectively as percentage of baseline stimulation. Bars represent means ± SEM, and asterisks ($p < 0.05$).

As shown in Figure 14A, WT and KO slices differed in LTP time course in response to the same stimulation paradigms. Following 4 TBS, the magnitude of e-LTP in KO slices significantly exceeded e-LTP in WT slices (WT mice, n = 10, KO mice, n = 9, $p < 0.05$). Referring to the student T-test, fEPSP slopes from KO slices were significantly different from WT slices during the initial 79.5 min (WT mice, n = 10, KO mice, n = 9, $p < 0.05$) and a few last time points (WT mice, n = 10, KO mice, n = 9, time points: 289.5-294.5 min, $p < 0.5$) while the greater part of LTP time courses remained indistinguishable (WT mice, n = 10, KO mice, n = 9, $p > 0.05$).

The bar diagram in Figure 14B summarizes the dependence of LTP magnitude as function of stimulus intensity. In WT slices, 4 TBS induced consistently greater e-LTP than 1 TBS while l-LTP was only induced by 4 TBS. In contrast, KO slices generated significantly larger e-LTP in response to 1 TBS and 4 TBS that exceeded WT e-LTP by 50% and 40%, respectively (1 TBS-WT mice, n = 5, 1 TBS-KO mice, n = 8, $p < 0.05$, 4 TBS-WT mice, n = 10, 4 TBS-KO mice, n = 9, $p < 0.05$). Nevertheless, regarding l-LTP in KO slices, neither of the two stimulation protocols could generate persistent elevation of fEPSP slopes. 4 TBS induced l-LTP in WT slices was significantly increased compared to KO slices (WT mice, n = 10, KO mice, n = 9, $p < 0.05$).Taken together these findings demonstrate that LTP magnitude and persistence depend on the presence of Arc/Arg3.1 in stimulated neurons and synapses. To test whether this effect depends on the expressed amount of Arc/Arg3.1, LTP and basal synaptic activity from heterozygous mice expressing roughly half of the amount of the normal Arc/Arg3.1 levels were investigated.

4.1.4 Intermediate LTP in HT mice

In the following LTP experiments, the impacts of partial Arc/Arg3.1 protein deletion were investigated. Therefore heterozygous mice (HT, Arc/Arg3.1$^{+/-}$) which express only one allele of Arc/Arg3.1 were included in the same experimental settings and compared to WT and KO mice.

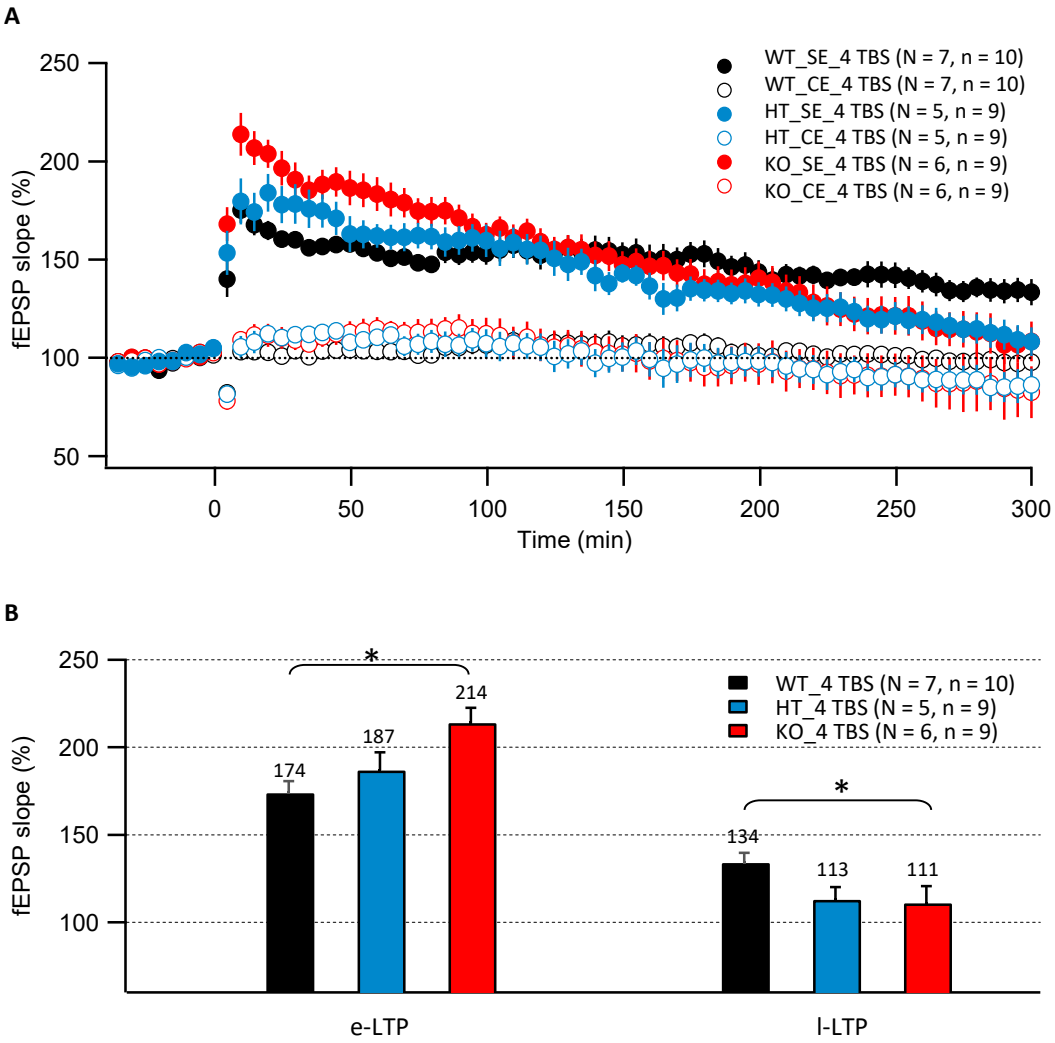

Figure 15: Intermediate LTP time course, e-LTP and l-LTP in HT mice. (A) After 4 TBS stimulation HT slices exhibited intermediate initial potentiation in fEPSP slopes while lasting fEPSP slopes tended to shift towards the LTP time course of KO slices (no significance between groups). **(B)** Comparison of 4 TBS induced e-LTP and l-LTP in WT, HT and KO slices in which the magnitude of HT slices in both, e-LTP and l-LTP, remained between WT and KO slices. Bars represent means ± SEM, and asterisks ($p < 0.05$).

Figure 15A shows the averaged LTP time course of HT slices (N = 6, n = 9) in comparison with WT and KO slices. Post 4 TBS-LTP induction, HT slices rapidly developed large e-LTP of 187 ±

10.23%, which was significantly higher than the baseline ($n = 9$, $p < 0.001$). FEPSP slopes remained enhanced for 140 min above control pathway ($n = 9$, $p < 0.05$) and for 269.5 min above baseline ($n = 9$, $p < 0.05$). It has to be noted that the corresponding control pathway did not remain stable at baseline levels (baseline prior TBS stimulation: 101 ± 0.41%) but decayed slightly to 86 ± 0.26%. Consequently, the difference between control and stimulation pathway became partly significant ($n = 9$, $p < 0.05$). L-LTP in the HT slices was 113 ± 7.19% but did not differ significantly from baseline ($n = 9$, $p > 0.05$) or from the control pathway ($n = 9$, $p > 0.05$). Comparison of 4 TBS-LTP time course between genotypes showed that HT slices exhibited slightly larger e-LTP than WT slices but failed to consolidate and decayed to baseline levels, similar to l-LTP in KO slices. However, fEPSP slopes post TBS application were not significantly different between genotypes (WT mice, $n = 10$, HT mice, $n = 9$, KO mice, $n = 9$, $p > 0.05$).

In Figure 15B, the averaged e-LTP and l-LTP are illustrated and compared between genotypes. In this bar diagram, HT slices clearly displayed an intermediate position in both, e-LTP and l-LTP, indicating a correlation between the magnitude of LTP and the level of Arc/Arg3.1 protein expression. One-way ANOVA indicated a statistically significant difference in e-LTP between WT and KO slices (WT mice, $n = 10$, KO mice, $n = 9$, $p < 0.05$) but no significant difference between HT and WT slices (WT mice, $n = 10$, HT mice, $n = 9$, $p > 0.05$) or between HT and KO slices (HT mice, $n = 9$, KO mice, $n = 9$, $p > 0.05$). L-LTP was not significantly different between WT, HT and KO slices (WT mice, $n = 10$, HT mice, $n = 9$, KO mice, $n = 9$, $p > 0.05$). However, the seize of l-LTP in WT and KO slices was significant in Mann-Whitney test (WT mice, $n = 10$, KO mice, $n = 9$, $p < 0.05$), as pictured in Figure 15B.

Interestingly, although the averaged LTP time course of HT slices decreased back to baseline stimulation, few individual slices exhibited elevated and stable LTP during the entire experiment. The following section analyzes the probability of stable l-LTP induction in all experiments and reveals genotype-dependent differences.

4.1.5 Induction of successful l-LTP

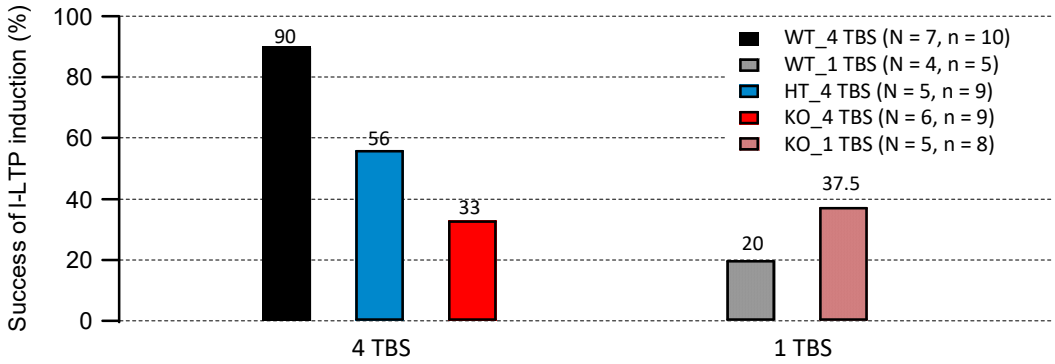

Figure 16: Successful l-LTP induction by 4 TBS and 1 TBS in WT, HT and KO mice. In response to 4 TBS, WT slices showed the highest percentage of successful l-LTP induction followed by lower percentages in HT and KO slices. Percentage of slices exhibiting successful l-LTP induction after 1 TBS was higher in KO compared to WT slices, but still lower than after 4 TBS in WT slices. Numbers above the bars indicate the probability of successful l-LTP induction calculated in percentage.

A single experiment was classified as successful when the value of l-LTP (measured between 270-300 min) was above 110% of the baseline. Figure 16 shows the percentage of successful l-LTP induction in WT, HT and KO mice in response to 1 and 4 TBS. In response to 4 TBS WT slices showed the highest percentage of successful l-LTP induction (90%, 9 out of 10 slices from 7 WT mice). HT slices exhibited lower percentage of successful l-LTP induction (56%, 5 out of 9 slices from 5 HT mice) while KO slices achieved the lowest success percentage (33%, 3 out of 9 from 6 KO mice). In response to 1 TBS, percentages of successful l-LTP induction clearly continued to fall in WT slices (20%,1 out of 5 slices from 4 WT mice) and remained at similar low levels in KO slices (37.5%, 3 out of 8 slices from 5 KO mice). Importantly, these results reveal that although rarely, stable l-LTP could be induced also in HT and KO slices. To study the time course of LTP in these rare cases, “successful” and “unsuccessful” 4 TBS experiments were averaged separately and compared.

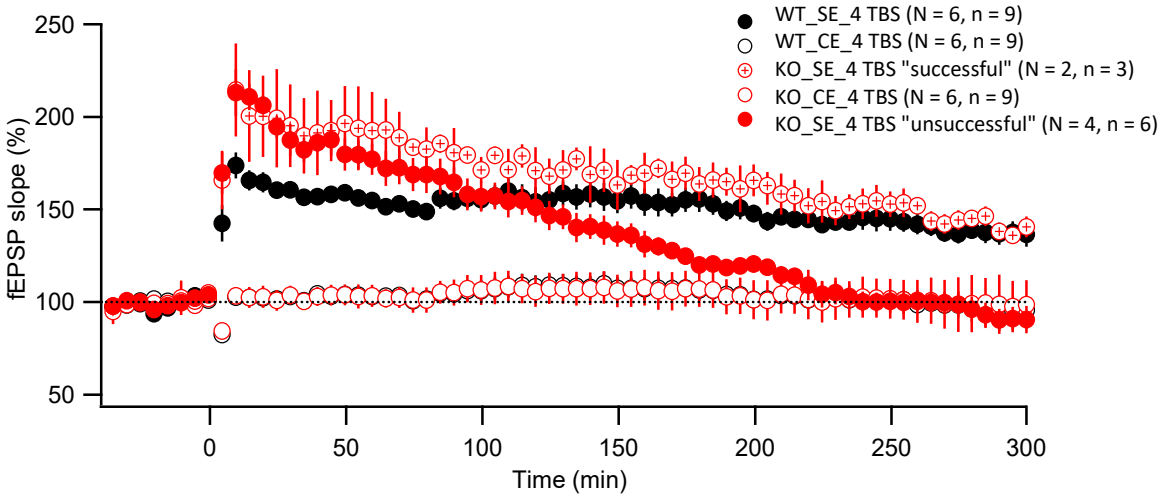

Figure 17: LTP time course of "successful" and "unsuccessful" l-LTP in WT and KO mice. Averaged time course of "successful" l-LTP in WT and KO slices and "unsuccessful" l-LTP in KO slices subjected to 4 TBS. KO slices generating "successful" l-LTP showed an e-LTP similar to "unsuccessful" KO slices, however, l-LTP in "unsuccessful" KO slices failed clearly while "successful" l-LTP experiments were as high as in WT slices.

Figure 17 shows the averaged LTP time course of "successful" l-LTP in WT (N = 6, n = 9) and KO slices (N = 2, n = 3) and "unsuccessful" l-LTP in KO slices (N = 4, n = 6). The LTP time course of "successful" l-LTP in KO slices showed large e-LTP of 212 ± 24.88% which was significantly increased compared to baseline (n = 3, $p < 0.001$) and significantly enhanced l-LTP of 142 ± 4.76% (n = 3, l-LTP to baseline: $p < 0.05$, l-LTP to CE: $p < 0.05$). E-LTP obtained from the LTP time course of “unsuccessful” l-LTP in KO slices was 215 ± 7.40% and resembled the e-LTP of LTP time course of "successful" l-LTP in KO slices (KO mice with "successful" l-LTP, n = 3, KO mice with "unsuccessful" l-LTP, n = 6, $p > 0.05$). However, l-LTP generated from LTP time course of "unsuccessful" l-LTP in KO slices measured 90 ± 6.47% and decayed back to baseline (n = 6, l-LTP to baseline: $p > 0.05$, l-LTP to CE: $p > 0.05$). In this KO subgroup fEPSP slopes remained elevated until 184.5 min compared to baseline (n = 6, $p < 0.001$-0.01, also time points: 199.5 and 204.5: $p < 0.05$) and until 199.5 min compared to control pathway (n = 6, $p < 0.001$-0.05, except time point: 194.5 $p > 0.05$). In WT slices, the averaged seize of e-LTP and l-LTP calculated from the LTP time course of "successful" l-LTP was respectively 173 ± 7.33% and 137 ± 5.36%.

Interestingly, linear curve fitting from 120 to 300 min in "successful" l-LTP in WT mice and KO mice (data not shown here) revealed that the slope was slightly higher in KO mice compared to WT mice (WT mice: 171 ± 1.43·x + 0.13 ± 0.01 and KO mice: 199 ± 2.37·x + 0.19 ± 0.01). Suggesting that "successful" l-LTP in KO mice might be transient and would continue decaying at later time points.

4.1.6 Altered fEPSP responses during TBS trains

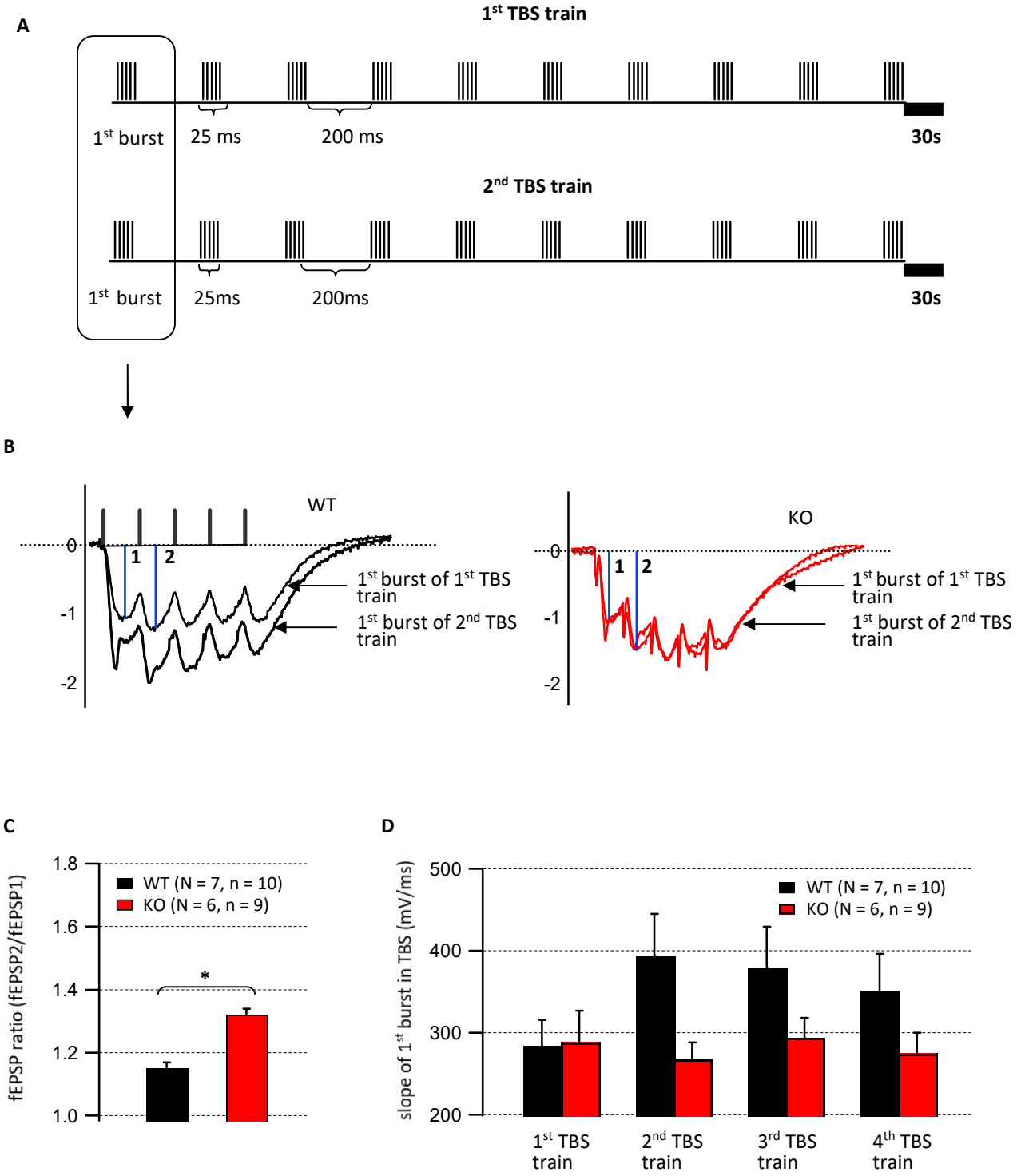

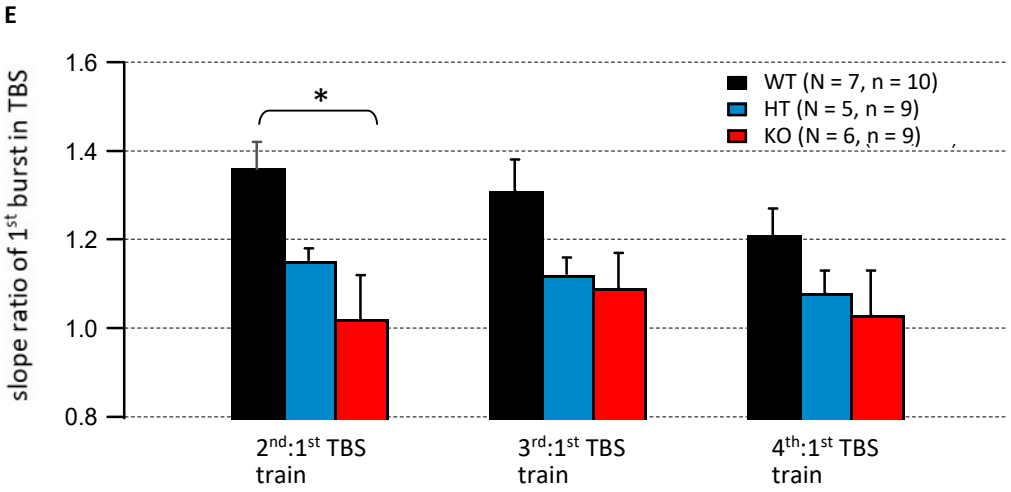

Figure 18: Analysis of fEPSP slopes in TBS trains in WT, HT and KO mice. (A) Schematic representation of the TBS stimulation protocol. 1st and 2nd TBS train, separated by 30s, contained each 10 bursts with 5 stimuli at an intra-burst rate of 200 Hz and inter-burst interval of 200 ms. An enlargement of the boxed window is shown in B. **(B)** Five stimuli from the respective 1st burst in the 1st and 2nd TBS train were plotted above exemplary fEPSP slopes from individual WT and KO slices. The inter-burst facilitation of fEPSP slopes from five stimuli resulting from 1st burst of the 2nd TBS train was increased in the WT slice compared to the KO slice. Blue bars indicate the seize of the first (1) and second (2) fEPSP amplitude from the 1st burst in 1st TBS train in both genotypes. The KO slice showed stronger intra-burst facilitation of the second fEPSP amplitude. **(C)** FEPSP ratio of second (2) to first (1) fEPSP amplitude from 1st burst in 1st TBS train in WT and KO mice. KO mice exhibited increased fEPSP ratio compared to WT mice. **(D)** Analysis of the slope of the 1st burst in 1st-4th TBS train in WT and KO mice. The slope of 1st burst in 1st TBS train was at similar seize in both genotype. Following the seize of the slopes from 1st burst in 2nd-4th TBS train, only WT mice showed increased slopes. **(E)** Slope ratio was calculated by the slope of 1st burst in 2nd-4th TBS train to 1st burst in 1st TBS train in WT, HT and KO mice. WT mice showed the greatest slope ratio compared to HT and KO mice. Bars represent means ± SEM, and asterisks ($p < 0.05$).

Next, fEPSP slopes evoked during TBS were analyzed from WT (N = 7, n = 10), HT (N = 5, n = 9) and KO slices (N = 6, n = 9). Figure 18A shows a schematic representation of the stimuli applied in the 1st and 2nd TBS train. TBS trains were delivered at 30 sec intervals. Each train consisted of 10 bursts of 5 stimuli, each applied at the rate of 200 Hz with inter-burst intervals of 200 ms. To compare inter-burst facilitation capacities, the total charge generated during the initial bursts in TBS trains was calculated from the slope under the 1st burst (5 stimuli) in the 1st and 2nd TBS train. An exemplary slope from WT and KO slice was represented in Figure 18B. The WT slice showed increased burst slope of 1st burst in 2nd TBS train while the KO slice appeared to generate similar slope of the 1st burst in the 1st and 2nd TBS train. Furthermore, greater facilitation of the second fEPSP (fEPSP2) to the first fEPSP (fEPSP1) amplitude within 1st burst in 1st TBS train was observed in the KO slice and marked with blue bars. This intra-burst facilitation was termed fEPSP ratio (fEPSP2/fEPSP1 amplitude of 1st burst in 1st TBS train) and was significantly larger in KO slices than in WT slices (Figure 18C, WT mice, n = 10, fEPSP ratio: 1.15 ± 0.02 mV, KO mice, n = 9, fEPSP ratio: 1.32 ± 0.02 mV, $p < 0.05$).

Subsequently, slopes of the 1st burst in the 1st-4th TBS train were averaged and compared between WT and KO slices (Figure 18D). The mean slope of the 1st burst in the 1st TBS train was similar between both genotypes and measured respectively 284 ± 31.99 mV/ms in WT slices and 288.4 ± 38.83 mV/ms in KO slices (WT mice, n = 10, KO mice, n = 9, $p > 0.05$). However, only in WT slices, the slope of the 1st burst increased to 393 ± 51.77 mV/ms in the 2nd TBS train, to 378.7 ± 50.32 mV/ms in the 3rd TBS train and to 351 ± 45.56 mV/ms in the 4th TBS train. In KO slices, the slope of the 1st burst remained nearly constant through all TBS trains (1st burst in 2nd TBS train: 267 ± 20.69 mV/ms, 1st burst in 3rd TBS train: 294 ± 24.60 mV/ms and 1st burst in 4th TBS train: 274 ± 25.67 mV/ms). Although the absolute burst slope values were clearly larger in WT compared to KO slices, this difference did not reach statistical significances (WT mice, n = 10, KO mice, n = 9, $p > 0.05$), possibly due to high inter-slice variability. To reduce this variability, the slope ratio of the 1st burst in 2nd-4th TBS train to 1st TBS train was calculated for each slice separately and thereafter averaged per group. Mean values of this slope ratio from WT and KO mice are shown in Figure 18E. The slope ratio of the 1st burst in 2nd TBS:1st TBS train was significantly lower in KO slices compared to WT slices (WT mice, n = 10, slope ratio of the 1st burst in 2nd TBS:1st TBS train: 1.36 ± 0.06, KO mice, n = 9, slope ratio of the 1st burst in 2nd TBS:1st TBS train: 1.02 ± 0.10, $p > 0.05$) while the slope ratios of the 1st burst in 3rd TBS:1st TBS train (WT mice: 1.31 ± 0.07, KO mice: 1.09 ± 0.08) and in the 4th TBS:1st TBS train (WT mice: 1.21 ± 0.06, KO mice: 1.03 ± 0.10) were more elevated in WT mice without reaching significant differences between genotypes (WT mice, n = 10, KO mice, n = 9, $p > 0.05$).

The same analysis performed on HT slices yielded values of TBS slope ratio that were intermediate between WT and KO slices (1st burst in 2nd TBS:1st TBS train: 1.15 ± 0.3, 1st burst in 3rd TBS:1st TBS train: 1.12 ± 0.04, 1st burst in the 4th TBS:1st TBS train: 1.08 ± 0.05) but were not significant compared to WT or KO slices (WT mice, n = 10, HT mice, n = 9, KO mice, n = 9, $p > 0.05$).

4.1.7 Analysis of basal synaptic transmission

In theory, alteration in the seize of synaptic strength between WT and KO mice could explain the reduction in l-LTP observed in KO mice. To test this hypothesis, the amplitudes of the fEPSP slope, fiber volley and the paired pulse facilitation ratio were measured and compared between genotypes. Input/output curves of the baseline fEPSP amplitude were measured and averaged over all stimulation and control pathways in WT, HT and KO slices. It is widely accepted that the slope of the evoked fEPSPs is correlated with synchronous depolarization of postsynaptic cells while its amplitude reflects the number of simultaneously activated neurons (Stringer et al. 1983). In the following figures, the input/output curves of fEPSP amplitudes were analyzed in two ways. First, the fEPSP amplitude was measured and plotted against the stimulus intensity and second, the ratio of the fEPSP over the FV amplitude was plotted against the stimulus intensity.

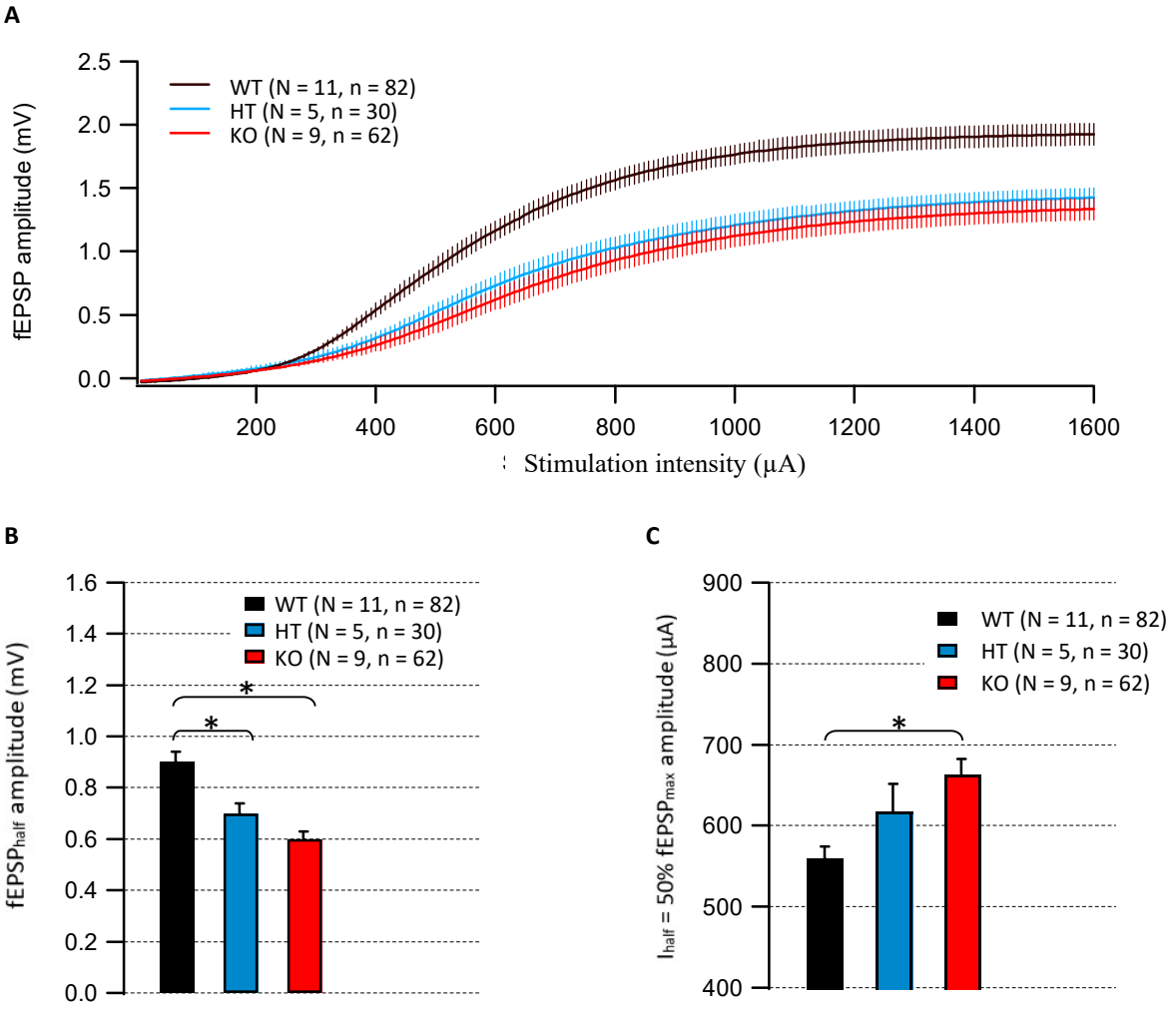

Figure 19: Input/output curves in WT, HT and KO mice. (A) Stimulation intensity was plotted against averaged fEPSP amplitude. Compared to WT, HT and KO slices showed reduced fEPSP amplitudes. **(B, C)** Bar diagrams of averaged values of $fEPSP_{half}$ amplitude and I_{half}. $FEPSP_{half}$ amplitude was lowest in KO slices, followed by HT and WT slices. I_{half} was highest in KO slices, intermediate in HT slices and lowest in WT slices. Bars represent means ± SEM, and asterisks ($p < 0.05$).

Figure 19A represents IO curves averaged from WT (N = 11, n = 82), HT (N = 5, n = 30) and KO slices (N = 9, n = 62). HT and KO slices showed initially flatter input/output curves and reached a lower plateau of fEPSP amplitudes compared to WT slices. The $fEPSP_{max}$-A at plateau level was 1.4 ± 0.08 mV in HT slices and 1.3 ± 0.06 mV in KO slices while WT slices reached the seize of 1.9 ± 0.09 mV. Bar diagrams in Figure 19B and 19C represent mean $fEPSP_{half}$ amplitude at I_{half} and I_{half}, respectively in all three genotypes. In contrast to WT slices ($fEPSP_{half}$-A: 0.9 ± 0.04 mV, I_{half}: 560 ± 15.27 µA), HT and KO slices generated smaller $fEPSP_{half}$-A (HT mice, $fEPSP_{half}$-A: 0.7 ± 0.04 mV, KO mice, $fEPSP_{half}$-A: 0.6 ± 0.03 mV) in response to higher stimulation intensity (HT mice, I_{half}: 617 ± 34.8 µA, KO mice, I_{half}: 662 ± 19.88 µA).

Statistical analysis using one-way ANOVA showed significant difference of the magnitude of $fEPSP_{half}$-A and I_{half} between genotypes. The $fEPSP_{half}$-A was significantly different in WT slices compared respectively to HT and to KO slices (WT mice, n = 82, HT mice, n = 30, KO mice, n = 62, respectively $p < 0.001$) while HT to KO mice did not show significant difference (HT mice, n = 30, KO mice, n = 62, $p > 0.05$). Values of I_{half} were only significantly distinct between WT and KO mice (WT mice, n = 82, KO mice, n = 62, $p < 0.001$).

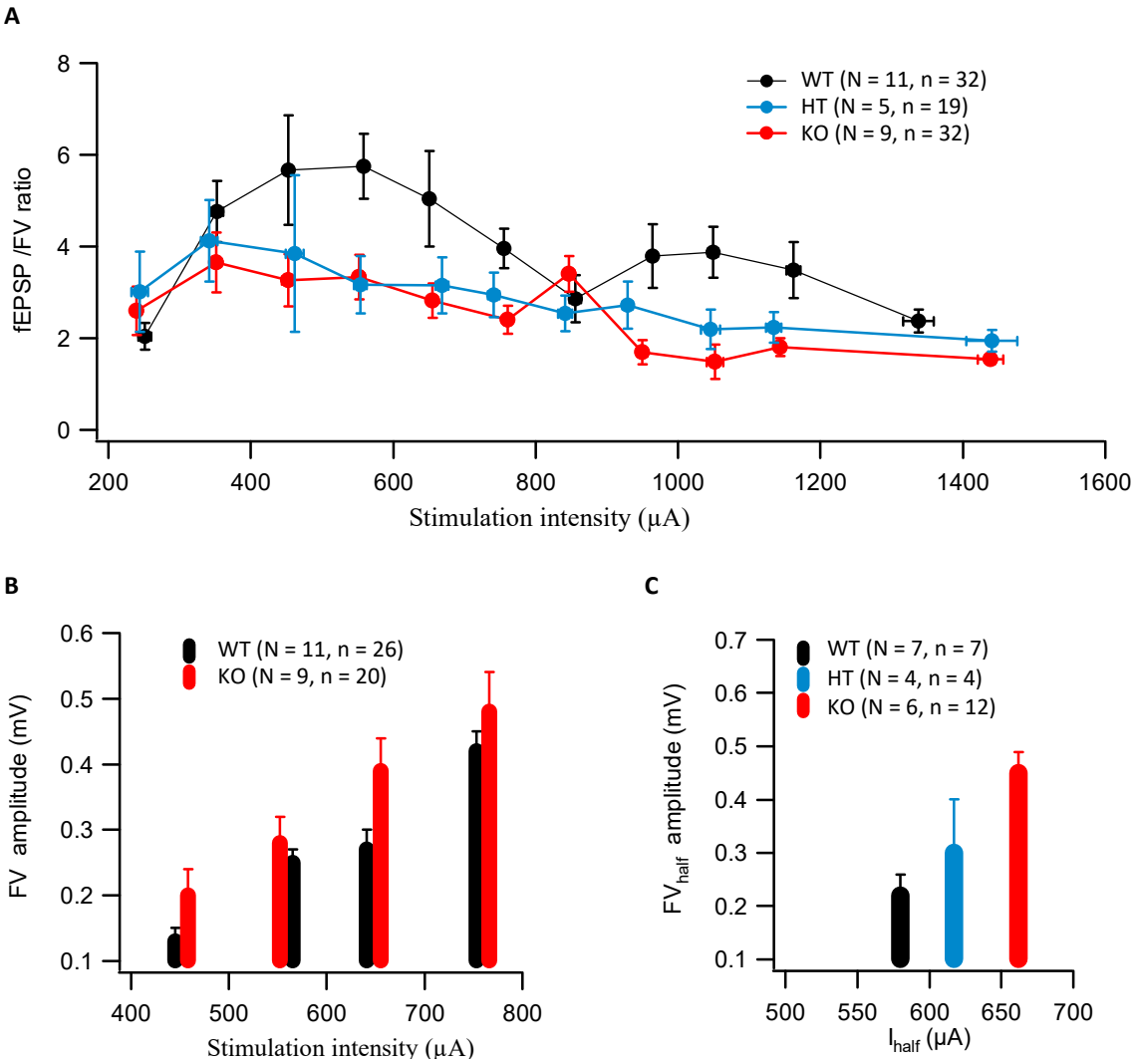

Figure 20: Basal synaptic transmission in WT, HT and KO mice. (A) HT and KO slices showed slightly reduced fEPSP/FV ratio compared to WT slices. **(B)** Bar plots showed mean FV amplitudes at four distinct stimulation intensities. KO slices exhibited increased FV amplitudes compared to WT slices. **(C)** Respective I_{half} applied in LTP experiments was plotted against the mean FV_{half} amplitude. Larger FV_{half} amplitudes in HT and KO slices compared to WT slices were found.

Next, fEPSP slopes were normalized to FV amplitudes (fEPSP/FV ratio), to account for possible differences in presynaptic excitability. In Figure 20A, stimulation intensities were plotted against fEPSP/FV ratio in WT (N = 11, n = 32), HT (N = 5, n = 19) and KO slices (N = 9,

n = 32). HT and KO slices exhibited lower fEPSP/FV ratio, especially at stimulation intensities between 400 and 600 µA, compared to WT slices. As demonstrated in Figure 20B, the absolute mean FV amplitude (FV-A) was calculated and averaged at four distinct stimulation intensities from WT (N = 11, n = 26) and KO slices (N = 9, n = 20). Consistently, each mean FV-A was larger in KO (0.2 ± 0.04 mV, 0.28 ± 0.04 mV, 0.39 ± 0.04 mV, 0.48 ± 0.06 mV) than in WT slices (0.3 ± 0.06 mV, 0.24 ± 0.06 mV, 0.25 ± 0.05 mV, 0.41 ± 0.06 mV), although this difference was not statistically significant (WT mice, n = 26, KO mice, n = 20, $p > 0.05$). Figure 20C shows the mean FV_{half} amplitude at I_{half} calculated for each individual LTP experiment in WT (N = 7, n = 7), HT (N = 4, n = 4) and KO slices (N = 6, n = 12). HT and KO slices exhibited slightly higher FV_{half} amplitudes (HT mice, FV_{half}-A: 0.30 ± 0.10 mV, KO mice, FV_{half}-A: 0.45 ± 0.08 mV) compared to WT slices (FV_{half}-A: 0.22 ± 0.04 mV) at I_{half}. These differences were not significant (WT mice, n = 7, HT mice, n = 4, KO mice, n = 12, $p > 0.05$), indicating that presynaptic excitability alone cannot explain the deficits in fEPSP amplitudes in the KO and HT slices.

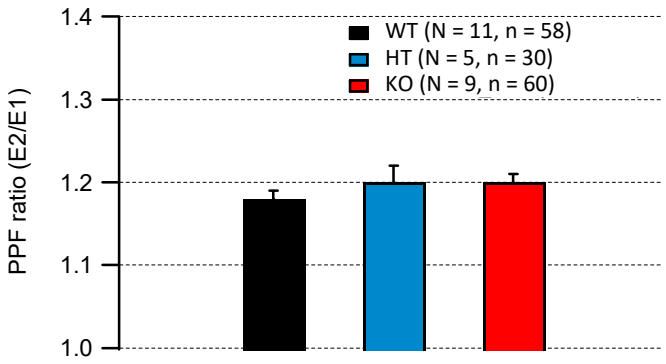

Figure 21: Paired pulse facilitation ratio in WT, HT and KO mice. The bar diagram represented similar magnitude of PPF ratio in WT, HT and KO slices. (E2/E1: fEPSP amplitude of Electrode 1 to fEPSP amplitude of Electrode 2).

To complete investigation of basal synaptic function, paired pulse facilitation tests were performed. In PPF test, a sequence of paired stimuli was delivered to the stimulation and control pathway, independently. The facilitation ratio was calculated in individual pathways, averaged from WT (N = 11, n = 58), HT (N = 5, n = 30) and KO slices (N = 9, n = 60) and illustrated in Figure 21. Here, all three genotypes showed similar PPF ratios of 1.18 ± 0.01, 1.2 ± 0.02 and 1.2 ± 0.01, respectively. These data suggests that presynaptic release mechanisms underlying PPF tests are not altered in the KO and HT mice.

4.2 LTP in conditional Arc/Arg3.1 mice

Arc/Arg3.1 is expressed in the hippocampus during early postnatal development (Gao et al. unpublished results). The role of Arc/Arg3.1 during this developmental period is not known yet. To address this question, mice with a floxed Arc/Arg3.1 allele were generated in our laboratory. In these mice, the open reading frame of Arc/Arg3.1 allele was flanked by LoxP sites (Arc/Arg3.1$^{f/f}$) (Plath et al. 2006). Arc/Arg3.1$^{f/f}$ mice were bred with CamKIIα-Cre mice (Casanova et al. 2001) to generate conditional KO mice (Arc/Arg3.1$^{f/f,\ Cre+}$, cKO mice). Immunoblotting and in situ hybridization demonstrated that Arc/Arg3.1 was completely and irreversibly removed between P7 (postnatal day 7) and P14 (postnatal day 14). In the conditional Arc/Arg3.1$^{f/f,\ Cre+}$ mice Arc/Arg3.1 is present until P14, whereas in the conventional KO mice, it is absent from the germ-line. In the following part of the thesis I studied how postnatal deletion of Arc/Arg3.1 in the Arc/Arg3.1$^{f/f,\ Cre+}$ mice affected e-LTP, l-LTP and basal synaptic transmission under experimental conditions identical to those used in conventional KO mice.

4.2.1 Stable l-LTP in control groups

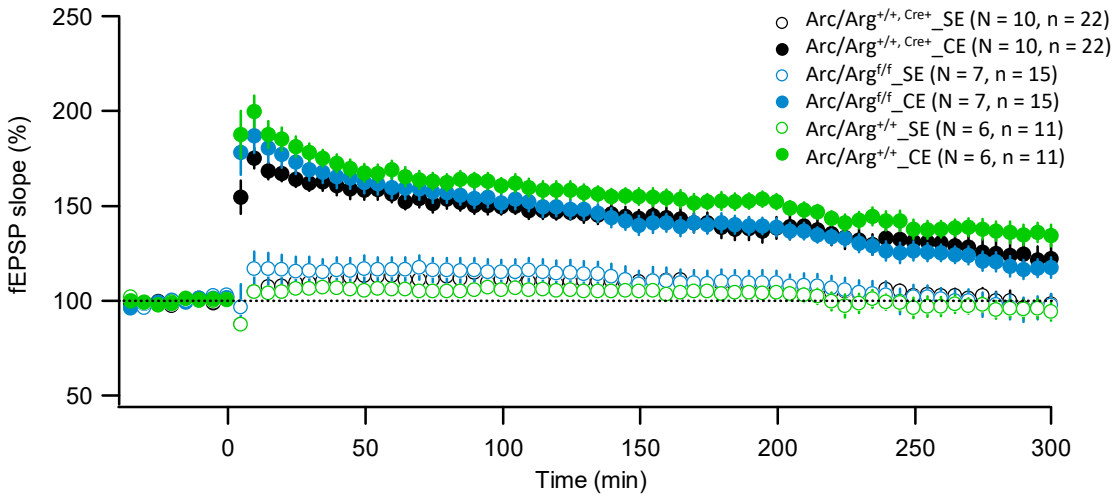

Figure 22: LTP time course in conditional control groups. Entire fEPSP slopes of LTP time course showed similar size of potentiation post 4 TBS application in Arc/Arg3.1$^{+/+,\ Cre+}$, Arc/Arg3.1$^{f/f}$ and Arc/Arg3.1$^{+/+}$ slices.

Although the cre recombinase system is widely applied for generating conditional knockout mice, some publications report that the cre recombinase enzyme and the loxP sites might cause off target effects, interfering with experimental results (Tronche et al. 2002). To rule out influences of cre-loxP system, synaptic function in control groups was verified. The control groups included three genetically different types of "wild-type" mice which carried either the loxP sites (Arc/Arg3.1$^{f/f}$), or wild-type mice expressing cre recombinase enzyme (Arc/Arg3.1$^{+/+,\ Cre+}$) or wild-type mice with no additional manipulations (Arc/Arg3.1$^{+/+}$).

Figure 22 shows the averaged LTP time course from Arc/Arg3.1$^{+/+,\ Cre+}$ (N = 10, n = 22), Arc/Arg3.1$^{f/f}$ (N = 7, n = 15) and Arc/Arg3.1$^{+/+}$ slices (N = 6, n = 11). After 40 min of baseline recording, 4 TBS trains were applied to the stimulation pathway of each genotype. All control groups rapidly responded with a similar increase in fEPSP slopes (Arc/Arg3.1$^{+/+,\ Cre+}$ mice, n = 22, e-LTP: 175 ± 6.25%, Arc/Arg3.1$^{f/f}$ mice, n = 15, e-LTP: 199 ± 8.74%, Arc/Arg3.1$^{+/+}$ mice, n = 11, e-LTP: 199 ± 11.61%, $p > 0.05$), which was highly significant compared to baseline (Arc/Arg3.1$^{+/+,\ Cre+}$ mice, n = 22, Arc/Arg3.1$^{f/f}$ mice, n = 15, Arc/Arg3.1$^{+/+}$ mice, n = 11, $p < 0.001$). The entire subsequent part of the LTP time course was indistinguishable between genotypes (Arc/Arg3.1$^{+/+,\ Cre+}$ mice, n = 22, l-LTP: 123 ± 7.20%, Arc/Arg3.1$^{f/f}$ mice, n = 15, l-LTP: 121 ± 5.65%,, Arc/Arg3.1$^{+/+}$ mice, n = 11, l-LTP: 136 ± 6.17%, $p > 0.05$) and remained significantly potentiated compared to corresponding baseline (Arc/Arg3.1$^{+/+,\ Cre+}$ mice, n = 22, $p < 0.001$-0.01, Arc/Arg3.1$^{f/f}$ mice, n = 15, $p < 0.01$-0.05 expect time points: 289.5 min and 299.5 min $p > 0.05$, Arc/Arg3.1$^{+/+}$ mice, n = 11, $p < 0.001$) and to control pathway (Arc/Arg3.1$^{+/+,\ Cre+}$ mice, n = 22, $p < 0.01$, Arc/Arg3.1$^{f/f}$ mice, n = 15, $p < 0.05$, Arc/Arg3.1$^{+/+}$ mice, n = 11, $p < 0.001$-0.01).

Additionally Arc/Arg3.1$^{+/+,\ Cre+}$, Arc/Arg3.1$^{f/f}$ and Arc/Arg3.1$^{+/+}$ mice were tested in input/output fEPSP curves, paired pulse facilitation and fEPSP/FV ratio whose results were comparable between genotypes (data not shown). These results demonstrate that cre recombinase and loxP site modifications did not appreciably affect synaptic transmission or LTP. Because Cre-recombinase poses the greater risk of off-target effects, all subsequent experiments were performed on Arc/Arg3.1$^{+/+,\ Cre+}$ mice and compared to Arc/Arg3.1$^{f/f,\ Cre+}$ mice.

4.2.2 Stable l-LTP in cKO mice

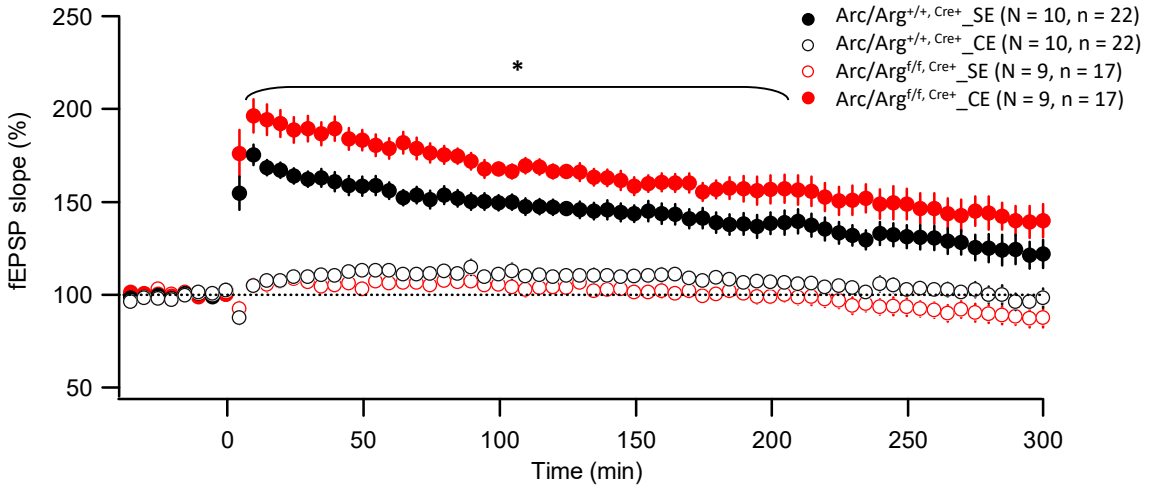

Figure 23: LTP time course in conditional Arc/Arg3.1 mice. LTP induced by 4 TBS, elicited stable LTP in Arc/Arg3.1$^{f/f,\ Cre+}$ slices which even exceeded LTP in Arc/Arg3.1$^{+/+,\ Cre+}$ slices. Significant difference of both stimulated pathways were indicated. Bars represent means ± SEM, and asterisks ($p < 0.05$).

Next, I investigated the functional consequences of postnatal deletion of Arc/Arg3.1 on LTP in the adult mice. The LTP time course from Arc/Arg3.1$^{+/+,\ Cre+}$ slices (N = 10, n = 22) and Arc/Arg3.1$^{f/f,\ Cre+}$ slices (N = 9, n = 17) are shown in Figure 23. Surprisingly and in contrast to conventional Arc/Arg3.1 deficient mice, Arc/Arg3.1$^{f/f,\ Cre+}$ mice showed a stable and persistent LTP. After 4 TBS application fEPSP slopes in Arc/Arg3.1$^{f/f,\ Cre+}$ slices potentiated rapidly to a level of 203 ± 8.95% (e-LTP) and were highly significant compared to baseline (n = 17, $p < 0.001$). Over 5 hours of recording fEPSP slopes stayed significantly elevated compared to baseline stimulation (n = 17, $p < 0.001$) and to control pathway (n = 17, $p < 0.001$). L-LTP measured 137 ± 9.62% and was significantly increased (n = 17, SE to baseline: $p < 0.001$, SE to CE $p < 0.01$-0.001). Comparing synaptic response from both genotypes, the LTP time course of Arc/Arg3.1$^{f/f,\ Cre+}$ mice was entirely higher than in Arc/Arg3.1$^{+/+,\ Cre+}$ mice and showed significant difference until 204.5 min post TBS application (Arc/Arg3.1$^{f/f,\ Cre+}$ mice, n = 17, Arc/Arg3.1$^{+/+,\ Cre+}$ mice, n = 22, $p < 0.01$-0.05). The following figures summarize e-LTP and l-LTP values in both genotypes and analyze the reliability of l-LTP induction in single experiments.

4.2.3 Comparison of LTP and induction of successful l-LTP

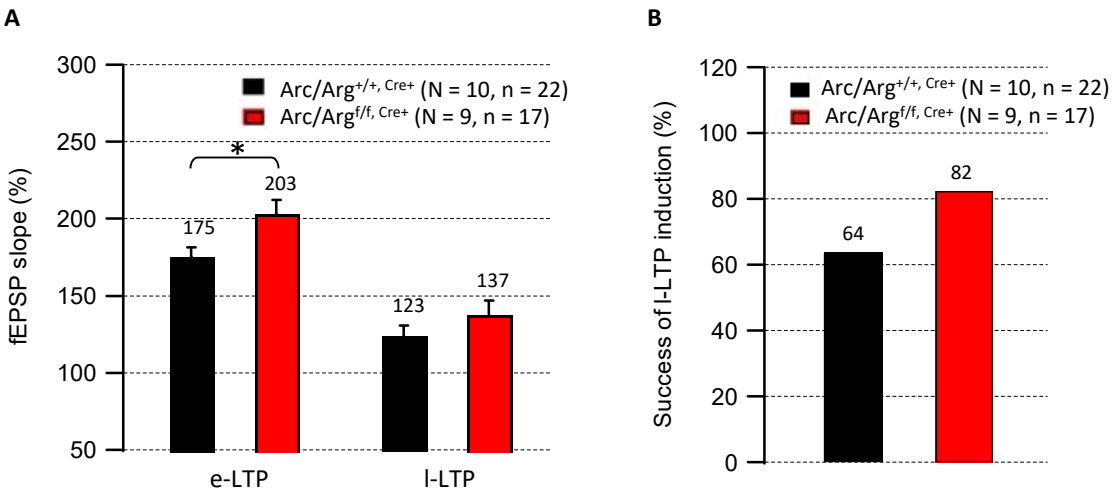

Figure 24: Summery of e-LTP, l-LTP and successful l-LTP induction in conditional Arc/Arg3.1 mice. (A) Bar diagram showed the significantly larger e-LTP in Arc/Arg3.1$^{f/f, Cre+}$ slices compared to Arc/Arg3.1$^{+/+, Cre+}$ slices. The seize of l-LTP was similar in both genotypes. Bars represent means ± SEM, numbers above the bars show mean value. Asterisks mark $P < 0.05$. **(B)** Higher percentage of successful l-LTP experiments in Arc/Arg3.1$^{f/f, Cre+}$ slices compared to Arc/Arg3.1$^{+/+, Cre+}$ slices. Numbers above the bars show mean percentage.

The different magnitudes of e-LTP and l-LTP in conditional slices are illustrated as bar diagrams and showed in Figure 24A. Similarly to conventional Arc/Arg3.1 KO slices (see Figure 15B), Arc/Arg3.1$^{f/f, Cre+}$ slices exhibited significantly larger e-LTP compared to Arc/Arg3.1$^{+/+, Cre+}$ slices (Arc/Arg3.1$^{+/+, Cre+}$ mice, n = 22, Arc/Arg3.1$^{f/f, Cre+}$ mice, n = 17, $p < 0.05$). L-LTP was slightly but not significantly higher in Arc/Arg3.1$^{f/f, Cre+}$ mice compared to Arc/Arg3.1$^{+/+, Cre+}$ slices (Arc/Arg3.1$^{+/+, Cre+}$ mice, n = 22, Arc/Arg3.1$^{f/f, Cre+}$ mice, n = 17, $p > 0.05$). Analysis of successful l-LTP induction (Figure 24B) revealed a higher percentage of successfully induced l-LTP in Arc/Arg3.1$^{f/f, Cre+}$ slices (82%, 14 out of 17 slices) than in Arc/Arg3.1$^{+/+, Cre+}$ slices (63%, 14 out of 22 slices). These findings demonstrate a reliable and comparable form of l-LTP in the hippocampal CA1 region in Arc/Arg3.1$^{+/+, Cre+}$ and Arc/Arg3.1$^{f/f, Cre+}$ mice which seem to be independent of Arg.3.1 protein expression. These results deviate from the instable l-LTP observed in the conventional Arc/Arg3.1 KO mice and suggest that Arc/Arg3.1 expression in early development influences the ability to recruit LTP in the adult mouse.

4.2.4 Similar fEPSP responses during TBS trains

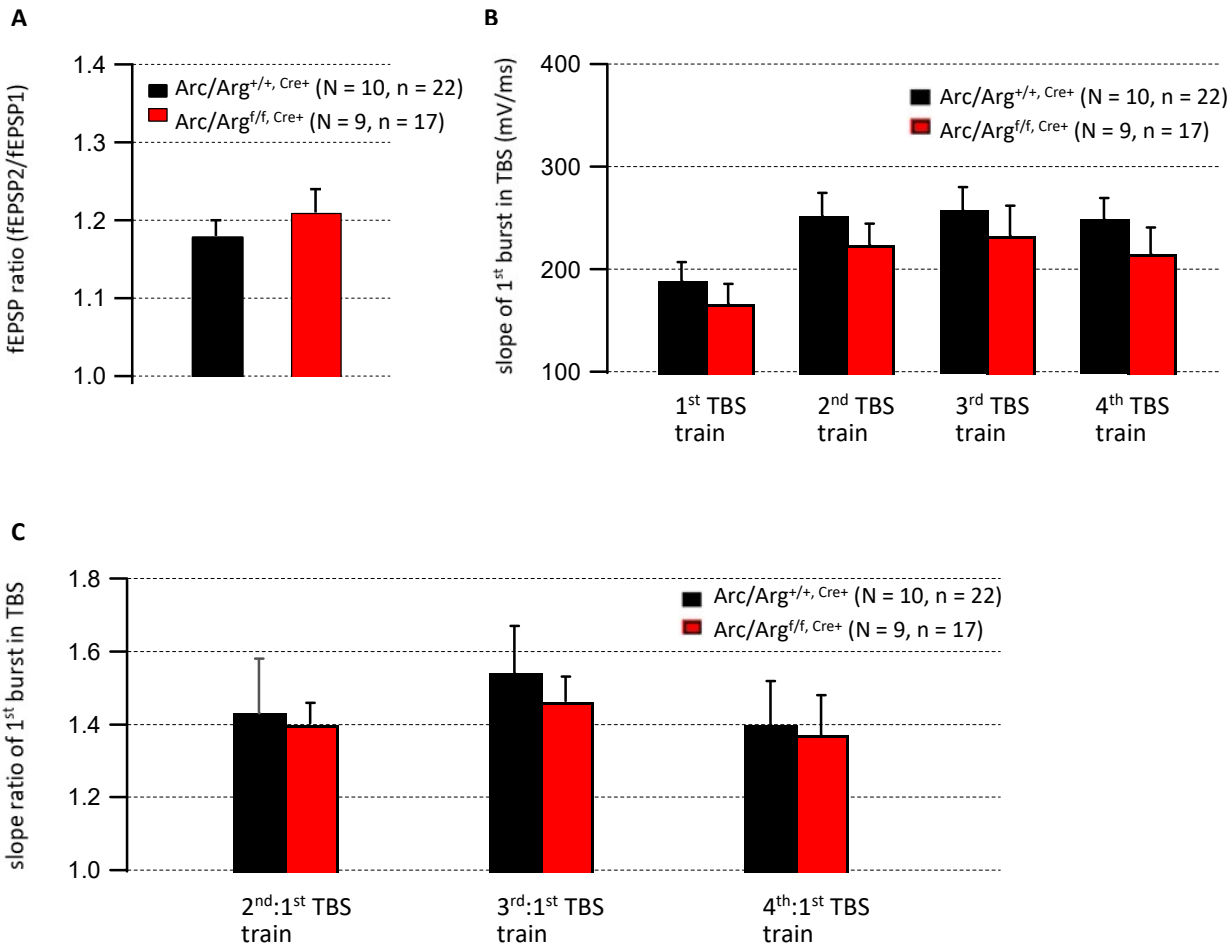

Figure 25: Analysis of fEPSP slopes in TBS trains in conditional Arc/Arg3.1 mice. (A) Bar diagram showed similar intra-burst facilitation from fEPSP ratio of the second (2) to the first (1) fEPSP amplitude of 1st burst in 1st TBS train in Arc/Arg3.1$^{+/+, Cre+}$ and Arc/Arg3.1$^{f/f, Cre+}$ slices. **(B)** FEPSP slope analysis of 1st burst respectively in 1st-4th TBS train in Arc/Arg3.1$^{+/+, Cre+}$ and Arc/Arg3.1$^{f/f, Cre+}$ slices. FEPSP slopes were not different between genotypes. **(C)** Comparable slope ratio of 1st burst in second, third and fourth TBS train to 1st burst in 1st TBS train in Arc/Arg3.1$^{+/+, Cre+}$ and Arc/Arg3.1$^{f/f, Cre+}$ slices.

Bar diagrams in Figure 25A-C show the analysis of mean fEPSP slope responses during TBS trains averaged from Arc/Arg3.1$^{+/+, Cre+}$ slices (N = 10, n = 22) and Arc/Arg3.1$^{f/f, Cre+}$ slices (N = 9, n = 17). As illustrated in Figure 25A, fEPSP ratios of the second fEPSP (fEPSP2) to first fEPSP (fEPSP1) amplitude of the 1st burst in 1st TBS train were comparable and not significant in both genotypes (Arc/Arg3.1$^{+/+, Cre+}$ mice, n = 22, Arc/Arg3.1$^{f/f, Cre+}$ mice, n = 17, $p > 0.05$). Here Arc/Arg3.1$^{+/+, Cre+}$ and Arc/Arg3.1$^{f/f, Cre+}$ slices displayed intra-burst facilitations in the seize of 1.18 ± 0.02 mV and 1.21 ± 0.03 mV. The next bar diagram demonstrates the mean slope of the 1st burst in the 1st-4th TBS train (Figure 25B). In Arc/Arg3.1$^{+/+, Cre+}$ slices, the mean slope of the 1st burst in the successive TBS trains (1st-4th TBS train) was respectively 189 ± 18.07

mV/ms, 252 ± 22.71 mV/ms, 256 ± 22.61 mV/ms and 249 ± 20.84 mV/ms while Arc/Arg3.1$^{f/f,\ Cre+}$ slices showed values of respectively 166 ± 19.09 mV/ms, 224 ± 20.52 mV/ms, 232 ± 20.19 mV/ms and 215 ± 21.77 mV/ms. During TBS trains, the magnitude of these slopes increased slightly and similarly in both genotypes without showing statistical significances (Arc/Arg3.1$^{+/+,\ Cre+}$ mice, n = 22, Arc/Arg3.1$^{f/f,\ Cre+}$ mice, n = 17, $p > 0.05$). Subsequently fEPSP slope ratios of 1st burst in second, third and fourth TBS train to 1st burst in 1st TBS train were calculated and compared, and are illustrated in Figure 35C. Arc/Arg3.1$^{+/+,\ Cre+}$ and Arc/Arg3.1$^{f/f,\ Cre+}$ slices showed similar values in all fEPSP slope ratios (Arc/Arg3.1$^{+/+,\ Cre+}$ mice, 1st burst in 2nd TBS:1st TBS train: 1.43 ± 0.15, 1st burst in 3rd TBS:1st TBS train: 1.45 ± 0.13, 1st burst in the 4th TBS:1st TBS train: 1.40 ± 0.12, Arc/Arg3.1$^{f/f,\ Cre+}$ mice, 1st burst in 2nd TBS:1st TBS train: 1.40 ± 0.06, 1st burst in 3rd TBS:1st TBS train: 1.46 ± 0.07, 1st burst in the 4th TBS:1st TBS train: 1.37 ± 0.11) and a minor increase of the fEPSP slope ratio of 1st burst in 3rd TBS:1st TBS train. Remarkably, Arc/Arg3.1$^{f/f,\ Cre+}$ mice tended to constantly smaller inter-burst facilitation values compared to Arc/Arg3.1$^{+/+,\ Cre+}$ slices. However no significant level was detected from the results of fEPSP slope ratios (Arc/Arg3.1$^{+/+,\ Cre+}$ mice, n = 22, Arc/Arg3.1$^{f/f,\ Cre+}$ mice, n = 17, $p > 0.05$).

4.2.5 Analysis of basal synaptic transmission

Input/output curves of the fEPSP amplitudes were analyzed to investigate potential differences in postsynaptic fEPSPs in slopes conditional Arc/Arg3.1 mice.

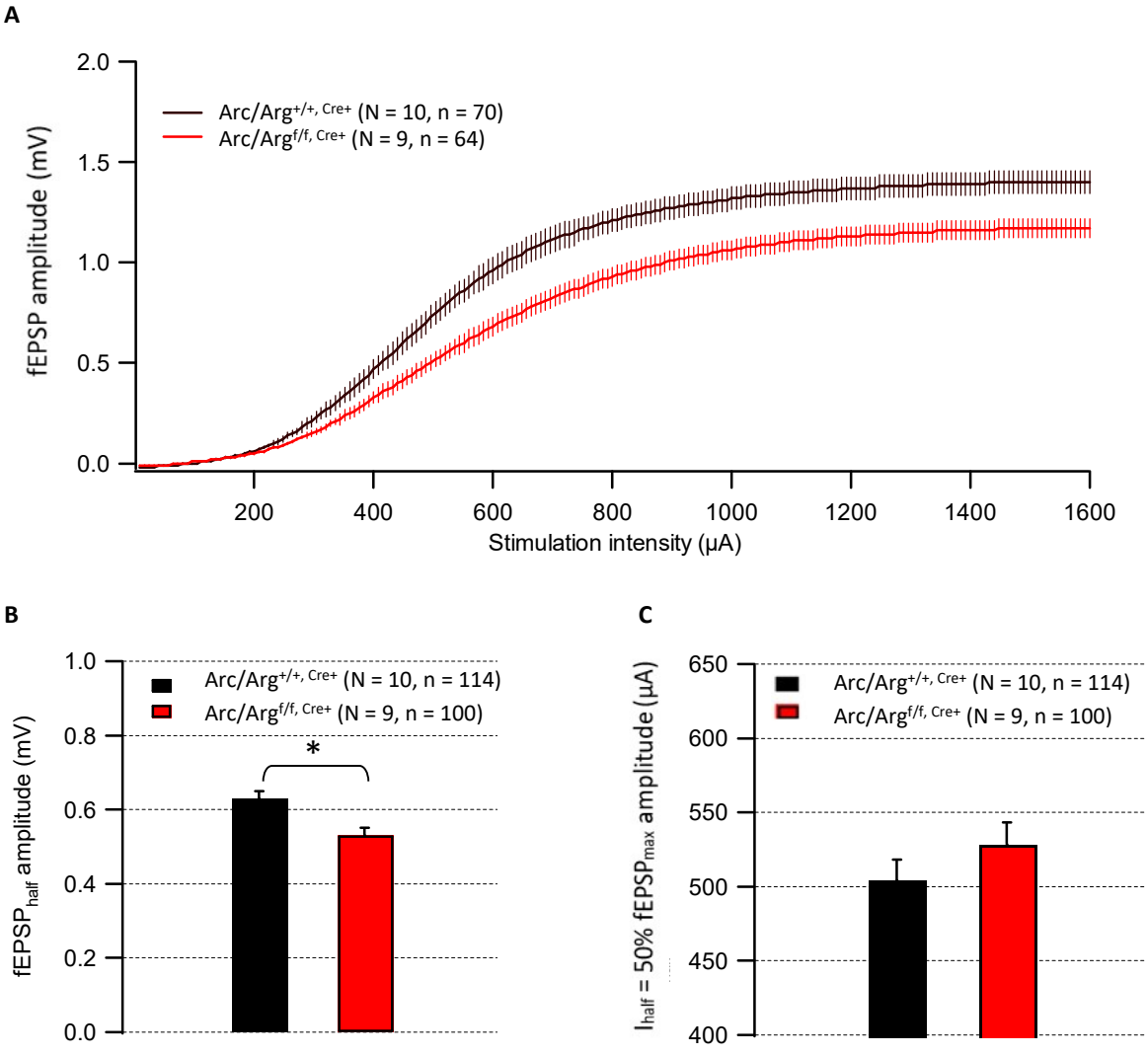

Figure 26: Input/output curves in conditional Arc/Arg3.1 mice. (A) Input/output curves, measured as stimulation intensity plotted against fEPSP amplitude, showed impaired postsynaptic cell responses at all stimulation intensities in Arc/Arg3.1$^{f/f,\ Cre+}$ mice compared to Arc/Arg3.1$^{+/+,\ Cre+}$ mice. **(B, C)** Bar diagrams of averaged magnitude of $fEPSP_{half}$ amplitude and I_{half}. Arc/Arg3.1$^{f/f,\ Cre+}$ slices showed significantly reduced $fEPSP_{half}$ amplitude in response to higher I_{half} application compared to Arc/Arg3.1$^{+/+,\ Cre+}$ slices. Bars represent means ± SEM, and asterisks ($p < 0.05$).

Figure 26A shows the averaged input/output curves from Arc/Arg3.1$^{+/+,\ Cre+}$ (N = 10, n = 70) and Arc/Arg3.1$^{f/f,\ Cre+}$ (N = 9, n = 64) mice. Arc/Arg3.1$^{f/f,\ Cre+}$ mice showed a flatter rising slope

in the input/output curve and lower plateau with $fEPSP_{max}$-A of 1.1 ± 0.05 mV, while Arc/Arg3.1$^{+/+,\ Cre+}$ mice reached $fEPSP_{max}$-A of 1.4 ± 0.06 mV. The bar diagrams in Figure 26B and 26C illustrate $fEPSP_{half}$ amplitudes at I_{half} and the stimulation intensities I_{half} in both genotypes. In Arc/Arg3.1$^{+/+,\ Cre+}$ mice, the mean I_{half} was of 504 ± 13.84 µA and elicited an averaged $fEPSP_{half}$-A of 0.63 ± 0.02 mV. In Arc/Arg3.1$^{f/f,\ Cre+}$ mice I_{half} was similar in the seize of 529 ± 15.06 µA and not significant compared to Arc/Arg3.1$^{+/+,\ Cre+}$ mice (Arc/Arg3.1$^{+/+,\ Cre+}$ mice, n = 114, Arc/Arg3.1$^{f/f,\ Cre+}$ mice, n = 100, $p > 0.05$). However, this I_{half} elicited significantly smaller $fEPSP_{half}$-A in the seize of 0.53 ± 0.02 mV (Arc/Arg3.1$^{+/+,\ Cre+}$ mice, n = 114, Arc/Arg3.1$^{f/f,\ Cre+}$ mice, n = 100, $p < 0.05$).

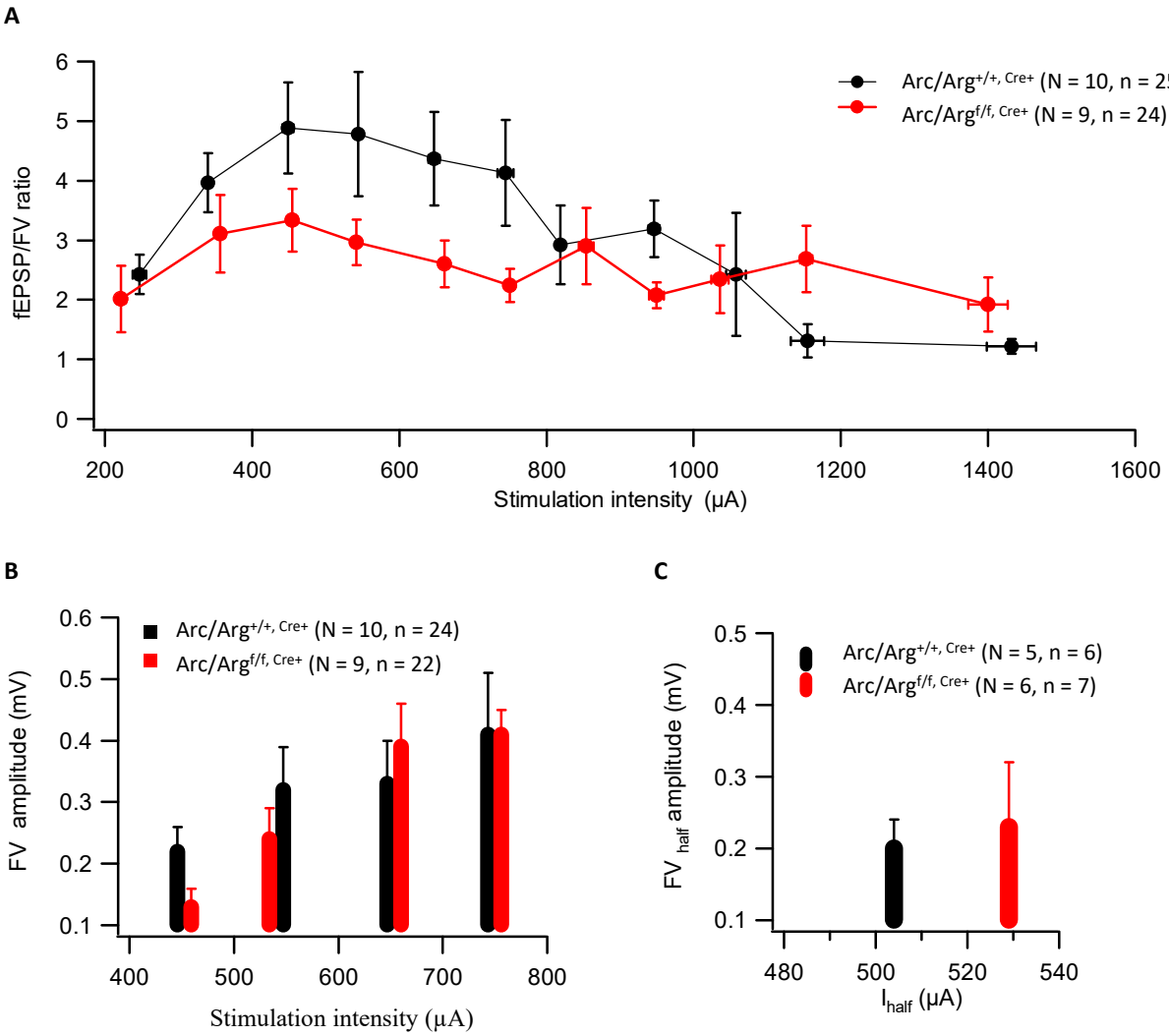

Figure 27: Basal synaptic transmission in conditional Arc/Arg3.1 mice. (A) Stimulation intensity was plotted against fEPSP/FV ratio and showed slightly reduced basal synaptic transmission in Arc/Arg3.1$^{f/f,\ Cre+}$ slices. **(B, C)** Bar diagrams showed mean FV amplitudes at four averaged stimulation intensities extracted from Figure 27A and mean FV_{half} amplitudes at I_{half}. Arc/Arg3.1$^{+/+,Cre+}$ and Arc/Arg3.1$^{f/f,\ Cre+}$ mice exhibited comparable results of both, FV amplitudes and FV_{half} amplitudes at I_{half}.

In Figure 27A, fEPSP/FV ratio was plotted against stimulation intensity to investigate presynaptic excitability from Arc/Arg3.1$^{+/+, Cre+}$ (N = 10, n = 25) and Arc/Arg3.1$^{f/f, Cre+}$ slices (N = 9, n = 24). Both genotypes showed similar fEPSP/FV ratios at all tested stimulation intensities. The bar diagram of Figure 27B illustrates and compares the mean FV-A at four averaged stimulation intensities extracted from Figure 27A from Arc/Arg3.1$^{+/+, Cre+}$ (N = 10, n = 24) and Arc/Arg3.1$^{f/f, Cre+}$ slices (N = 9, n = 22). Here, no significant difference between these mice was detected (Arc/Arg3.1$^{+/+, Cre+}$ mice, n = 24, FV amplitudes: 0.22 ± 0.04, 0.32 ± 0.07, 0.33 ± 0.07, 0.41 ± 0.10, Arc/Arg3.1$^{f/f, Cre+}$ mice, n = 22, FV amplitudes: 0.13 ± 0.03, 0.24 ± 0.05, 0.39 ± 0.07, 0.41 ± 0.04, $p > 0.05$). Likewise FV amplitudes, mean FV_{half} amplitudes at I_{half} averaged from Arc/Arg3.1$^{+/+, Cre+}$ (N = 5, n = 6) and Arc/Arg3.1$^{f/f, Cre+}$ slices (N = 6, n = 7) were indistinguishable (Figure 27C, Arc/Arg3.1$^{+/+, Cre+}$ mice, n = 6, FV_{half}-A: 0.20 ± 0.04 mV, Arc/Arg3.1$^{f/f, Cre+}$ mice, n = 7, FV_{half}-A: 0.23 ± 0.04 mV, $p > 0.05$).
In total, these findings indicate that at low frequency stimulation conditional Arc/Arg3.1$^{f/f, Cre+}$ mice exhibited normal FV amplitudes whereas postsynaptic fEPSP amplitudes seemed to be impaired, compared to Arc/Arg3.1$^{+/+, Cre+}$ mice.

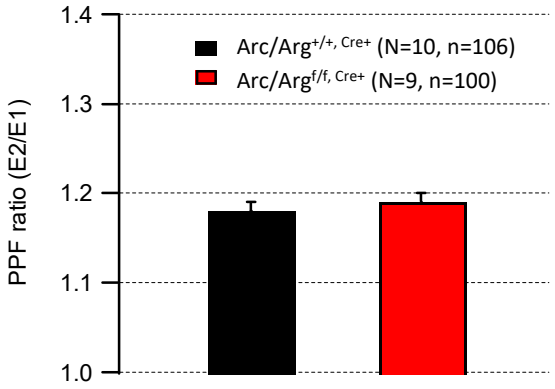

Figure 28: Paired pulse facilitation ratio in conditional Arc/Arg3.1 mice. Arc/Arg3.1$^{+/+, Cre+}$ and Arc/Arg3.1$^{f/f, Cre+}$ slices showed similar seize of PPF ratio (E2/E1: fEPSP amplitude of Electrode 1 to fEPSP amplitude of Electrode 2).

The PPF ratio was averaged and analyzed from Arc/Arg3.1$^{+/+, Cre+}$ (N = 10, n = 106) and Arc/Arg3.1$^{f/f, Cre+}$ slices (N = 9, n = 100). As shown in Figure 28, very similar PPF ratios were obtained between genotypes and measured respectively 1.18 ±0.01 in Arc/Arg3.1$^{+/+, Cre+}$ and 1.19 ± 0.01 in Arc/Arg3.1$^{f/f, Cre+}$ slices (Arc/Arg3.1$^{+/+, Cre+}$ mice, n = 106, Arc/Arg3.1$^{f/f, Cre+}$ mice, n = 100, $p > 0.05$). Together, these findings indicate similar presynaptic release capacity in both genotypes.

4.3 Comparison of synaptic deficits in both mouse lines

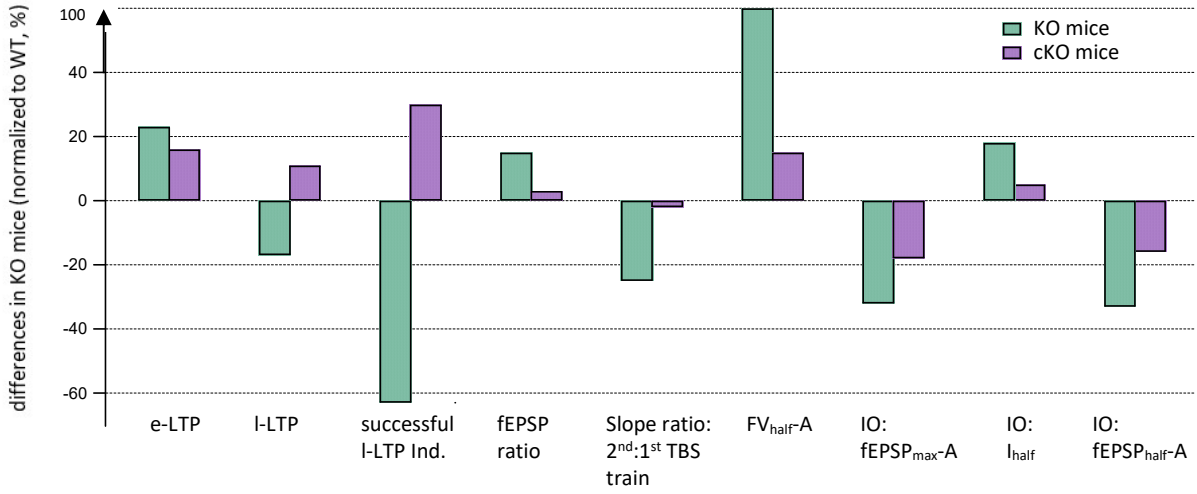

Figure 29: Schematic summary of altered synaptic transmission and plasticity in KO and cKO mice. Various measures of KO and cKO plasticity. Values of KO and cKO were normalized to their respective WT littermates values and presented as Δ change in percentage. Conventional KO mice exhibited more alterations of synaptic transmission and plasticity compared to conditional KO mice (Ind.: induction).

The bar diagram in Figure 29 summarizes selected data from previous tests obtained in conventional and conditional Arc/Arg3.1 KO mice. To illustrate differences from both mouse lines, values of conventional KO mice (KO mice) were normalized to their corresponding wild-type littermates (WT mice) whereas values from conditional KO mice (cKO, Arc/Arg3.1$^{f/f,\ Cre+}$ mice) were normalized to littermates carrying the Cre transgene (Arc/Arg3.1$^{+/+,\ Cre+}$ mice). The measured values were plotted as Δ change in percent (100% was subtracted). Generally, conventional KO mice display stronger deviations from WT compared to conditional Arc/Arg3.1$^{f/f,\ Cre+}$ mice. Post-TBS induced e-LTP differences were similarly increased in both mouse lines (KO mice, Δ e-LTP: +23%, cKO mice, Δ e-LTP: +16%) while the magnitude of l-LTP and percentage of successful l-LTP induction showed opposite alterations (KO mice, Δ l-LTP: -17%, Δ successful l-LTP induction: -63%, cKO mice, Δ l-LTP: +11%, Δ successful l-LTP induction: +30%). Analysis of fEPSP ratio and slope ratio of 1st burst in TBS trains (2nd:1st TBS train) showed significant differences in conventional Arc/Arg3.1 KO mice whereas Arc/Arg3.1$^{f/f,\ Cre+}$ mice were barely affected (KO mice, Δ fEPSP ratio: +15%, Δ slope ratio: -25%, cKO mice, Δ fEPSP ratio: +3%, Δ slope ratio: -2%). Parameters of basal synaptic transmission were also more strongly altered in the conventional mouse line. FV_{half}-A exhibited a high percentage difference of +105% in conventional KO mice while a much smaller difference of +15% was observed in cKO mice. Basic synaptic transmission parameters obtained from input/output curves showed greater alterations in conventional KO mice compared to conditional Arc/Arg3.1$^{f/f,\ Cre+}$ mice (KO mice, Δ $fEPSP_{max}$-A: -32%, Δ I_{half}: +18%, Δ $fEPSP_{half}$-A: -33%, cKO mice: Δ $fEPSP_{max}$-A -18%, Δ I_{half}: +5%, Δ $fEPSP_{half}$-A: -16%).

Parameters	HT mice	KO mice	cKO mice
e-LTP	↑	↑	↑
l-LTP	↓	↓	≅
TBS slope ratio	↓	↓	≅
fEPSP from IO curves	↓/↓	↓	↓
Arc/Arg3.1 remaining amount	50%	0%	0%
Time of Arc/Arg3.1 presence	>E0	--	<P14

Figure 30: Tabular summary of altered synaptic transmission and plasticity in HT, KO and cKO mice. Selected parameters were extracted from Figure 29 and the effects of the absence of Arc/Arg3.1 protein were compared between HT, KO and cKO mice. Similar to conventional KO mice, HT mice showed increased e-LTP and reduced l-LTP, TBS slope ratio and fEPSP slopes from IO curves. Additionally, the Arc/Arg3.1 remaining amount and distinct time points of Arc/Arg3.1 removal were opposed. Only HT mice posed 50% of Arc/Arg3.1 protein amount. The Arc/Arg3.1 gene was present from E0 (embryonic day 0) onwards in HT mice, was always absent in KO mice and was present until P14 in the cKO mice. Small arrows symbolize a weak effect and big arrows a stronger effect of Arc/Arg3.1 absence.

The tabular of Figure 30 shows a summary table of the main parameters of basal and plastic transmission (extracted from Figure 29) in conventional KO and HT mice, and conditional Arc/Arg3.1$^{f/f,\ Cre+}$ mice. Similar to conventional KO mice, HT mice showed elevated initial potentiation (e-LTP) and reduced capacities of long-term potentiation (l-LTP), TBS slope facilitation and basal synaptic response. However, the alterations in synaptic response were similar to conventional KO mice, HT mice were generally less severe affected from the absence of Arc/Arg3.1 protein. Since Arc/Arg3.1 protein deletion occurred only partially (ca. 50%), the results from HT mice might indicate a gene-dose dependent effect of Arc/Arc3.1 protein deletion.

The tabular also illustrates the distinct time points of Arc/Arg3.1 protein deletion. The complete lack of Arc/Arg3.1 protein after P14 from cKO mice reduced especially baseline synaptic transmission, while the reduction or complete lack of Arc/Arg3.1 protein before P14 in the conventional mice affected more severely long-term potentiation, TBS response and baseline transmission. Concerning the amount of increased e-LTP, the elevation seem to be dose dependent and was the most exceeded in the conventional KO mice with complete deletion of Arc/Arg3.1 protein before P14.

5 DISCUSSION

Previous publications demonstrated the major role of Arc/Arg3.1, in consolidation of long-term memory and synaptic plasticity. In this study, I aimed to investigate in detail, the role of Arc/Arg3.1 in TBS-LTP. A form of LTP which links natural neural activity patterns to protein synthesis and to memory formation. In conventional Arc/Arg3.1 KO mice, I investigated TBS-LTP induction probability and persistence and compared the results to WT and heterozygous mice. The study reveals an essential role for Arc/Arg3.1 protein in converting early LTP to late LTP in a manner dependent on the amount of Arc/Arg3.1 present in the brain. Unexpectedly, in the conditional Arc/Arg3.1 deficient mice, TBS-LTP was not impaired. These data suggest that the development stage at which Arc/Arg3.1 is removed could determine its effect on TBS-LTP.

5.1 LTP in conventional KO mice

5.1.1 Stimulus pattern depending long-term potentiation

Similarly to previous reports, the present study used different stimulation paradigms to induce either transient LTP or persistent LTP, separately, in the CA1 region of the hippocampus and showed that transient LTP induction depends on the number of applied TBS trains. In conventional WT slices, 4 TBS trains induced e-LTP and l-LTP whereas a single TBS train induced only e-LTP. In Arc/Arg3.1 KO slices e-LTP was significantly larger after 1 and 4 TBS application than in WT slices and persisted for a longer time. Following LTP time course of KO slices, synaptic responses decayed to baseline after 1 and 4 TBS application and did not consolidate into l-LTP. Notably, l-LTP was successfully induced by a single train of TBS in a limited number of individual LTP experiments in WT and KO mice.

LTP induced by repetitive TBS trains was significantly different in conventional WT and KO mice. As expected, in response to 4 TBS, WT mice showed persistently elevated fEPSP slopes during the entire LTP time course. This persistent LTP was reliably induced in almost all individual LTP experiments. In contrast, 4 TBS trains in Arc/Arg3.1 KO mice induced larger e-LTP which, in most experiments, did not consolidate into l-LTP. However, similar to 1 TBS induced successful l-LTP, a small number of individual experiments in KO slices remained potentiated in the order of l-LTP after 4 TBS stimulation. In the analysis of the LTP time course of only successful induced l-LTP in WT and KO mice (Figure 17), KO mice might still decay to baseline beyond 5 hours of recording time but at a slower rate compared to the majority of KO slices which could reflect an interposed form of LTP (between e-LTP and l-LTP). In recent literature, evidence in support of further categorization of LTP has emerged (Volianskis and Jensen 2003, Raymond 2007, Park et al. 2014). Additionally to e- and l-LTP, they defined a third, intermediate form of LTP which was reported to be storable for hours, to require protein synthesis but not to implicate gene transcription. The magnitude of this

form of LTP depended of the amplitude of stimulation frequency and its decay could be induced by synaptic activation. The extended categorization of LTP might reconcile the finding that l-LTP could still be induced in a few individual Arc/Arg3.1 KO slices and just represents a third form of LTP in these slices. Alternatively, this l-LTP might result from different mechanisms for l-LTP consolidation which are independent of Arc/Arg3.1 protein expression.

5.1.2 Enhanced e-LTP in KO mice

Experiments from conventional Arc/Arg3.1 KO mice have shown that e-LTP is inducible and intact after strong theta burst stimulation, while l-LTP establishment differed in WT and KO mice. In KO slices, the initial fEPSP slopes were increased in response to 1 TBS and 4 TBS and generated in both LTP time courses an exceeding magnitude of e-LTP which was significantly elevated compared to WT mice. The similar initial enhancement of LTP has also been demonstrated in recent reports. Plath and colleagues investigated the LTP time course of HFS-LTP in conventional Arc/Arg3.1 KO mice in which e-LTP exceeded of approximately 40% e-LTP in wild-type mice and decayed back to baseline after 90 minutes of recording (Plath et al 2006). The following part of the work provided several attempts of explanation, but the specific mechanisms underlying this effect are not known yet.

1. A consistent finding in literature is that Arc/Arg3.1 interferes with the endocytic pathway of dynamin and endophilin and regulate AMPA receptor trafficking. Distinct regions of Arc/Arg3.1 interact with dynamin's PH (plextrin homology) domain and endophilin's BAR (Bin/amphiphysin/Rvs) domain and were found together at the postsynaptic density (PSD) where AMPA receptor endocytosis occurs (Chowdhury et al. 2006). Via these endocytic components, Arc/Arg3.1 can initiate the internalization of AMPA receptors and thus, reduce the amount of surface AMPA receptors of the postsynaptic membrane. Conversely, and in accord with these findings, Arc/Arg3.1 KO mice posses a higher amount of postsynaptic AMPA receptors and remove only a reduced number of AMPA receptors in response to synaptic activity. These altered mechanisms in KO mice might evoke the exceeding peck in e-LTP, and reflect the important role of Arc/Arg3.1 protein in the early phase of LTP formation. Furthermore, the absence of Arc/Arg3.1 and its consequent increase of AMPA receptor function was also shown to provide a cell-wide effect on neuronal activity. In the model of homeostatic plasticity, homeostatic synaptic scaling of AMPA receptors is mediated by Arc/Arg3.1 and was suggested to complement the Hebbian plasticity. The homeostatic scaling mechanisms were thought to compensate for acute changes in synaptic strength and are required to maintain neuronal output in the normal range in order to avoid neuronal unrestrained potentiation or saturation without changing the relative strength of individual synapses (Shepherd et al. 2006). Since Arc/Arg3.1 KO mice have reduced capacities of homeostatic plasticity, it can be supposed that the increased amount and function of AMPA receptors may contribute to more synaptic response after stimulation.

2. A second explanation might be a change in the composition of AMPAR subunits that contribute to diverse levels of excitatory synaptic potentiation. A recent report from Shepherd and colleagues observed increased surface levels of GluR1-AMPA receptors in Arc/Arg3.1 KO neurons and proposed a shift in the subunit composition of AMPARs toward more GluR1-containing AMPA receptors (Shepherd et al. 2006). The type of GluR1-AMPAR is permeable to Ca^{2+} ions and hence is capable of reinforcing postsynaptic Ca^{2+} dependent signaling pathways (Cull-Candy et al. 2006). Possible increase in GluR1-AMPARs at the synapse could facilitate and enhance initial fEPSP slopes during LTP maintenance. This is in accord with work demonstrating that adult GluR-A (GluR1)-deficient mice could not establish LTP in response to tetanus stimulation (Mack et al. 2001).
3. A third explanation could be the recruitment of silent synapses. Previous studies of the hippocampal CA1 region proposed that a certain contingent of synapses exists which express only NMDA receptors and are thus non-functional and remain silent at normal resting potentials (Liao et al. 1995). During LTP induction and NMDA receptor activation, these synapses could be stimulated and switched to a more functional state (Isaac et al. 1995). Although it remains to be elucidated whether the switch from silent to functional synapses is due to pre-existing AMPARs or to insertion of new AMPARs into the postsynaptic membrane, the concept of silent synapses could coincide with the present data. The obtained results from the input/output curves and their calculated parameters ($fEPSP_{half}$-A, I_{half}) showed that conventional and conditional KO mice produce smaller fEPSPs at basal stimulation compared to their corresponding WT mice. This effect might reflect the presence of more silent and less functional synapses in the conventional and conditional KO mice, compared to WT mice. The higher fraction of silent synapses would reduce the baseline of fEPSP amplitude but would lead to a proportionally larger e-LTP when converted into functional synapses by the LTP induction stimulus. Although previous studies reported overall normal morphology and numbers of spines in conventional KO CA1 cells, a direct test of silent synapses was not performed yet (Plath et al. 2006).
An interesting finding in my study was that KO mice showed significant elevated fEPSP ratio of 1^{st} burst in 1^{st} TBS train (Figure 18C) compared to WT mice. This might reflect altered existing cellular mechanisms or cellular equipment of different signaling molecules which respond in an hypersensitive and very rapid manner to extern high frequency stimulation. This hypersensitive activation of fEPSP response may also be accounted for the exceeding peck of e-LTP in KO mice.

5.1.3 Consolidation of l-LTP in KO mice

Synaptic plasticity in the hippocampal CA1 area can lead to modifications of synaptic structure believed to underlie memory formation. Long-term consolidation of CA1 plasticity requires NMDA receptor activation, induction of IEG expression and novel protein synthesis (Abraham et al. 1991, Huang and Kandel 1994, Tsien et al. 1996, Abraham and Williams 2003). The IEG Arc/Arg3.1 is regulated by NMDA receptor activation (Bloomer et al. 2008)

and was shown to be necessary for consolidation of l-LTP (Plath et al. 2006). My results demonstrate that TBS-induced LTP fails to consolidate into l-LTP, as previously reported for pairing-induced LTP and DG-LTP (Plath et al. 2006). Several possible explanations are considered below, although additional evidence is still needed.

Impaired l-LTP in KO mice

To verify the canonical hypothesis that Arc/Arg3.1 protein is necessary to establish stable l-LTP, long-lasting (5 hours) LTP was measured in conventional Arc/Arg3.1 KO mice. These experiments confirmed the decay of LTP within 3 hours post TBS stimulation, similar to the decay rate of pairing-induced LTP in CA1 (Plath et al. 2006). Interestingly, individual LTP experiments in KO slices did not uniformly fail to form l-LTP but occasionally generated stable l-LTP. These observations from l-LTP experiments suggest that the probability of inducing stable l-LTP is reduced in the Arc/Arg3.1 KO mice despite a strong induction protocol, but not completely extinguished. These results equally show that a form of l-LTP can still be induced in absence of Arc/Arg3.1, however the mechanism underlying l-LTP stability in the KO slices might be different to those supporting l-LTP in WT slices. Alternatively, l-LTP in the KO slices might reflect an adaptation to the constitutive loss of Arc/Arg3.1. It is also plausible that successful l-LTP in the KO slices is maintained longer than the decaying LTP, but might eventually also decay at a later time point beyond the recording time used here.

My data is also similar to previously reported impaired l-LTP in living rats and in corresponding in vitro experiments. The group of Guzowski showed that intrahippocampal infusion of antisense oligodeoxynucleotides, which inhibited Arg3.1 protein expression, leads to impairment of long-term potentiation and long-term consolidation in spatial learning (Guzowski et al. 2000). It is widely accepted that both, long-term memory formation *in vivo* and l-LTP consolidation *in vitro*, require activity-regulated expression of Arg3.1 gene and protein. In this study, the absence of Arc/Arg3.1 in conventional KO slices resulted in severe l-LTP impairment and thus, is in line with previous reports.

TBS stimulation did not only induce distinct levels of long-term potentiation in Arc/Arg3.1 WT and KO mice, but also resulted in a different increase of cell responses during TBS trains. The analysis of burst slopes in TBS trains showed enhanced inter-burst facilitation in WT mice compared to KO littermates. Especially, the slope of the 1st burst of the 2nd TBS train demonstrated the highest facilitation value, while the magnitude of burst slope of the 1st TBS train was comparable to KO mice. The lack of inter-burst facilitation as measured from the slope ratio of the 1st burst in 2nd TBS:1st TBS train, was significant between genotypes. These differences of facilitation capacities in TBS trains might arise the hypothesis that intact long-term potentiation in WT mice require preceding inter-burst facilitation and that in return, the impairment of l-LTP in the KO mice is a result from inadequate inter-burst facilitation. In literature, several evidences can be found to understand the mechanisms of burst facilitation and correlation to LTP maintenance. For example, Kramer and colleagues showed that the amount of facilitation within theta burst trains correlates with the magnitude of

induced long-term potentiation (Kramer et al. 2004). The group induced TBS-LTP over 60 minutes in BDNF treated slices and control slices and showed that fEPSP slopes are not only increased in BDNF-LTP but also within the applied theta burst trains. According to this group, the increased inter-burst (BDNF-) facilitation within one TBS train was suggested to regulate the amplitude of subsequent bursts in this TBS train and to initiate the maintenance of long-lasting potentiation. Similarly to my study, WT mice showed elevated inter-burst facilitation and intact l-LTP after TBS stimulation. Since Kramer and colleagues demonstrated the positive effect of BDNF amplification within TBS bursts and TBS-LTP, it is thinkable that the absence of Arc/Arg3.1 protein in KO mice has the reverse effect on both, burst facilitation and l-LTP. Thus, intact burst facilitation within TBS trains may be a condition of the establishment of l-LTP and might indicate a role of Arc/Arg3.1 protein expression in the mechanisms of inter-burst facilitation within TBS trains.

On a cellular level, a widely accepted convention is that the immediate enhancement of cell responses after synaptic stimulation is due to activated NMDARs, postsynaptic Ca^{2+} influx and the entailed Ca^{2+} dependent signaling cascades (Malenka et al. 1992, Bliss and Collingridge 1993, Bredt and Nicoll 2003). The rise of Ca^{2+} ions initiates series of cellular changes that ultimately lead to the persistent enhancement of synaptic transmission. By consequence, impaired TBS-induced activation of NMDARs in the KO mice, would reduce the amount of postsynaptic Ca^{2+} influx and thereby, generate smaller inter-burst facilitation within TBS trains. Alternatively, low postsynaptic Ca^{2+} concentration might also result from other altered or dysfunctional Ca^{2+} sources which are known to elevate postsynaptic Ca^{2+} after synaptic stimulation. For example, the voltage-dependent Ca^{2+} channels are a rich source of Ca^{2+} ions and can be activated by tetanic LTP protocols (Cavazzini et al. 2005). A second example of a postsynaptic Ca^{2+} source is the endoplasmic reticulum. Its activity-dependent release of Ca $^{2+}$ ions occurs through ryanodine and inositol (1,4,5)-triphosphate receptors which in turn, are reinforced by the increase of cytosolic Ca^{2+} ions and furthermore promote Ca^{2+}-induced Ca^{2+}release (Raymond 2007). Alterations of one of these mechanisms in KO mice might reduce postsynaptic Ca^{2+} concentrations and could account for the reduced cellular potentiation after TBS stimulation. However, in this postsynaptic model, the detailed role of Arc/Arg3.1 protein involvement remained unclear.

Another possible explanation for the association of burst facilitation and l-LTP might result from the large debate of the locus of LTP. On the one hand the postsynaptic model including AMPA receptor trafficking is universally agreed upon, but on the other hand, there is also some evidence for presynaptic expression mechanisms of LTP which might be altered in KO mice. The group Schulz and colleagues reexamined changes in pared pulse facilitation (PPF), and found a significant increased and decrease in PPF which was correlated inversely with the expression of LTP (Schulz et al. 1994). This group presumed that smaller initial PPF was correlated with an increase in PPF with LTP, which was associated with an increase in the number of release sites or the probability release of neurotransmitter release or both. It has to be added that these observations were made in individual slices and were not observed in the average of PPF analysis. In this study, the fEPSP ratio from Arc/Arg3.1 KO mice showed

an immediate initial stronger intra-burst facilitation which was significant higher, while inter-burst facilitation did not increase across TBS trains compared to WT mice. This vague hypothesis might provide an indication of a presynaptic contribution to LTP and might be affected by the absence of Arc/Arg3.1 protein.

Formation of stable LTP implicates long-term structural changes like the expansion of the postsynaptic density (PSD) and enlargement of dendritic spines (Fukazawa et al. 2003). These processes were shown to depend on F-actin polymerization and are regulated by sustained Arc/Arg3.1 protein synthesis (Messaoudi et al. 2007). Evidence from several studies have shown that phosphorylation of cofilin is the major regulator of F-actin polymerization and that inhibition of Arc/Arg3.1 protein synthesis leads to dephosphorylation of cofilin which in turn, reduces nascent F-actin at synaptic stimulated dendrites (Messaoudi et al. 2007). A recent study has identified the actin binding protein WAVE3 as an Arc/Arg3.1 binding-partner, however, it is not known yet how Arc/Arg3.1 synthesis regulate cofilin phosphorylation (Bramham et al. 2008). On a morphological level, time-lapse imaging studies provided evidence that spine expansion and stabilization is associated with TBS-LTP and new protein synthesis (Yang et al. 2008). In another study, the group of Chen and colleagues demonstrated that TBS-LTP in the hippocampal CA1 neurons leads to an increase in the number of phospho-cofilin positive spines in stimulated spines which correlates with larger PSD sites (Chen et al. 2007). According to these studies, KO mice might posses reduced capacities in the strengthening of dendritic spines via F-actin polymerization after TBS stimulation, and thereby fail in long-term LTP consolidation. Although, different brain morphology between WT and KO mice were not discovered yet (Plath et al. 2006).

5.1.4 Gene-dose dependent deficits in HT mice

Heterozygous mice express lower amounts of Arc/Arg3.1 protein compared to WT mice throughout their development and adulthood. In the current study, the effects of this reduced amount of Arc/Arg3.1 protein expression on synaptic function and plasticity was investigated. Generally, the results obtained from Arc/Arg3.1 HT mice show deficits that are intermediate between WT and KO littermates. In HT slices, e-LTP amplitude was intermediate between WT and KO mice. The LTP subsequently decayed to baseline like KO slices, albeit more slowly. The probability of l-LTP induction was in the seize of 50% and thus higher than in KO slices but lower than in WT slices. In accord with the previously mentioned correlation between l-LTP and facilitation within TBS trains, l-LTP failure was also accompanied by a reduction of the TBS slope ratio which was comparable to KO slices. Similar results from mice expressing a limited amount of Arc/Arg3.1 protein have been reported by other groups (Guzowski et al. 2000, Messaoudi et al. 2007). They investigated Arc/Arg3.1 function on synaptic efficacy via disruption of Arc/Arg3.1 protein translation by using of antisense oligodeoxynucleotides (ODNs). The ODNs were applied in form of intrahippocampal infusion into dentate gyrus *in vivo* and *in vitro* and leaded to a quantitative

decrease of roughly 50% of Arc/Arg3.1 protein. My findings agree with these reports and showed that Arc/Arg3.1 gene deletion impairs LTP consolidation in a gene- and protein-dose dependent manner. Since the l-LTP induction probability was 50% in HT mice, the amount of Arc/Arg3.1 protein expression might be at threshold levels for l-LTP induction. It is thinkable that a certain amount of Arc/Arg3.1 protein deletion resulted in impairment of l-LTP while values above that defined amount could generate intact l-LTP. However, since the amount of genetic reduction of Arc/Arg3.1 gene mostly occurs in an enlarged interval in individual animals, the exact threshold of l-LTP induction cannot be determined and was not further analyzed in this study.

Basal synaptic transmission recorded in HT mice remained intermediate between WT and KO mice and reflected the gene-dose effects of partial Arc/Arg3.1 gene deletion. The magnitude of $fEPSP_{half}$-A lay below WT mice and above KO mice while stimulation intensity at I_{half} in HT mice was greater compared to WT mice but smaller compared to KO mice. However, the averaged input/output curve of HT mice tended to the input/output curve obtained from KO mice. Since presynaptic function was similar in all three genotypes, the reduced postsynaptic function is likely to result from smaller or fewer synapses in HT and KO mice.

It will be of interest to identify the threshold of Arc/Arg3.1 protein expression for l-LTP induction and provide more evidence for the correlation between the amount of Arc/Arg3.1 protein expression and the l-LTP induction, for example via western blot testing.

5.1.5 Basal synaptic transmission in KO mice

Basal synaptic transmission was analyzed in KO, HT and WT mice to detect differences between genotypes which could be related to the failure of LTP consolidation. The fEPSP amplitudes were similar in HT and KO mice, but lower over the total fEPSP input/output curves compared to WT mice. In contrast to WT mice, KO mice required significant higher I_{half} to induce smaller $fEPSP_{half}$ amplitude, likewise HT mice. Since postsynaptic fEPSP amplitudes reflected the sum of simultaneously activated postsynaptic neurons, KO mice might activate only a reduced number of postsynaptic neurons or stimulate a subpopulation of synapses with remarkable less excitability capacities, resulting from reduced NMDA receptor activation and subsequent Ca^{2+} influx. Alternatively, reduced fEPSP amplitudes might be a result from a larger number of silent synapses in the KO mice, that were refractive to low stimulation and that were not detected by the previous studies (Isaac et al. 1995, Liao et al. 1995). The same tendency as fEPSP input/output curves could be demonstrated in the analysis of fEPSP/FV ratio which excluded a presynaptic contribution to excitability. The altered basal synaptic capacities in KO mice may also be ascribed to morphological changes. However, the group Plath and colleagues investigated the same conventional KO mice and reported no crucial morphological differences between brain structure, seize and density of synapses in KO and WT mice (Plath et al. 2006). They also visualized dendritic trees, spine density and PSD in hippocampal CA1 pyramidal cells and found no significant difference between WT and KO mice.

Interestingly, KO mice showed a slight increase in FV and FV_{half} amplitudes, compared to WT mice. This increase might come from diverse parameters like the number of presynaptic fibers or excitability of these, an elevated probability of transmitter release or number of release sites. However, presynaptic release mechanisms underlying PPF tests are similar in KO and WT mice. Recent publication of Mikuni and colleagues demonstrated a role of Arc/Arg3.1 protein expression in activity-dependent synapse elimination in the developing cerebellum (Mikuni et al. 2013). Generally, it is known that around birth an exceeded number of synapses and connections can be found in many regions of the brain. At early postnatal age, these redundant pre-existing circuits undergo strict selection and elimination processes which are necessary for the formation of functional and mature neuronal circuits (Kano and Hashimoto 2009). The group of Mikuni showed that activity-induced elimination of pre-existing climbing fibers to Purkinje cells synapses is Arc/Arg3.1 protein dependent and that the absence of Arc/Arg3.1 protein significantly increases the number of redundant climbing fibers (Mikuni et al. 2013). In accordance with the latter report, hippocampal presynaptic fibers might be augmented in KO mice because of inadequate elimination processes at the early postnatal age in the absence of Arc/Arg3.1 protein and generate thereby slightly elevated FV amplitudes. By consequence, an elevated number of fibers would converge on CA1 pyramidal cells and possibly impair or partly block postsynaptic excitability. This hypothesis may explain the altered capacities in basal synaptic transmission in KO mice, but was not yet directly tested in literature.

5.2 Consolidation of l-LTP in conditional KO mice

Although adult conventional and conditional Arc/Arg3.1 mice are equally devoid of Arc/Arg3.1 protein in the cortex and hippocampus, conventional KO mice exhibited impaired l-LTP whereas conditional KO mice showed stable l-LTP in the averaged LTP time course, that even slightly exceeded the seize of l-LTP in conditional WT littermates. Furthermore, the rate of successful l-LTP induction from individual experiments was much higher in conditional KO mice than in conventional KO mice and slightly elevated compared to conditional WT mice.
A main difference between conventional and conditional Arc/Arg3.1 KO mice is the time point of Arc/Arg3.1 deletion. Conventional KO mice lack Arc/Arg3.1 during their entire lifespan whereas in conditional KO mice Arc/Arg3.1 is present until the second postnatal week (unpublished results from Gao et al., Hamburg). The presence of Arc/Arg3.1 during this early development might be sufficient to change the synapses in CA1 region. In line with this hypothesis, Mikuni and colleagues have shown that selective elimination of initial abundant climbing fibers in the cerebellum at the time of birth is mediated by postsynaptic activity-dependent Purkinje cells via Arc/Arg3.1 gene (Mikuni et al. 2013). Since Arc/Arg3.1 knockdown in cultures slices resulted in significant impairment of synapse elimination, this process is considered as essential for the establishment of mature and intact neuronal network. Referring to my data, the increased fiber volley amplitudes measured at different

stimulation intensities in conventional KO slices might be an indication for impaired elimination of presynaptic input and reflect immature neuronal circuits. Interestingly, fiber volley amplitudes were not altered in conditional Arc/Arg3.1 deficient mice and thus, might account for a more intact neuronal circuit due to a later deletion of Arc/Arg3.1 protein expression.

Resuming the results from fEPSP ratio, slope of the 1st burst in 1st-4th TBS train, slope ratio and l-LTP maintenance, no significant difference could be detected between conditional WT and KO mice. In contrast to conventional KO mice, which showed altered intra- and inter-burst facilitation capacities within TBS trains, conditional KO mice seem to preserve the ability of all these forms of potentiation. Taken together these observations from both mouse lines, increased burst facilitation within TBS trains seem to precede stable l-LTP formation and might reveal a correlation or condition that could reflect a general rule of plasticity. This correlation or condition could arise either because facilitation within TBS trains is required for l-LTP induction, or because both are co-modified in absence of Arc/Arg3.1 protein.

A general view has emerged that Arc/Arg3.1 regulates the cellular mechanisms and structural changes for stable l-LTP maintenance. Following high-frequency stimulation, Arc/Arg3.1 protein becomes enriched in stimulated dendritic spines and initiates the expansion of PSD and enlargement of these spines (Bramham 2008). The local Arc/Arg3.1 protein synthesis promotes long-term F-actin polymerization and interacts with its major regulators of F-actin dynamics, cofilin. (Fukazawa et al. 2003, Yang et al. 2008, Bramham 2008). In its phosphorylated state cofilin is inactive and supports facilitation of the enlargement of F-actin filaments, however, how Arc/Arg3.1 synthesis regulates cofilin phosphorylation is not known yet (Bramham 2008). Hence, the question has raised how conditional Arc/Arg3.1 deficient mice generate stable l-LTP without expressing this essential protein. Several explanatory approaches could be accounted for this finding.

1. A simple explanation is that the network in the conventional Arc/Arg3.1 KO mice is more impaired than in the conditional Arc/Arg3.1 KO mice and thereby, the latter could recruit better or still intact cellular mechanisms of synaptic plasticity. Furthermore, conditional Arc/Arg3.1 KO mice have more time to develop normal hippocampal neuronal circuits and synapses because Arc/Arg3.1 protein deletion occurred at a later time point compared to conventional KO mice.

2. It has to be noted that the animal breeding of conditional cre mice in our laboratory underwent a plethora of genetic crossings and thereby might be subjected to genetic shift in the genome or to diverse side effects of cre transgene. The genome might be altered in favor of possible compensatory cellular mechanisms which prolong only temporary LTP potentiation and mimic l-LTP maintenance. Following this suggestion, it is thinkable that a longer recording time of LTP experiments post theta burst stimulation might lead to l-LTP decay and reconcile the different findings in conditional KO mice. In behavioral studies of our laboratory, the deficits in long-term memory consolidation were observed after an interval of 24 hours.

3. At a cellular level, stable l-LTP is not due to a specific signaling pathway but implicates a diversity of possible signaling cascades which could be activated simultaneously, amplified by themselves, overlapping or even interfering (cross-talk) between each other (Waltereit and Weller 2003). Downstream NMDAR activation and Ca^{2+} influx multiple second messenger and IEG are identified and proposed to mediate l-LTP consolidation but none of them seem to be indispensable for l-LTP formation. For example, Huang and Kandel demonstrated that TBS induced l-LTP formation in the hippocampal CA1 region depends on the cAMP-PKA signal (Huang and Kandel 1994) while other groups showed intact l-LTP formation in the presence of PKA inhibitors (Abbas et al. 2009, Villers et al. 2012). It is widely accepted that the calmodulin-cAMP-PKA-MAPK pathway is activated and acts on the transcription factors CREB that in turn, initiates the transcription of Arc/Arg3.1 gene (Nguyen and Kandel 1997, Waltereit and Weller 2003, Bramham et al. 2010, Lisman et al. 2012). However, the Ca^{2+} signal can also activate other signaling pathways like the PKC-Ras-Raf signal cascade which converges on CREB or other factors and thereby, up-regulates IEGs such as Arc/Arg3.1, c-fos, zif268 or CREB targets; all are signaling molecules previously implicated in l-LTP formation (Link et al.1995, Jones et al. 2001, Waltereit and Weller 2003). Following LTP induction, phosphorylation by diverse protein kinases such as cAMP-PKC, PKA, CaMKII or the atypical form of PKC: PKMζ, are thought to be critical for the regulation of AMPA receptors (Serrano et al. 2005, Lee and Kirkwood 2011). An increase in the number of AMPA receptors via phosphorylation of these proteins might be an alternative pathway to Arc/Arg3.1 protein regulated pathways, and thereby establish intact long-term potentiation in KO mice. It can also be suggested that over-expression of one of these signaling cascades might be sufficient to mediate structural changes and strengthening of the dendritic spines and via this mechanisms generate normal long-term consolidation.

Another contributing regulatory mechanism of AMPA receptor trafficking was recently describes by protein ubiquitination. Generally, ubiquitination is a reversible post-translational modification that controls multiple processes like protein degradation, endocytosis, and the sorting and trafficking of transmembrane proteins (Widagdo et al. 2017). In recently stimulated neurons, ubiquitination of AMPA receptors is mediated via ligand-binding, subsequent postsynaptic membrane depolarization and following Ca^{2+} signaling cascade including Ca^{2+} activated CaMKII and leads to internalization of AMPA receptors (Widagdo et al. 2017). However, this mechanism is not considered as a crucial controlling mechanism for synaptic plasticity, inhibition of ubiquitination of AMPA receptors might increase the synaptic potentiation capacities in KO mice.

5.3 Developmental effects of Arc/Arg3.1 protein

In this study, the knockdown of Arc/Arg3.1 protein in the conventional and conditional mouse line has provided different impacts on synaptic plasticity. Contrary to the expectations, the absence of Arc/Arg3.1 protein did not show sever deficits of long-term

potentiation in conditional KO mice, like in conventional KO mice. The magnitude of e-LTP in both KO mouse lines was similarly increased compared to the respective control group, however conventional KO mice tended to higher values of e-LTP than conditional KO mice. Comparison of burst facilitation capacities and l-LTP maintenance showed a correlation in both KO mouse lines. Conditional KO mice showed similar intra-burst facilitation and growing inter-burst facilitation in TBS trains which was followed by intact l-LTP induction while conventional KO mice generated exactly the opposite cell responses within TBS trains and failed to induce l-LTP. Furthermore, basal synaptic transmission was more severe affected from Arc/Arg3.1 deletion in conventional KO mice than in conditional KO mice. Taken these findings together, the time point of Arc/Arg3.1 protein deletion might explain these different results in both mouse lines and thus, define a function for Arc/Arg3.1 in the embryonic development, distinct to its role in synaptic plasticity. In literature, recent reports showed evidence that early Arc/Arg3.1 protein expression is associated with the survival and maturation of new dentate granule cells (Kuipers et al. 2009). It was reported that progenitor cells in the adult dentate gyrus provide the constant supply of neuronal precursors, and that only a small fraction of these cells develop into mature dentate granule cells (Kuipers et al. 2009). To understand these selection processes, Arc/Arg3.1 protein expression was induced by high-frequency stimulation in newborn dentate granule cells at diverse time points of the first four postnatal weeks and was thought to act as a specific marker for the integration of these cells in the pre-existing hippocampal circuits. Interestingly, newborn granule cells did not increase in Arc/Arg3.1 protein expression after HFS evokes Arc/Arg3.1 induction, and showed a certain refractory nature during the early postnatal period (Kuipers et al. 2009), although 1-3 week-old neurons were reported to have lower threshold for LTP induction relative to pre-existing dentate granule cells (Bramham et al. 2010). Furthermore, the group of Bramham described early post-mitotic and spontaneous expression of Arc/Arg3.1 protein in newborn granule cells which was correlated to their integration into hippocampal neuronal network, suggesting a unique property of Arc/Arg3.1 among IEG (Bramham et al. 2010). In these undifferentiated cells, Arc/Arg3.1 protein might act directly in the nucleus, where it initiates proliferation and differentiation of cells and is implicated in transcription and post-translational modification (Bramham et al. 2010). Moreover, Kuipers and colleagues described an early formation of glutamatergic synapses of newborn granule cells which require preceding Arc/Arg3.1 protein expression at the 1-7 postnatal day (Kuipers et al. 2009). Although, the mechanisms how Arc/Arg3.1 protein interacts on neurogenesis remain to be explored, Arc/Arg3.1 protein expression plays a role in the establishment and formation of pre-existing hippocampal neuronal circuits and its prenatal absence evoke dysfunction in these cellular networks.

5.4 Conclusions

This study investigated the consequences of a conventional and a conditional genetic deletion of Arc/Arg3.1 gene to synaptic strength and plasticity. In the conventional Arc/Arg3.1 KO mouse line, complete absence of Arc/Arg3.1 protein during embryogenesis, developmental and adulthood might lead to altered wiring of neuronal circuits in the hippocampus. This was indicated by impaired basal synaptic transmission and long-term plasticity. In contrast, conditional Arc/Arg3.1 KO mice underwent Arc/Arg3.1 protein deletion at a later time point and showed less altered basal synaptic transmission and intact long-term potentiation. In the latter mouse line, pre-existing hippocampal circuits might have already reached a certain level of maturation at birth, and thus acquire less severe deficits in synaptic plasticity after Arc/Arg3.1 protein deletion. The comparison of the impact of Arc/Arg3.1 protein deletion in both mouse lines showed the essential role of Arc/Arg3.1 in synaptic plasticity but also suggest a novel function of Arc/Arg3.1 protein in neurogenesis. However, the mechanisms by which Arc/Arg3.1 protein interact in these processes might be different, and remain an interesting and important object of research.

6 SUMMARY

Long-term potentiation had been widely studied in several brain regions to gain a better understanding of molecular mechanisms believed to underlie learning and memory. The fundamental basis for the acquisition and storage of new information is the ability of neuronal circuits, in particular within the hippocampus, to modify synaptic strength through Hebbian and non-Hebbian mechanisms. Long-lasting synaptic plasticity can be evoked by activation of NMDA receptors leading to functional and morphological alterations in activated synapses. Up-regulation of immediate early genes and novel protein synthesis are required for consolidating synaptic plasticity long enough to support memory. One of these IEG is Arc/Arg3.1 which plays an essential role in memory and plasticity consolidation.

The current study investigated the role of Arc/Arg3.1 in LTP elicited by a behaviorally inspired theta-burst-stimulation (TBS). Conventional (KO, Arc/Arg3.1$^{-/-}$) and conditional KO (Arc/Arg3.1$^{f/f,\ Cre+}$, cKO) mice in which Arc/Arg3.1 was deleted either in the germline (KO, Arc/Arg3.1$^{-/-}$ mice) or early after birth (cKO, Arc/Arg3.1$^{f/f,\ Cre+}$ mice) were examined to explore the effects of Arc/Arg3.1 expression during development on adult synaptic transmission and plasticity. Moreover, conventional heterozygous (HT) KO mice were investigated to reveal gene-dose response of Arc/Arg3.1 on synaptic transmission and plasticity. In conventional WT mice LTP was correlated with stimulation strength and duration; in agreement with previous reports. A transient LTP was induced by a single TBS train whereas 4 consecutive TBS trains elicited persistent LTP. In conventional KO mice e-LTP was abnormally large in response to 1 and 4 TBS while l-LTP decayed to baseline after 5 hours of stimulation. The summed fEPSP slopes during the TBS and the fEPSP amplitudes were strongly reduced in KO compared to WT mice, indicating altered short-term modulation and basal synaptic transmission. Heterozygous KO mice exhibited reduced baseline and TBS-evoked fEPSP amplitudes, increased e-LTP and decreased l-LTP compared to WT littermates. In most measures, values of HT mice were intermediate between those of WT and KO littermates, indicating gene-dose response effects of Arc/Arg3.1 on synaptic transmission and plasticity. Conditional removal of Arc/Arg3.1 after postnatal day 14 (P14) generated adult cKO mice that were completely devoid of Arc/Arg3.1, but experienced normal Arc/Arg3.1 expression during early development. These conditional KO mice exhibited relatively normal TBS slopes and l-LTP, elevated e-LTP but significantly reduced baseline fEPSP amplitudes compared to their WT littermates. These findings indicate that Arc/Arg3.1 expression before P14 is sufficient to install the mechanisms responsible for the TBS slope amplification and for the recruitment of l-LTP. Differently, expression of Arc/Arg3.1 after P14 is needed for establishing baseline synaptic transmission.

Taken together, my findings confirm an important role for Arc/Arg3.1 in synaptic transmission and plasticity and differentiate dose from time-dependent effects. Arc/Arg3.1 might mediate these effects by influencing the number of CA1 synapses, their strength and their plasticity through trafficking of glutamate receptors. My work helps to direct future experiments on the role of Arc/Arg3.1 during normal and pathological brain development.

7 ZUSAMMENFASSUNG

Die Langzeitpotenzierung (LTP) in den verschiedenen Gehirnregionen war Gegenstand zahlreicher Studien und ermöglicht uns ein besseres Verständnis der zugrundeliegenden molekularen Mechanismen, die für die Bildung des Langzeitgedächtnisses verantwortlich sind, zu gewinnen. Die grundlegende Voraussetzung für den Erwerb und die Speicherung von neuen Informationen ist die Fähigkeit neuronaler Schaltkreise, insbesondere der Schaltkreise in der Region des Hippocampus, die Stärke der zugehörigen Synapsen durch Hebb'sche und nicht Hebb'sche Mechanismen zu modifizieren. Dauerhafte synaptische Plastizität kann durch aktivierte NMDA Rezeptoren funktionelle und morphologische Veränderungen in stimulierten Synapsen hervorrufen. Es ist bekannt, dass eine ausreichende Hochregulierung von "immediate early genes" (IEGs) und die Synthese von neuen Proteinen nötig sind, um die Bildung des Langzeitgedächtnisses zu induzieren. Eines dieser IEGs, welchem eine entscheidende Rolle bei der Bildung des Langzeitgedächtnisses und dessen plastische Konsolidierungsprozesse zugeschrieben wird, ist Arc/Arg3.1.

Im Rahmen dieser Arbeit wurde die Funktion von Arc/Arg3.1 in der durch Theta-burst-Stimulierung erzeugten Langzeitpotenzierung untersucht. Konstitutive (KO, Arc/Arg3.1$^{-/-}$) und konditionelle KO (Arc/Arg3.1$^{f/f,\ Cre+}$, cKO) Mäuse, in denen Arc/Arg3.1 jeweils in der Keimbahn (KO, Arc/Arg3.1$^{-/-}$Mäuse) oder in den ersten Tagen nach der Geburt (cKO, Arc/Arg3.1$^{f/f,\ Cre+}$ Mäuse) entfernt wurde, wurden in die Experimente eingeschlossen, um die Auswirkungen von Arc/Arg3.1 Expression während der Entwicklung auf die adulte synaptische Transmission und Plastizität zu studieren. Außerdem wurden konstitutive heterozygote (HT) KO Mäuse untersucht, um einen etwaigen Gendosis abhängigen Effekt der Arc/Arg3.1 Deletion auf die synaptische Transmission und Plastizität aufzuzeigen. Übereinstimmend mit früheren Studien, korrelierte LTP in den konstitutiven WT Mäusen mit der zugeführten Intensität und der Dauer der Stimulation. Demnach generierten schwache Stimulierungsprotokolle (1 TBS) transientes LTP, während stärkere Stimulierungsprotokolle (4 TBS) langanhaltendes LTP hervorriefen. In konstitutiven KO Mäusen war e-LTP nach 1 und 4 TBS ungewöhnlich hoch, wohingegen l-LTP nach 5 Stunden Stimulierung auf das Niveau der Baseline abfiel. Im Gegensatz zu den WT Mäusen, zeigten KO Mäuse einen Abfall des summierten "fEPSP slopes" während der TBS Gabe und reduzierte fEPSP Amplituden. Dieses Ergebnis deutet auf eine Veränderung in der kurzzeitigen Modulation und der basalen synaptischen Transmission hin. Verglichen mit den WT Mäusen, zeigten heterozygote KO Mäuse reduzierte Baseline fEPSP Amplituden und reduzierte "fEPSP slopes" während der TBS Gabe sowie erhöhte e-LTP und erniedrigte l-LTP Werte. In den meisten Messungen lagen die Werte der HT Mäusen zwischen den Werten der WT und KO Mäusen, und ließen somit einen Gen-Dosis abhängigen Effekt von Arc/Arg3.1 bezüglich der synaptischen Transmission und der Plastizität vermuten. Die konditionelle Entfernung von Arc/Arg3.1 nach dem 14. postnatalen Tag (P14) erzeugte zwar cKO Mäuse, die gänzlich frei von der Arc/Arg3.1 Expression waren, jedoch während der frühen Entwicklung normale Arc/Arg3.1 Expression

aufwiesen. Konditionelle KO Mäuse besaßen relativ normale "TBS slope" und l-LTP Werte, erhöhte e-LTP Werte sowie signifikant reduzierte Baseline fEPSP Amplituden im Vergleich zu der zugehörigen WT Kontrollgruppe. Diese Ergebnisse deuten darauf hin, dass Arc/Arg3.1 Expression vor dem 14. Lebenstag ausreichend ist, um Mechanismen der "TBS slope" Amplifikation und der Langzeitpotenzierung zu aktiveren. Im Gegensatz dazu, erfordert die Stärke der basalen synaptischen Transmission die Expression von Arc/Arg3.1 auch nach dem 14. Lebenstag.

Zusammengefasst bestätigen meine Ergebnisse die wichtige Rolle von Arc/Arg3.1 in der synaptischen Transmission und Plastizität und differenzieren zwischen einem Gen-Dosis und einem zeitlich abhängigem Effekt der Arc/Arg3.1 Expression. Arc/Arg3.1 könnte diese Effekte durch die Anzahl der CA1 Synapsen, ihrer Stärke oder ihrer Plastizität via Glutamat Rezeptor-Trafficking regulieren. Meine Arbeit soll ein Wegweiser für zukünftige Experimente sein und diese darin unterstützen, neue Funktionen von Arc/Arg3.1 während der normalen und der pathologischen Entwicklung des Gehirns aufzudecken.

8 APPENDIX

8.1 Index of abbreviations

A	Amplitude
ACSF	Artificial cerebrospinal fluid
AMPAR	α-amino-3-hydroxy-5-methyl-4-isoxazolepropionic acid receptor
ANOVA	Analysis of variance
AP	Action potential
Arc/Arg3.1	Activity-regulated cytoskeleton-associated protein/activity-regulated gene
AS	Antisense
avg	Average
BAR	Bin/amphiphysin/Rvs
BDNF	Brain-derived neurotrophic factor
bp	Base pair
CA 1-4	Cornu ammonis area 1-4
$CaCl_2$	Calcium chloride
CH	Chamber
CamKIIα	Calcium/calmodulin-dependent kinase IIα
CaMKII(β)	Calcium/calmodulin-dependent protein kinase II (β)
cAMP	Cyclic adenosine monophosphate
CE	Control pathway, from control electrode
CH 1-4	Chamber 1-4
cKO	Conditional knockout
Cl^-	Chloride ion
CO_2	Carbon dioxide
Cre	Cyclization recombination
CRE	cAMP response element
CREB	CRE-binding protein
d/+	Heterozygous
DG	Dentate gyrus
DNA	Desoxyribonucleic acid
E0	Embryonic day 0
eIF2α/4E	Eukaryotic initiation factor 2α/4E
E-LTP	Early long-term potentiation
EM	Electron microscope
ERK	Extracellular-signal-regulated kinase
fEPSP	Field excitatory postsynaptic potential
fEPSP-A	Field excitatory postsynaptic potential amplitude
$fEPSP_{max}$-A	Maximal field excitatory postsynaptic potential amplitude

$fEPSP_{half}$-A	Half-maximal field excitatory postsynaptic potential amplitude
FV	Fiber volley
FV-A	Fiber volley amplitude
GABA	Gamma-aminobutyric acid
GluR1-4	Glutamate receptor 1-4
GluR-A-D	Glutamate receptor A-D
hAPP	Human amyloid precursor protein
HCO_3^-	Hydrogen carbonate ion (bicarbonate)
HT	Heterozygous
I	Current
I_{half}	Current needed to generate $fEPSP_{half}$-A
IPSP	Inhibitory postsynaptic potential
IO curve	Input/output curve
KCl	Potassium chloride
KO	Knockout
L-LTP	Late long-term potentiation
LoxP	Locus of X-over of P1
MAPK	Mitogen-activated protein kinase
mGluR	Metabotropic glutamate receptor
$MgSO_4$	Magnesium sulfate
MNK1	MAP kinase integrating kinase-1
mRNA	Messenger ribonucleic acid
n	Number of slices
N	Number of mice
NaCl	Sodium chloride
$NaHCO_3$	Sodium hydrogen carbonate
NaH_2PO_4	Sodium dihydrogen phosphate
NMD	Non-sense mediated RNA decay
NMDAR	N-methyl-D-aspartate receptor
NR1, NR2	N-methyl-D-aspartate receptor type 1, type 2
NO	Nitric oxide
O_2	Oxygen
ODN	Oligodeoxynucleotides
ORF	Open reading frame
P 7, 14	Postnatal day 7, 14
PEST	Riche in proline (P), glutamate (E), serine (S) and threonine (T)
PH	Plextrin homology
PI3K	Phosphoinositide 3-kinase
PKA	Protein kinase A
PKC	Protein kinase C
PPF	Paired pulse facilitation

PSD	Postsynaptic density
Raf	Rapidly accelerated fibrosarcoma
Ras	Rat sarcoma
RE	Recording electrode
SARE	Synaptic-activity responsive element
SE	Stimulation pathway, from stimulation electrode
sem	Standard error of measurement
SRE	Serum response element
STP	Short-term potentiation
TBS	Theta burst stimulation
TrkB	Tropomyosin receptor kinase B
UBE3A	Ubiquitin-protein ligase E3A
WT	Wild-type

8.2 Index of Figures

8.3 Literatures

Abbas, A. K., Dozmorov M., Li R., Huang F. S., Hellberg F., Danielson J., Tian Y., Ekstrom J., Sandberg M. and Wigstrom H. **(2009)**. Persistent LTP without triggered protein synthesis. Neurosci Res 63(1), 59-65.

Abeliovich, A., Chen C., Goda Y., Silva A. J., Stevens C. F. and Tonegawa S. **(1993)**. Modified hippocampal long-term potentiation in PKCγ-mutant mice. Cell 75(7), 1253-1262.

Abraham, W. C., Dragunow M. and Tate W. P. **(1991)**. The role of immediate early genes in the stabilization of long-term potentiation. Mol Neurobiol 5(2-4), 297-314.

Abraham, W. C., Demmer J., Richardson C., Williams J., Lawlor P., Mason S. E., Tate W. P. and Dragunow M. **(1993)**. Correlations between immediate early gene induction and the persistence of long-term potentiation. Neuroscience 56(3), 717–727.

Abraham, W. C. and Huggett, A. **(1997)**. Induction and reversal of long-term potentiation by repeated high-frequency stimulation in rat hippocampal slices. Hippocampus 7(2), 137–145.

Abraham, W. C, Greenwood J. M. , Logan B. L., Mason-Parker S. E. and Dragunow M. **(2002)**. Induction and experience-dependent reversal of stable LTP lasting months in the hippocampus. J Neurosci 22(21), 9626–34.

Abraham, W. C. and Williams J. M. **(2003)**. Properties and mechanisms of LTP maintenance. Neuroscientist 9(6), 463–474.

Andersen, P., Sundberg S. H., Sveen O. and Wigström H. (**1977**). Specific long-lasting potentiation of synaptic transmission in hippocampal slices. Nature 266(5604), 736-737.

Arancio, O., Kiebler M., Lee C., Lev-Ram V., Tsien R., Kandel E. and Hawkins R. **(1996).** Nitric oxide acts directly in the presynaptic neuron to produce long-term potentiation in cultured hippocampal neurons. Cell 87(6), 1025–1035.

Barria, A., Muller D., Derkach V., Griffith L. C. and Soderling T. R. **(1997)**. Regulatory phosphorylation of AMPA-type glutamate receptors by CaM-KII during long-term potentiation. Science 276(5321), 2042–2045.

Bliss, T. V. and Gardner-Medwin A. R. **(1973)**. Long-lasting potentiation of synaptic transmission in the dentate area of the unanaesthetized rabbit following stimulation of the perforant path. J Physiol 232(2), 357–374.

Bliss, T. V. and Lømo T. (**1973**). Long-lasting potentiation of synaptic transmission in the dentate area of the anaesthetized rabbit following stimulation of the perforant path. J Physiol *232*(2), 331-356.

Bliss, T. V. and Collingridge G. L. (**1993**). A synaptic model of memory: long-term potentiation in the hippocampus. Nature 361(6407), 31-39.

Blitzer, R. D., Wong T., Nouranifar R., lyengar R. and Landau E. M. **(1995)**. Postsynaptic cAMP pathway gates early LTP in hippocampal CA1 region. Neuron 15(6), 1403-1414.

Bloomer, W. A., Van Dongen H. M. and Van Dongen A. M. **(2008)**. Arc/Arg3.1 translation is controlled by convergent N-methyl-D-aspartate and Gs-coupled receptor signaling pathways. J Biol Chem 283(1), 582–592.

Bortolotto, Z. A. and Collingridge G. L. **(2000)**. A role for protein kinase C in a form of metaplasticity that regulates the induction of long-term potentiation at CA1 synapses of the adult rat hippocampus. Eur J Neurosci 12(11), 4055–4062.

Bramham, C. R. and Wells D. G. (**2007**). Dendritic mRNA: transport, translation and function. Nat Rev Neurosci 8(10), 776–789.

Bramham, C. R. **(2008).** Local protein synthesis, actin dynamics, and LTP consolidation. Curr Opin Neurobiol 18(5), 524-531.

Bramham, C. R., Worley P. F., Moore M. J. and Guzowski J. F. **(2008)**. The immediate early gene Arc/Arg3. 1: regulation, mechanisms, and function. J Neurosci 28(46), 11760-11767.

Bramham, C. R., Alme M. N., Bittins M., Kuipers S. D., Nair R. R., Pai B., Panja D., Schubert M., Soule J., Tiron A. and Wibrand K. (**2010**). The Arc of synaptic memory. Exp Brain Res 200(2), 125–140.

Brandon, E. P., Idzerdat R. L. and McKnightt G. S. **(1997)**. PKA isoforms, neuronal pathways, and behaviour: making the connection. Curr Opin Neurobiol 7(3), 397-403.

Bredt, D. S. and Nicoll R. A. **(2003)**. AMPA receptor trafficking at excitatory synapses. Neuron 40(2), 361–379.

Casanova, E., Fehsenfeld S., Mantamadiotis T., Lemberger T., Greiner E., Stewart A. F. and Schütz G. **(2001)**. A CamKIIα iCre BAC allows brain-specific gene inactivation. Genesis 31(1), 37-42.

Cavazzini, M., Bliss T. and Emptage N. **(2005)**. Ca2+ and synaptic plasticity. Cell calcium 38(3-4), 355-367.

Chen, G., Kolbeck R., Barde Y. A., Bonhoeffer T. and Kossel A. **(1999)**. Relative contribution of endogenous neurotrophins in hippocampal long-term potentiation. J Neurosci 19(18), 7983-7990.

Chen, L. Y., Rex C. S., Casale M. S., Gall C. M. and Lynch G. **(2007)**. Changes in synaptic morphology accompany actin signaling during LTP. J Neurosci 27(20), 5363-5372.

Chowdhury, S., Shepherd J. D., Okuno H., Lyford G., Petralia R. S., Plath N., Kuhl D., Huganir R. L. and Worley P. F. **(2006)**. Arc/Arg3.1 interacts with the endocytic machinery to regulate AMPA receptor trafficking. Neuron 52(3), 445–459.

Cole, A. J., Saffen D. W., Baraban J. M. and Worley P. F. **(1989)**. Rapid increase of an immediate early gene messenger RNA in hippocampal neurons by synaptic NMDA receptor activation. Nature 340(6233), 474-476

Collingridge, G. L. and Bliss T. V. P. (**1987**). NMDA receptors-their role in long-term potentiation. Trends Neurosci 10(7), 288-293.

Constantine-Paton, M. and Cline H. T. **(1998)**. LTP and activity-dependent synaptogenesis: the more alike they are, the more different they become. Curr Opin Neurobiol 8(1), 139-148.

Costa-Mattioli, M., Sossin W. S., Klann E. and Sonenberg N. **(2009)**. Translational control of long-lasting synaptic plasticity and memory. Neuron 61(1), 10–26.

Cull-Candy, S., Kelly L. and Farrant M. **(2006)**. Regulation of $Ca2+^{+}$-permeable AMPA receptors: synaptic plasticity and beyond. Curr Opin Neurobiol 16(3), 288 –297.

Daumas, J. C., Halley H., Francés B. and Lassalle J.-M. **(2009)**. Activation of metabotropic glutamate receptor type 2/3 supports the involvement of the hippocampal mossy fiber pathway on contextual fear memory consolidation. Learn Mem 16(8), 504-507.

David, G. A. **(1993)**. Emerging principles of intrinsic hippocampal organization. Curr Opin Neurobiol 3(2), 225 –229.

Davies, C. H., Starkey S. J., Pozza M. F. and Collingridge G. L. **(1991)**. GABA autoreceptors regulate the induction of LTP. Nature 349(6310), 609-611.

Davis, H. P., Small S. A., Stern Y., Mayeux R., Feldstein S. N. and Keller F. R. **(2003)**. Acquisition, recall, and forgetting of verbal information in long-term memory by young, middle aged, and elderly individuals. Cortex 39(4-5), 1063–1091.

Douglas, R. M. and Goddard G. V. **(1975)**. Long-term potentiation of the perforant path-granule cell synapse in the rat hippocampus. Brain Res 86(2), 205-215.

Eichenbaum, H. **(2000)**. A cortical-hippocampal system for declarative memory. Nat Rev Neurosci 1(1), .41-50.

English J. D. and Sweatt J. D. **(1997)**. A requirement for the mitogen-activated protein kinase cascade in hippocampal long term potentiation. J Biol Chem 272(31), 19103–19106.

Esteban, J. A., Shi S. H., Wilson C., Nuriya M., Huganir R. L. and Malinow R. **(2003)**. PKA phosphorylation of AMPA receptor subunits controls synaptic trafficking underlying plasticity. Nat Neurosci 6(2), 136–143.

Frey, U., Huang Y. Y. and Kandel E. R. **(1993)**. Effects of cAMP simulate a late stage of LTP in hippocampal CA1 neurons. Science 260(5114), 1661–1664.

Frey, U., Frey S., Schollmeier F. and Krug M. **(1996)**. Anisomycin of actinomycin D, a RNA synthesis inhibitor on long-term potentiation in rat hippocampal neurons in vivo and in vitro. J Physiol 490(3), 703–711.

Frey, U. and Morris R. G. **(1997)**. Synaptic tagging and long-term potentiation. Nature 385(6616), 533-536.

Fukazawa, Y., Saitoh Y., Ozawa F., Ohta Y., Mizuno K. and Inokuchi K. **(2003)**. Hippocampal LTP is accompanied by enhanced F-actin content within the dendritic spine that is essential for late LTP maintenance in vivo. Neuron 38(3), 447-460.

Giese, K. P., Fedorov N. B., Filipkowski R. K. and Silva A. J. **(1998)**. Autophosphorylation at Thr286 of the α calcium-calmodulin kinase II in LTP and learning. Science 279(5352), 870–873.

Greer, P. L., Hanayama R., Bloodgood B. L., Mardinly A. R., Lipton D. M., Flavell S. W., Kim T. K., Griffith E. C., Waldon Z., Maehr R., Ploegh H. L., Chowdhury S., Worley P. F., Steen J. and Greenberg M. E. **(2010)**. The Angelman Syndrome protein Ube3A regulates synapse development by ubiquitinating arc. Cell 140(5), 704–716.

Guzowski, J. F., Mcnaughton B. L., Barnes C. A. and Worley P. F. **(1999)**. Environment-specifc expression of the immediate-early gene Arc in hippocampal neuronal ensembles. Nat Neurosci 2(12), 1120–1124.

Guzowski, J. F., Lyford G. L., Stevenson G. D., Houston F. P., McGaugh J. L., Worley P. F. and Barnes C. A. **(2000)**. Inhibition of activity-dependent Arc protein expression in the rat hippocampus impairs the maintenance of long-term potentiation and the consolidation of long-term memory. J Neurosci 20(11), 3993–4001.

Guzowski, J. F., Setlow B., Wagner E. K. and McGaugh J. L. **(2001)**. Experience-dependent gene expression in the rat hippocampus after spatial learning: a comparison of the immediate-early genes Arc, c-fos, and zif268. J Neurosci 21(14), 5089-5098.

Hartmann, M., Heumann R. and Lessmann V. **(2001)**. Synaptic secretion of BDNF after high-frequency stimulation of glutamatergic synapses. EMBO J 20(21), 5887-5897.

Hebb, D. O. (**1949**). The organization of behavior: a neuropsychological theory. John Wiley and Sons, New York

Hering, H. and Sheng M. **(2001)**. Dendritic spines: structure, dynamics and regulation. Nat Rev Neurosci 2(12), 880–888.

Hjelmstad, G. O., Nicoll R. A. and Malenka R. C. **(1997)**. Synaptic refractory period provides a measure of probability of release in the hippocampus. Neuron 19(6), 1309–1318.

Huang, Y.-Y. and Kandel E. R. **(1994)**. Recruitment of long-lasting and protein kinase A-dependent long-term potentiation in the CA1 region of hippocampus requires repeated tetanization. Learn Mem 1(1), 74-82.

Huang, Y.-Y. and Kandel E. R. **(2005)**. Theta frequency stimulation induces a local form of late phase LTP in the CA1 region of the hippocampus. Learn Mem 12(6), 587-593.

Huang, F., Chotiner J. K. and Steward O. **(2007)**. Actin polymerization and ERK phosphorylation are required for Arc/Arg3.1 mRNA targeting to activated synaptic sites on dendrites. J Neurosci 27(34), 9054–9067.

Isaac, J. T., Nicoll R. A. and Malenka R. C. **(1995)**. Evidence for silent synapses: implications for the expression of LTP. Neuron 15(2), 427–434.

Jones, M. W., Errington M. L., French P. J., Fine A., Bliss T. V. P., Garel S., Charnay P., Bozon B., Laroche S. and Davis S. **(2001)**. A requirement for the immediate early gene Zif268 in the expression of late LTP and long-term memories. Nat Neurosci 4(3), 289–296.

Kanai, Y., Dohmae N. and Hirokawa N. **(2004)**. Kinesin transports RNA: isolation and characterization of an RNA-transporting granule. Neuron 43(4), 513–525.

Kandel, E. R. **(2001)**. The molecular biology of memory storage: a dialogue between genes and synapses. Science 294(5544), 1030–1038.

Kang, H. and Schuman E. M. **(1995)**. Long-lasting neurotrophin-induced enhancement of synaptic transmission in the adult hippocampus. Science 267(5204), 1658–1662.

Kang, H. and Schuman E. M. **(1996)**. A requirement for local protein synthesis in neurotrophin-induced hippocampal synaptic plasticity. Science 273(5280), 1402-1406.

Kang, H., Welcher A. A., Shelton D. and Schuman E. M. **(1997)**. Neurotrophins and time: different roles for TrkB signaling in hippocampal long-term potentiation. Neuron 19(3), 653-664.

Kano M. and Hashimoto K. **(2009)**. Synapse elimination in the central nervous system. Curr Opin Neurobiol 19(2), 154–161.

Karpova, A., Mikhaylova M., Thomas U., Knopfel T. and Behnisch T. **(2006)**. Involvement of protein synthesis and degradation in long-term potentiation of Schaffer collateral CA1 synapses. J Neurosci 26(18), 4949–4955.

Kato, K., Clark G. D., Bazan N. G. and Zorumski C. F. **(1994)**. Platelet-activating factor as a potential retrograde messenger in CA1 hippocampal long-term potentiation. Nature 367(6459), 175-179.

Katz, B. and Miledi R. **(1968)**. The role of calcium in neuromuscular facilitation. J Physiol 195(2), 481–492.

Kawashima, T., Okuno H., Nonaka M., Adachi-Morishima A., Kyo N., Okamura M., Takemoto-Kimura S., Worley P. F. and Bito H. **(2009)**. Synaptic activity-responsive element in the Arc/Arg3.1 promoter essential for synapse-to-nucleus signaling in activated neurons. Proc Natl Acad Sci USA 106(1), 316–321.

Konorski, J. (**1948**). Conditioned reflexes and neuron organization. CUP Archive.

Korte, M., Carroll P., Wolf E., Brem G., Thoenen H. and Bonhoeffer T. **(1995)**. Hippocampal long-term potentiation is impaired in mice lacking brain-derived neurotrophic factor. Proc Natl Acad Sci USA 92(19), 8856–8860.

Kramar, E. A., Lin B. , Lin C., Arai A. C., Gall C. M. and Lynch G. **(2004)**. A Novel Mechanism for the Facilitation of Theta-Induced Long-Term Potentiation by Brain-Derived. Neurotrophic Factor. J Neurosci 24(22), 5151–5161.

Krucker, T., Siggins G. R. and Halpain S. (**2000)**. Dynamic actin filaments are required for stable long-term potentiation (LTP) in area CA1 of the hippocampus. Proc Natl Acad Sci USA 97(12), 6856-6861.

Kuhl, D. and Skehel P. **(1998)**. Dendritic localization of mRNAs. Curr Opin Neurobiol 8(5), 600–606.

Kuipers, S. D., Tiron A., Soule J., Messaoudi E., Trentani A. and Bramham C. R. **(2009)**. Selective survival and maturation of adult-born dentate granule cells expressing the immediate early gene Arc/Arg3.1. PLoS One 4(3), e4885.

Larson, J., Wong D. and Lynch G. **(1986)**. Patterned stimulation at the theta frequency is optimal for the induction of hippocampal long-term potentiation. Brain Res 368(2), 347-350.

Larson, J. and Lynch G. **(1988)**. Role of N-methyl-D-aspartate receptors in the induction of synaptic potentiation by burst stimulation patterned after the hippocampal θ-rhythm. Brain Res 441(1-2), 111–118.

Lee H.-K. and Kirkwood A. (**2011**). AMPA receptor regulation during synaptic plasticity in hippocampus and neocortex. Semin Cell Dev Biol 22(5), 514–520.

Leßmann, V. and Brigadski T. **(2009)**. Mechanisms, locations, and kinetics of synaptic BDNF secretion: an update. Neurosci Res 65(1), 11-22.

Liao, D., Hessler N. A. and Malinow R. **(1995).** Activation of postsynaptically silent synapses during pairing-induced LTP in CA1 region of hippocampal slice. Nature 375(6530), 400-4004.

Link, W., Konietzko U., Kauselmann G., Krug M., Schwanke B., Frey U. and Kuhl D. **(1995)**. Somatodendritic expression of an immediate early gene is regulated by synaptic activity. Proc Natl Acad of Sci USA 92(12), 5734-5738.

Lisman, J. **(1989).** A mechanism for the Hebb and the anti-Hebb processes underlying learning and memory. Proc Natl Acad Sci USA 86(23), 9574-9578.

Lisman, J. E. and Zhabotinsky A. M. **(2001)**. A model of synaptic memory: a CaMKII/PP1 switch that potentiates transmission by organizing an AMPA receptor anchoring assembly. Neuron 31(2), 191–201.

Lisman, J., Yasuda R. and Raghavachari S. **(2012)**. Mechanisms of CaMKII action in long-term potentiation. Nat Rev Neurosci 13(3), 169-182.

Lo, D. C. **(1995)**. Neurotrophic factors and synaptic plasticity. Neuron 15(5), 979–981.

Lu, Y., Ji Y., Ganesan S., Schloesser R., Martinowich K., Sun M., Mei F., Chao M. V. and Lu B. **(2011)**. TrkB as a potential synaptic and behavioral tag. J Neurosci 31(33), 11762-11771.

Lyford, G. L., Yamagata K., Kaufmann W. E., Barnes C. A., Sanders L. K., Copeland N. G., Gilbert D. J., Jenkins N. A., Lanahan A. A. and Worley P. F. **(1995)**. Arc, a growth factor and activity-regulated gene, encodes a novel cytoskeleton-associated protein that is enriched in neuronal dendrites. Neuron 14(2), 433-45.

Mack, V., Burnashev N., Kaiser K. M., Rozov A., Jensen V., Hvalby O., Seeburg P. H., Sakmann B. and Sprengel R. **(2001)**. Conditional restoration of hippocampal synaptic potentiation in GluR-A-deficient mice. Science 292(5526), 2501–2504.

Malenka, R. C., Lancaster B. and Zucker R. S. **(1992)**. Temporal limits on the rise in postsynaptic calcium required for the induction of long-term potentiation. Neuron 9(1), 121-128.

Malenka, R. C. and Nicoll R. A. **(1999)**. Long-term potentiation--a decade of progress?. Science 285(5435), 1870–1874.

Martin, K. C., Brada M. and Kandel E. R. **(2000)**. Local protein synthesis and its role in synapse-specific plasticity. Curr Opin Neurobiol 10(5), 587–592.

McNaughton, B. L., Douglas R. M. and Goddard G. V. **(1978)**. Synaptic enhancement in fascia dentata: cooperativity among coactive afferents. Brain Res 157(2), 277-293.

Megías, M., Emri Z., Freund T. F. and Gulyas A. I. **(2001)**. Total number and distribution of inhibitory and excitatory synapses on hippocampal CA1 pyramidal cells. Neuroscience 102(3), 527–540.

Mellor, H. and Parker P. J. **(1998)**. The extended protein kinase C superfamily. Biochem J 332(2), 281-292.

Messaoudi, E., Bårdsen K., Srebro B. and Bramham C. R. **(1998)**. Acute intrahippocampal infusion of BDNF induces lasting potentiation of synaptic transmission in the rat dentate gyrus. J Neurophysiol 79(1), 496-499.

Messaoudi, E., Kanhema T., Soule J., Tiron A., Dagyte G., da Silva B. and Bramham C. R. **(2007)**. Sustained Arc/Arg3.1 synthesis controls long-term potentiation consolidation through regulation of local actin polymerization in the dentate gyrus in vivo. J Neurosci 27(39), 10445–10455.

Messas, C. S., Mansur L. L. and Martins Castro L. H. **(2008)**. Semantic memory impairment in temporal lobe epilepsy associated with hippocampal sclerosis. Epilepsy Behav 12(2), 311-316.

Mikuni, T., Uesaka N., Okuno H., Hirai H., Deisseroth K., Bito H. and Kano M. **(2013)**. Arc/Arg3.1 is a postsynaptic mediator of activity-dependent synapse elimination in the developing cerebellum. Neuron 78(6), 1024–1035.

Minichiello, L., Calella A., Medina D., Bonhoeffer T., Klein R. and Korte M. **(2002)**. Mechanism of TrkB-mediated hippocampal long-term potentiation. Neuron 36(1), 121-137.

Mody, I. and Pearce R. A. (**2004**). Diversity of inhibitory neurotransmission through GABAA receptors. Trends Neurosci 27(9), 569-575.

Moga, D. E., Calhoun W. E., Chowdhury A., Worley P., Morrison J. H. and Shapiro M. L. **(2004)**. Activity-regulated cytoskeletal-associated protein is localized to recently activated excitatory synapses. Neuroscience 125(1), 7–11.

Monyer, H., Burnashev N., Laurie D. J., Sakmann B. and Seeburg P. H. (**1994**). Developmental and regional expression in the rat brain and functional properties of four NMDA receptors. Neuron 12(3), 529 –540.

Nguyen, P. V., Abel T. and Kandel E. R. **(1994)**. Requirement of a critical period of transcription for induction of a late phase of LTP. Science 265(5175), 1104-1107.

Nguyen, P. V. and Kandel E. R. **(1996)**. A macromolecular synthesis-dependent late phase of LTP requiring cAMP in the medial perforant pathway of rat hippocampal slices. J Neurosci 16(10), 3189-3198.

Nguyen, P. V. and Kandel E. R. **(1997)**. Brief theta-burst stimulation induces a transcription-dependent late phase of LTP requiring cAMP in area CA1 of the mouse hippocampus. Learn Mem 4(2), 230–243.

Nicoll, R. A. and Malenka R. C. **(1999)**. Expression mechanisms underlying NMDA receptor-dependent long-term potentiation. Ann N Y Acad Sci 868(1), 515-525.

Okuno, H., Akashi K., Ishii Y., Yagishita-Kyo N., Suzuki K., Nonaka M., Kawashima T., Fujii H., Takemoto-Kimura S., Abe M., Natsume R, Chowdhury S., Sakimura K., Worley P. F. and Bito H. **(2012)**. Inverse synaptic tagging of inactive synapses via dynamic interaction of Arc/Arg3.1 with CaMKIIβ. Cell 149(4), 886–898.

Otmakhov, N., Tao-Cheng J. H., Carpenter S., Asrican B., Dosemeci A., Reese T. S., Lisman J. **(2004)**. Persistent accumulation of calcium/calmodulin-dependent protein kinase II in dendritic spines after induction of NMDA receptor-dependent chemical long-term potentiation. J Neurosci 24(42), 9324–9331.

Palop, J. J., Chin J., Roberson E. D., Wang J., Thwin M. T., Bien-Ly N., Yoo J., Ho K. O., Yu G., Kreitzer A., Finkbeiner S., Noebels J. L. and Mucke L. **(2007)**. Aberrant excitatory neuronal activity and compensatory remodeling of inhibitory hippocampal circuits in mouse models of Alzheimer's disease. Neuron 55(5), 697–711.

Panja, D., Dagyte G., Bidinosti M., Wibrand K., Kristiansen Å., Sonenberg N.and Bramham C. R. **(2009)**. Novel translational control in Arc-dependent long term potentiation consolidation in vivo. J Biol Chem 284(46), 31498-31511.

Panja, D. and Bramham C. R. **(2013)**. BDNF mechanisms in late LTP formation: A synthesis and breakdown. Neuropharmacology 76, 664–676.

Park, S., Park J. M., Kim S., Kim J-A., Shepherd J. D., Smith-Hicks C. L., Chowdhury S., Kaufmann W., Kuhl D., Ryazanov A. G., Huganir R. L., Linden D. J. and Worley P. F. **(2008)**. Elongation factor 2 and fragile X mental retardation protein control the dynamic translation of Arc/Arg3.1 essential for mGluR-LTD. Neuron 59(1), 70–83.

Park, P., Volianskis A., Sanderson T. M., Bortolotto Z. A., Jane D. E., Zhuo M., Kaang B.-K. and Collingridge G. L. **(2014)**. NMDA receptor-dependent long-term potentiation comprises a family of temporally overlapping forms of synaptic plasticity that are induced by different patterns of stimulation. Phil Trans R Soc B 369(1633), 20130131.

Peebles, C. L. and Finkbeiner S. **(2007)**. RNA decay back in play. Nat Neurosci 10(9), 1083.

Peebles, C. L., Yoo J., Thwin M. T., Palop J. J., Noebels J. L. and Finkbeiner S. **(2010)**. Arc regulates spine morphology and maintains network stability in vivo. Proc Natl Acad Sci USA 107(42), 18173–18178.

Pittenger C., Huang Y. Y., Paletzki R. F., Bourtchouladze R., Scanlin H., Vronskaya S. and Kandel E. R. **(2002)**. Reversible inhibition of CREB/ATF transcription factors in region CA1 of the dorsal hippocampus disrupts hippocampus-dependent spatial memory. Neuron 34(3)**,** 447–462.

Plath, N., Ohana O., Dammermann B., Errington M. L., Schmitz D., Gross C., Mao X., Engelsberg A., Mahlke C., Welzl H., Kobalz U., Stawrakakis A., Fernandez E., Waltereit R., Bick-Sander A., Therstappen E., Cooke S. F., Blanquet V., Wurst W., Salmen B., Bösel M. R., Lipp H.-P., Grant S. G. N., Bliss T. V. P., Wolfer D. P. and Kuhl D. **(2006)**. Arc/Arg3. 1 is essential for the consolidation of synaptic plasticity and memories. Neuron 52(3), 437-444.

Pozza, M. F., Manuel N. A., Steinmann M., Froestl W. and Davies C. H. (**1999**). Comparison of antagonist potencies at pre-and post-synaptic GABAB receptors at inhibitory synapses in the CA1 region of the rat hippocampus. Br J Pharmacol 127(1), 211-219.

Ramón y Cajal, S. F. (**1894**). The Croonian lecture.—"La fine structure des centres nerveux." Proc R Soc Lond 55(331-335), 444-468.

Rao, V. R., Pintchovski S. A., Chin .J, Peebles C. L., Mitra S. and Finkbeiner S. **(2006)**. AMPA receptors regulate transcription of the plasticity-related immediate-early gene Arc. Nat Neurosci 9(7), 887–895.

Raymond, C. R. **(2007)**. LTP forms 1, 2 and 3: different mechanisms for the 'long' in long-term potentiation. Trends Neurosci 30(4), 167-175.

Rex, C. S., Kramar E. A., Colgin L. L., Lin B., Gall C. M. and Lynch G. **(2005)**. Long-term potentiation is impaired in middle-aged rats: regional specificity and reversal by adenosine receptor antagonists. J Neurosci 25(25), 5956–5966.

Roberson, E. D., English J. D. and Sweatt J. D. **(1996)**. A biochemist's view of long-term potentiation. Learn Mem 3(1), 1–24.

Sans, N., Vissel B., Petralia R. S., Wang Y. X., Chang K., Royle G. A., Wang C. Y., O'Gorman S., Heinemann S. F. and Wenthold R. J. **(2003)**. Aberrant formation of glutamate receptor complexes in hippocampal neurons of mice lacking the GluR2 AMPA receptor subunit. J Neurosci 23(28), 9367–9373.

Scharf, M. T., Woo N. H., Lattal K. M., Young J. Z., Nguyen P. V. and Abel T. **(2002)**. Protein synthesis is required for the enhancement of long-term potentiation and long-term memory by spaced training. J Neurophysiol 87(6), 2770–2777.

Schulz, P. E., Cook E. P. and Johnston D. **(1994)**. Changes in Paired-Pulse Facilitation suggest presynaptic involvement in long-term potentiation. J Neurosci 14(9), 5325–5337.

Schulz, P. E. **(1997).** Long-term potentiation involves increases in the probability of neurotransmitter release. Proc Natl Acad Sci USA 94(11), 5888–5893.

Scoville, W. B. and Milner B. **(1957)**. Loss of recent memory after bilateral hippocampal lesions. J Neurol Neurosurg Psychiatry 20(1), 11-21.

Serrano, P., Yao Y. D. and Sacktor T. C. **(2005)**. Persistent phosphorylation by protein kinase Mζ maintains late-phase long-term potentiation. J Neurosci 25(8), 1979–1984.

Shankar, G. M., Li S., Mehta T. H., Garcia-Munoz A., Shepardson N. E., Smith I., Brett F. M., Farrell M. A., Rowan M. J., Lemere C. A., Regan C. M., Walsh D. M., Sabatini B. L. and Selkoe D. J. **(2008)**. Amyloid-β protein dimers isolated directly from Alzheimer's brains impair synaptic plasticity and memory. Nat Med 14(8), 837-842.

Shepherd, J. D., Rumbaugh G., Wu J., Chowdhury S., Plath N., Kuhl D., Huganir R. L. and Worley P. F. **(2006)**. Arc/Arg3.1 mediates homeostatic synaptic scaling of AMPA receptors. Neuron 52(3), 475–484.

Shepherd, J. D. and Huganir R. L. **(2007).** The cell biology of synaptic plasticity: AMPA receptor trafficking. Annu Rev Cell Dev Biol 23, 613-643.

Shepherd, J. D. and Bear M. F. **(2011)**. New views of Arc, a master regulator of synaptic plasticity. Nat Neurosci 14(3), 279-284.

Song, I. and Huganir R. L. **(2002)**. Regulation of AMPA receptors during synaptic plasticity. Trends Neurosci. 25(11), 578–588.

Staubli, U. and Lynch G. **(1987)**. Stable hippocampal long-term potentiation elicited by 'theta' pattern stimulation. Brain Res 435(1-2), 227-234.

Steward, O. **(1976)**. Topographic organization of the projections from the entorhinal area to the hippocampal formation of the rat. J Comp Neurol 167(3), 285–314.

Steward, O., Wallace C. S., Lyford G. L. and Worley P. F. **(1998)**. Synaptic activation causes the mRNA for the IEG Arc to localize selectively near activated postsynaptic sites on dendrites. Neuron 21(4), 741–751.

Steward, O. and Worley P. F. **(2001)**. Selective targeting of newly synthesized Arc mRNA to active synapses requires NMDA receptor activation. Neuron 30(1), 227–240.

Stringer, I., Greenfield L. J., Hackete J. T. and Guyenet P. G. **(1983)**. Blockade of long-term potentiation by phencyclidine and σ opiates in the hippocampus in vivo and in vitro. Brain Res 280(1), 127-138.

Tronche, F., Casanova E., Turiault M., Sahly I. and Kellendonk C. **(2002)**. When reserve genetics meets physiology: the use of site-specific recombinases in mice. FEBS Letters 529(1), 116-121.

Tsien, J. Z., Huerta P. T. and Tonegawa S. **(1996)**. The essential role of hippocampal CA1 NMDA receptor-dependent synaptic plasticity in spatial memory. Cell 87(7), 1327–1338.

Tzingounis, A. V. and Nicoll R. A. **(2006)**. Arc/Arg3.1: linking gene expression to synaptic plasticity and memory. Neuron 52(3), 403–407.

Villers, A., Godaux E. and Ris L. **(2012)**. Long-lasting LTP requires neither repeated trains for its induction nor protein synthesis for its development. PLoS ONE 7(7), e40823.

Volianskis, A. and Jensen M. S. **(2003)**. Transient and sustained types of long-term potentiation in the CA1 area of the rat hippocampus. J Physiol 550(2), 459–492.

Waltereit, R., Dammermann B., Wulff P., Scafidi J., Staubli U., Kauselmann G., Bundman M. and Kuhl D. **(2001)**. Arg3.1/Arc mRNA induction by Ca^{2+} and cAMP requires protein kinase A and mitogen-activated protein kinase/extracellular regulated kinase activation. J Neurosci 21(15), 5484-5493.

Waltereit, R. and Weller M. **(2003)**. Signaling from cAMP/PKA to MAPK and synaptic plasticity. Mol Neurobiol 27(1), 99–106.

Waung, M. W., Pfeiffer B. E., Nosyreva E. D., Ronesi J. A. and Huber K. M. **(2008)**. Rapid translation of Arc/Arg3.1 selectively mediates mGluR-dependent LTD through persistent increases in AMPAR endocytosis rate. Neuron 59(1), 84–97.

Wenthold, R. J., Petralia R. S., Blahos J. and Niedzielski A. S. **(1996)**. Evidence for multiple AMPAR complexes in hippocampal CA1/CA2 neurons. J Neurosci 16(6), 1982-1989.

Widagdo, J., Guntupalli S., Jang S. E. and Anggono V. (**2017**). Regulation of AMPA receptor trafficking by trotein ubiquitination. Front Mol Neurosci 10, 347.

Woo, N. H., Duffy S. N., Abel T. and Nguyen P. V. **(2003)**. Temporal spacing of synaptic stimulation critically modulates the dependence of LTP on cyclic AMP dependent protein kinase. Hippocampus 13 (2), 293–300.

Yang, Y., Wang X. B., Frerking M. and Zhou Q. **(2008)**. Spine expansion and stabilization associated with long-term potentiation. J Neurosci 28(22), 5740-5751.

Zhao, C., Teng E. M., Summers R. G. , Ming G. L. and Gage F. H. (**2006**). Distinct morphological stages of dentate granule neuron maturation in the adult mouse hippocampus. J Neurosci 26(1), 3–11.

8.4 Acknowledgments

I would like to express my gratitude to my supervisor Prof. Dr. Dietmar Kuhl who gave me the studentship, the interesting issue of my dissertation and the possibility to experience research work in the laboratory.

Very special thanks goes to my advisor Dr. Ora Ohana in many ways. She was the person who taught me mice preparation and handling of experimental techniques with her expertise, motivation and encouragement. I appreciate her time and her help during critical moments of experiments. Her encouragement created an agreeable working atmosphere and accompanied me through my thesis. I also wanted to thank her for taking out time from her busy schedule to proofread my thesis.

I must also acknowledge all members working in the laboratory who contributed to accomplish this work, especially for providing the mouse lines, for answering my subject-specific questions as well as computer or for technical support. Thanks also go to who supports me with statistical advice for any time of need.

Finally, I would like to thank my family who supports me during my studies and my laboratory work, and who was always very patient with me and without whose support I would not have finished this thesis.

8.5 Curriculum vitae

Lebenslauf wurde aus datenschutzrechtlichen Gründen entfernt.

8.6 Eidesstaatliche Erklärung

Ich versichere ausdrücklich, dass ich die Arbeit selbständig und ohne fremde Hilfe verfasst, andere als die von mir angegebenen Quellen und Hilfsmittel nicht benutzt und die aus den benutzten Werken wörtlich oder inhaltlich entnommenen Stellen einzeln nach Ausgabe (Auflage und Jahr des Erscheinens), Band und Seite des benutzten Werkes kenntlich gemacht habe.
Ferner versichere ich, dass ich die Dissertation bisher nicht einem Fachvertreter an einer anderen Hochschule zur Überprüfung vorgelegt oder mich anderweitig um Zulassung zur Promotion beworben habe.
Ich erkläre mich einverstanden, dass meine Dissertation vom Dekanat der Medizinischen Fakultät mit einer gängigen Software zur Erkennung von Plagiaten überprüft werden kann.

Unterschrift: .....